VIBRATION REDUCTION OF STRUCTURES BY USING NONLINEAR TUNED VIBRATION ABSORBERS

A THESIS SUBMITTED TO
THE GRADUATE SCHOOL OF NATURAL AND APPLIED SCIENCES
OF
MIDDLE EAST TECHNICAL UNIVERSITY

BY

MUHAMMED EMIN DOĞAN

IN PARTIAL FULFILLMENT OF THE REQUIREMENTS
FOR
THE DEGREE OF MASTER OF SCIENCE
IN
MECHANICAL ENGINEERING

SEPTEMBER 2019

Approval of the thesis:

VIBRATION REDUCTION OF STRUCTURES BY USING NONLINEAR TUNED VIBRATION ABSORBERS

submitted by **MUHAMMED EMIN DOĞAN** in partial fulfillment of the requirements for the degree of **Master of Science in Mechanical Engineering Department, Middle East Technical University** by,

Prof. Dr. Halil Kalıpçılar
Dean, Graduate School of **Natural and Applied Sciences**

Prof. Dr. M. A. Sahir Arıkan
Head of Department, **Mechanical Engineering**

Prof. Dr. Ender Ciğeroğlu
Supervisor, **Mechanical Engineering, METU**

Examining Committee Members:

Assoc. Prof. Dr. Mehmet Bülent Özer
Mechanical Engineering, METU

Prof. Dr. Ender Ciğeroğlu
Mechanical Engineering, METU

Assoc. Prof. Dr. Yiğit Yazıcıoğlu
Mechanical Engineering, METU

Assist. Prof. Dr. Orkun Özşahin
Mechanical Engineering, METU

Assist. Prof. Dr. Çağlar Başlamışlı
Mechanical Engineering, Hacettepe University

Date: 09.09.2019

I hereby declare that all information in this document has been obtained and presented in accordance with academic rules and ethical conduct. I also declare that, as required by these rules and conduct, I have fully cited and referenced all material and results that are not original to this work.

Name, Surname: Muhammed Emin Doğan

Signature:

ABSTRACT

VIBRATION REDUCTION OF STRUCTURES BY USING NONLINEAR TUNED VIBRATION ABSORBERS

Doğan, Muhammed Emin
Master of Science, Mechanical Engineering
Supervisor: Prof. Dr. Ender Ciğeroğlu

September 2019, 85 pages

Tuned Vibration Absorbers (TVA) are commonly used in reducing undesirable vibrations of mechanical structures. However, TVAs work in a very limited frequency range and if the excitation frequency is outside of this range, they become ineffective. In order to solve this problem, researchers started to consider nonlinear TVAs for vibration attenuation. In this study, dynamic behavior of a Linear systems coupled with a nonlinear TVA is investigated. The system is subjected to sinusoidal base excitation. Parameters of the nonlinear TVA is optimized to minimize vibration values of the primary system. Assumed modes method is used to model the Euler-Bernoulli beam. Nonlinear differential equations of motion are converted to a set of nonlinear algebraic equations by using Harmonic balance Method (HBM). The resulting set of nonlinear algebraic equations is solved by Newton's Method with Arc-Length continuation. Nonlinearities used in the TVA are cubic stiffness, which is referred as Nonlinear Energy Sink (NES) in the literature; cubic damping and dry friction damping. Hill's method is used to evaluate stability of the solutions obtained. Results of the system with optimum nonlinear TVAs are compared with that of optimum linear TVA. Although, NES show to exhibit good vibration reduction performance, which is in parallel with the results given in literature, due to instability of the frequency

domain solutions, it is observed that, actually, it is not as effective as other nonlinear TVAs.

Keywords: Tuned Vibration Absorber, Nonlinear Energy Sink, Optimization, Friction

ÖZ

DOĞRUSAL OLMAYAN AYARLI TİTREŞİM SÖNÜMLEYİCİ KULLANILARAK YAPI ÜZERİNDEKİ TİTREŞİMLERİN AZALTILMASI

Doğan, Muhammed Emin
Yüksek Lisans, Makina Mühendisliği
Tez Danışmanı: Prof. Dr. Ender Ciğeroğlu

Eylül 2019, 85 sayfa

Ayarlı Titreşim Sönümleyicileri (ATS) mekanik yapılan üzerindeki istenmeyen titreşimi azaltmak için kullanılır. Fakat ATS'ler sınıtlı bir frekans aralığında çalışırlar. Eğer tahrik frekansı bu aralığın dışındaysa, ATS'ler etkili olmamaya başlar. Bu problem çözmek için birçok araştırmacı doğrusal olmayan ATS'ler üzerinde çalışmaya başlamıştır. Bu çalışmada, doğrusal olmayan ATS ile birleştirilmiş doğrusal bir sistemin dinamik davranışı incelenmektedir. Sistem tabandan tahrik edilmektedir. Ana sistemin titreşim seviyesini minimize edecek şekilde doğrusal olmayan ATS'nin parametreleri optimize edilmektedir. Mod varsayım yöntemi kullanılarak Euler-Bernouli kirişi modellenmektedir. Doğrusal olmayan diferansiyel denklemler harmonik denge metodu ile doğrusal olmayan cebirsel denklemlere çevrilmektedir. Bu denklem seti de yay Devamlı Yay Uzunluğu ve Newton metodu kullanılarak çözülmektedir. Sistemde kullanılan doğrusal elemanlar kübik katılık, kübik damper ve sürtünmedir. Hill metodu ile elde edilen çözümlerin kararlılığı kontrol edilmiştir. Doğrusal olmayan katılık kullanılan ATS'ler literatürde Doğrusal olmayan enerji çukuru diye de geçer. Optimize edilmiş doğrusal olmayan ATS'lerin performansı ile optimum doğrusal ATS'lerin performansı karşılaştırılır.

Anahtar Kelimeler: Ayarlı Titreşim Sönümleyicisi, Doğrusal Olmayan Enerji Çukuru, Optimizasyon, Sürtünme

To my family…

ACKNOWLEDGEMENTS

I would like to thank my thesis advisor Prof. Dr. Ender Ciğeroğlu for his excellent supervision and leading guidance from the beginning to the end of my thesis work.

I would like to thank colleagues, my team leader Mahmut Miraç Ünlüer and my director Tahir Fidan for their help during the thesis period.

I would like to thank Elif Nur Taşçı for her valuable support and encouragement.

I would like to thank my family, my father Mehmet Doğan, my mother Melek Doğan and my sister Şeyma for their support over many years. Finally, I would like to thank my lovely niece Melike for the joy that she brings my life.

TABLE OF CONTENTS

LIST OF TABLES

TABLES

LIST OF FIGURES

FIGURES

LIST OF ABBREVIATIONS

ABBREVIATIONS

TVA: Tuned Vibration Absorber

FTVA: Tuned Vibration Absorber with Friction Damper

HBM: Harmonic Balance Method

DOF: Degree of Freedom

SDOF: Single Degree of Freedom

MDOF: Multi Degrees of Freedom

FFT: Fast Fourier Transform

LIST OF SYMBOLS

SYMBOLS

$x_b(t)$: Displacement of primary system in time domain.

$\dot{x}_b(t)$: Velocity of primary system in time domain.

$\ddot{x}_b(t)$: Acceleration of primary system in time domain.

m_b : Mass of primary system

k_b : Mass of primary system

h_b : Structural damping of primary system

$u(t)$: Base Excitations

$m_{TVA,i}$: Mass of ith TVA

$k_{TVA,i}$: Stiffness of ith TVA

$c_{TVA,i}$: Linear damping of ith TVA

x_{rel} : Relative displacement between TVA and primary system

$\mathbf{x}(t)$: Displacement vector in time domain

$\dot{\mathbf{x}}(t)$: Velocity vector in time domain

$\ddot{\mathbf{x}}(t)$: Acceleration vector in time domain

$\mathbf{M}$: Mass matrix

$\mathbf{K}$: Stiffness matrix

$\mathbf{H}$: Structural damping matrix

$\mathbf{C}$: Damping matrix

F_{NL} :Nonlinear transfer function

f_{non} :Nonlinear force element

$\mathbf{f}_{non}$:Nonlinear force vector

$\mathbf{x}^s$:Sine component of displacement vector in frequency domain

$\mathbf{x}^c$:Cosine component of displacement vector in frequency domain

$\mathbf{x}$:Displacement vector in frequency domain

$f_n{}^s$:Sine component of Fourier representation of nonlinear force element

$f_n{}^c$:Cosine component of Fourier representation of nonlinear force element

$\mathbf{f}_n$:Fourier representation of nonlinear force vector

s :Arc-length continuation parameter

$\boldsymbol{\sigma}(t)$:Perturbation element

$\mathbf{z}(t)$:Periodic term in perturbation element

$W(y,t)$:Displacement of beam

$\phi_i(y)$:i$^{\text{th}}$ mode shape

α :Mass coefficient in damping matrix

β :Stiffness coefficient in damping matrix

c_c :Cubic damping parameter

k_c : Cubic stiffness parameter

μN : Slip load

k_t : Contact Stiffness

CHAPTER 1

INTRODUCTION

Tuned Vibration Absorbers (TVA) are commonly used in reducing undesirable vibrations of mechanical structures. It generally consists of a mass, a spring and a damper which is attached to a structure. The aim is to reduce the dynamic response of the primary system at a certain frequency by tuning the frequency of the TVA to that frequency. It is especially useful when the inherent damping of the primary system is low.

There are many application areas. It is widely used in civil engineering to eliminate excessive response of towers. Similarly, it is used in bridges, wind turbine, etc. It is also used in electric cables, which is known as Stockbridge damper. Moreover, it is used in many mechanical systems to avoid excessive vibration response [1].

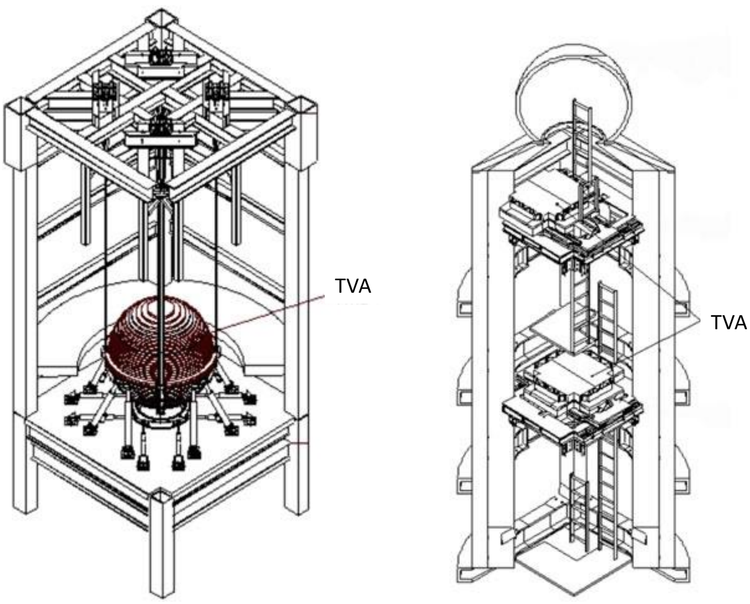

Figure 1.1. Schematic of the TMD systems installed in Taipei 101, Taiwan.

Retrieved from [1]

In literature, Tuned Vibration Absorber is also referred, Tuned Mass Damper, Dynamic Vibration Absorber ,and Frahm Damper. In this study, Tuned Vibration Absorber is used. Notice, Tuned Liquid Column Damper, which is a form of TVA with liquid columns, is not included in this study.

In this study, a base excited linear mechanical system connected to TVAs equipped with linear and nonlinear elements is considered. Single and multiple TVAs are optimized. By the use of multiple TVAs and nonlinear elements, it is aimed to suppress the vibrations of the structures in a broader frequency range.

At the beginning of the study, a literature review is presented in CHAPTER 2. Historical development and studies related to TVA for the undamped primary system are presented in the first paragraph. In second paragraph, studies related to TVA for the damped primary system are presented. In the third paragraph, the studies related to the use of multiple TVAs for single resonance are presented. In the fourth paragraph, the studies related to a continuous system coupled with TVAs are presented. In the fifth paragraph, first nonlinear TVA studies are presented. In the sixth paragraph, studies related to TVA with friction dampers are presented. Finally, in last paragraph, studies related to TVA with cubic stiffness are presented.

In CHAPTER 3, methods, used in this study is represented. This chapter divided 4 subchapters. In the first subchapter, Harmonic Balance Method is presented. In the second subchapter Newton Method with Arch-Length Continuation is represented. In the third subchapter, Hill's Method is presented. Lastly in the forth subchapter, Assumed Modes Method is presented.

In CHAPTER 4, the mathematical modeling of the systems is presented. It is divided into two subchapters, which are modeling in discrete and continuous system. The behavior of different TVA configurations are investigated in a discrete system. The nonlinear elements used in this study are cubic damping, cubic stiffness, dry friction damping, and their combinations. Also, the linear system is studied in this chapter.

In CHAPTER 5, results are presented. In this chapter, optimum values for different TVA configurations are presented. It is divided into two subchapters. In the first subchapter, optimum results for discrete systems are presented. In the second chapter, optimum results of TVA for continuous system is presented.

Finally, in the last chapter, CHAPTER 6, conclusion and future works are presented. Studies and important findings are summed in the conclusion. In future work subchapter, the subjects excluded in this study are discussed to further improve this study.

In the appendix, optimum results for different boundary conditions are presented. For clarity, they are not presented in CHAPTER 5.

CHAPTER 2

LITERATURE REVIEW

TVA like systems was first used by Watts [2] in 1883. In 1909, Frahm [3] patented the classic TVA, which was consisted of a mass and a spring. Ormondroyd and Den Hartog [4] carried out the first theoretical investigation on TVA. TVA without damping can reduce the response of the main system to almost zero at the previous resonance point under harmonic excitation. However the addition of TVA two new resonance near the tuned frequency. Therefore, it is useful for a single stationary frequency; however, excitation is rarely stationary in real applications. Viscous damper is considered to reduce vibration response in a broader band [5]. The study is that of a TVA with viscous damper attached an undamped SDOF system, which subjected to harmonic excitation. It had been noticed, frequency response curves of the main mass, which is plotted for different damping values pass through two invariant points. Optimization is performed by using these invariant points. The ratio of the natural frequencies of the TVA and the main system is altered until the response of the invariant points is equal. Respectively, damping of TVA is adjusted such that the slope of the frequency response curve at invariant points become zero. (See Figure 2.1). Researchers studied to obtain closed form solution for this optimization problem.

Real systems, however, contain damping and invariant points do not exist in the frequency response curve. Bapat and Kumaraswamy [6] investigated an optimization for the damped system. It has been noticed that fixed point optimization works for the slightly damped system. Toshihiro and Ikeda [7] obtained empirical formulae for the TVA parameters with the condition that damping is light. Randall, Halsted, and Taylor [8] presented computational graphs that determine the optimum values of TVA for the damped system. The represented solution offered much more accurate results than those achieved by classical methods.

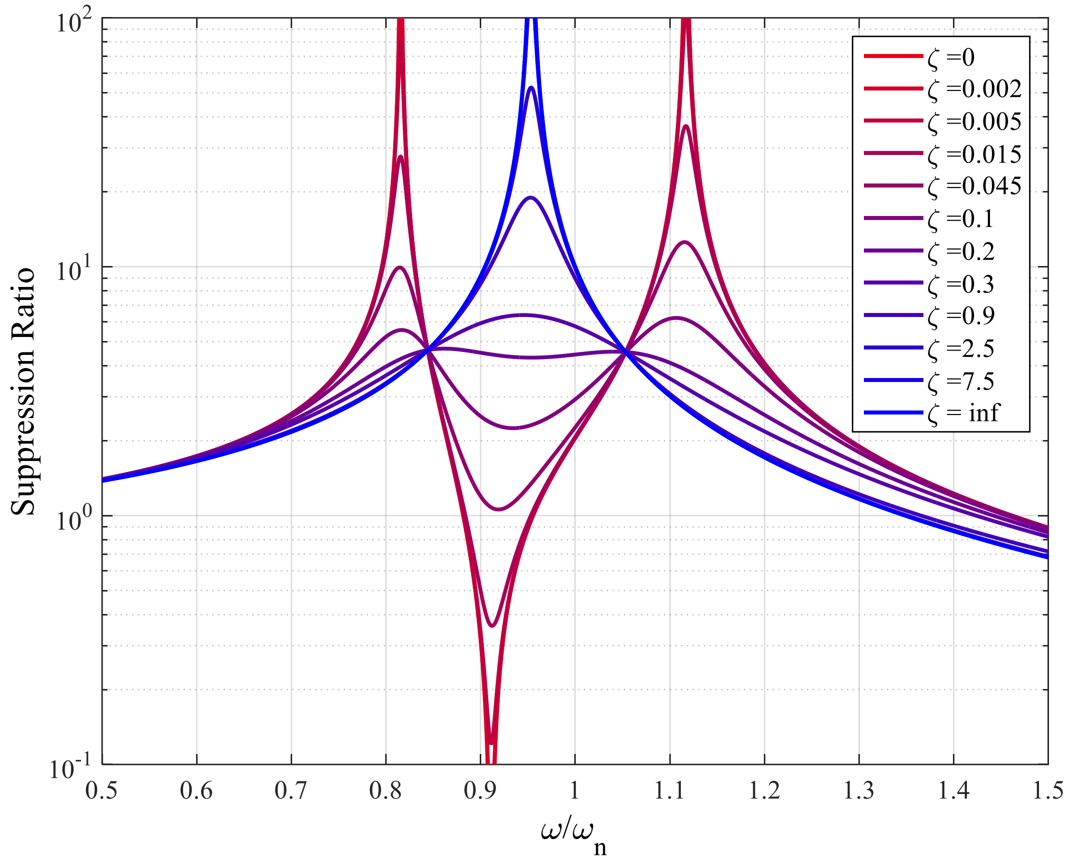

Figure 2.1. Invariant Points and Change in Damping Value

To improve effective bandwidth, multiple TVA is considered. In such cases, More than one TVAs are used to suppress a single resonance peak. Iwanami and Seto [9] investigated dual TVA. The study showed that dual TVA eliminates the drawback of single TVA, which is very sensitive to the variation of parameters. Moreover, it reduces transmissibility better in the resonance region. Igusa and Xu [10] showed that multiple TVA is more effective and robust than single TVA, which has equal total mass under harmonic excitation. Many researchers are still interested in multiple TVA.

The application absorber to a continuous system, which is more realistic and accurate, has been studied extensively. Young [11] made the first study on the application of TVA to the continuous system. Neubert [12] studied on axially excited beam with one or two TVAs in steady state. It was stated that second TVA has an advantage if TVAs are tuned for separated resonances. In addition, the effect of the location of the TVA was studied. Jaquot [13] studied on optimization of TVA for Euler-Bernoulli beam subjected to sinusoidal excitation. Assumed mode method for single mode approximation is used to establish the analogy between SDOF system and beam. Optimum TVA parameters is determined for the equivalent SDOF system by using the theory in earlier works. Warburton and Ayorinde [14] extended Jaquet's study for plates and cylindrical shells and improved the accuracy for beams. Özgüven and Çandır [15] studied on structurally damped beam with two TVA, which is subjected to harmonic excitation. TVAs were optimized to suppress first two resonance of the beam. It had been noted that optimization parameters for TVA tuned to second resonance are not affected the existence of the one tuned to first resonance. However, the opposite is not true. Esmailzadeh and Jalili [16] extended the theory for Timoshenko beams.

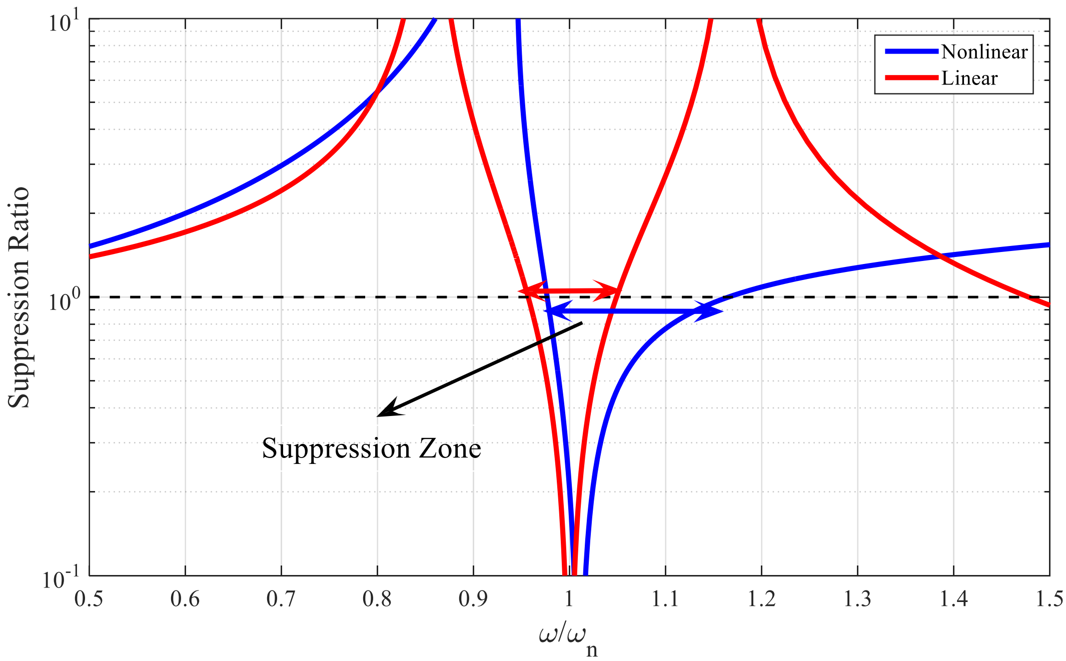

Figure 2.2. Suppression Zones with Linear and Nonlinear TVA

Although many researchers still interested in linear vibration absorber, there are many researches on nonlinear vibration absorber to further improve the effectiveness of

TVA. Roberson [17] introduced nonlinear TVA. The study focused on improving suppression bandwidth, which is the frequency bandwidth with amplitude less than unity. (See Figure 2.2) In the study, undamped TVA with linear and nonlinear spring was considered. Significant improvement is observed when comparing to the linear one. Hunt and Nissen [18] studied on damped nonlinear TVA. The research demonstrated that suppression band is twice as wide as which produced by a linear TVA. Natsiavas [19] studied on stability of the nonlinear system to avoid dangerous effects which are possible due to the presence of the nonlinearity.

Inaudi and Kelly [20] introduced TVA with friction dampers (FTVA). The system exhibits both linear and hysteretic behavior. Statistical linearization method had been used and optimum parameters were calculated for SDOF linear system. It is found out that, FTVA exhibits convenient behaviors, achieves the same level of performance that an optimized linear TVA would provide. The advantage of FTVA is its robustness to environmental temperature change. Ricciardelli and Vickery [21] used FTMD. They studied the response of a linear single DOF system, where FTMD is connected by using an equivalent linearized damping for single harmonic motion. They also obtained optimum slip parameters for harmonic excitation. Gewei and Basu [22] studied the response of a linear SDOF system with FTMD under both harmonic and random excitation. For harmonic excitation, harmonic balance method is used to obtain a periodic response. In the case of random excitation, statistical linearization method is used. Carmona, Avila and Dose [23] proposed an FTMD to control excessive floor vibration. Linearized friction model is used. Linearized FTMDs are attached to the floor. Analysis is carried out by using finite element method. They suggested and optimized multi FTMDs for certain load cases. Pisal and Jangid [24] studied on linear SDOF system with FTMD under both harmonic and earthquake excitation. They used state-space method to solve the system. Sinha and Trikutam [25] studied the optimization of a SDOF linear system with FTMD in steady state. They used harmonic balance method to solve the nonlinear system. Genetic algorithm with minimax approach is used for optimization.

Weakly nonlinear systems are not able to react effectively on a wide range of frequency because of its dependency on amplitude level. However, strongly nonlinear system reacts effectively on a broader frequency band. Systems with this consideration bring a new concept, which is Nonlinear Energy Sink (NES). This concept also covers grounded vibration absorber i.e. the nonlinear element is located between vibration absorber and ground. It has been noticed that nonlinear attachment exhibits irreversible transient energy transfer [26]-[27]. Jiang, McFarland, Bergman, and Vakakis [28] studied NES in steady state dynamics. Gendelman, Gourdon, and Lamarque [29] studied the effects of NES on the main system. They found out, system under periodic excitation exhibits quasiperiodic behavior around the main resonance of the system. Parseh, Morteza and, Ghasemi [30] studied steady state dynamics of linear Euler-Bernouli beam with NES under harmonic forcing. The nonlinear element in the NES is cubic stiffness. They stated that NES performs better than linear TVA if the forcing is the same or less than designed force. Linear TVA performs better if the forcing is above the design consideration. Gourc, Elce, Kercshen, Michon, Aridon, and Hot [31] studied on performance comparison of linear TVA and NES. They stated that properly tuned linear TVA outperforms NES. Moreover, they claim that in previous studies, which compares linear TVA and NES, designing procedure was not properly proposed

CHAPTER 3

METHODS

3.1. Harmonic Balance Method

Harmonic Balance Method (HBM) is used to calculate steady state response of nonlinear differential equations. In HBM, responses and nonlinear forces are represented in terms of Fourier series and substituted into nonlinear differential equations which results in a set of nonlinear algebraic equations.

The idea is, to express periodic solution in the form

$$x_j(\omega t) = x_j{}^0 + \sum_{p=1}^{N} x_j{}^{s,p} \sin(p\omega t) + x_j{}^{c,p} \cos(p\omega t) \tag{3.1}$$

Consider equation of motion of a nonlinear system under harmonic excitation

$$\mathbf{M}\ddot{\mathbf{x}}(t) + \left(\mathbf{C} + \frac{\mathbf{H}}{\omega}\right)\dot{\mathbf{x}}(t) + \mathbf{K}\mathbf{x}(t) + \mathbf{f}_{non}\left(\mathbf{x}(t)\right) = \mathbf{f}_{exc}(t) \tag{3.2}$$

$\mathbf{f}_{non}$ is nonlinear force vector. Elements in the nonlinear force vector can be expressed as

$$f_{non,j}(\theta) = f_{NL}\left(x_{rel}(\theta)\right) \tag{3.3}$$

Where f_{NL} is nonlinear transfer function, x_{rel} is the relative displacement between DOFs where nonlinear element is connected, and $\theta = \omega t$. Each element in the nonlinear force vector calculated by HBM individually. As a result, amplitude depended sine and cosine coefficients and bias term of the nonlinear internal forcing are obtained. Governing equations are shown in the Equation (3.4)

$$
\begin{aligned}
f_{n,j}{}^{0} &= \frac{1}{2}\int_{0}^{2\pi} f_{non,j}\left(\theta\right)d\theta \\
f_{n,j}{}^{s,p} &= \frac{1}{2}\int_{0}^{2\pi} f_{non,j}\left(\theta\right)\sin\left(p\theta\right)d\theta \\
f_{n,j}{}^{s,p} &= \frac{1}{2}\int_{0}^{2\pi} f_{non,j}\left(\theta\right)\cos\left(p\theta\right)d\theta
\end{aligned}
\tag{3.4}
$$

Equation (3.1) is substituted into Equation (3.2) and coefficients of the nonlinear force vector is obtained by Equation (3.4). As a result, nonlinear algebraic equation is obtained. N+1 algebraic equation is obtained for each DOF.

$$
\begin{bmatrix} \mathbf{K} & \mathbf{0} & \mathbf{0} \\ \mathbf{0} & -\omega^2\mathbf{M}+\mathbf{K} & -\mathbf{H}-\omega\mathbf{C} \\ \mathbf{0} & -\mathbf{H}-\omega\mathbf{C} & -\omega^2\mathbf{M}+\mathbf{K} \end{bmatrix}
\begin{Bmatrix} \mathbf{x}^0 \\ \mathbf{x}^s \\ \mathbf{x}^c \end{Bmatrix}
+ \begin{Bmatrix} \mathbf{f}_n{}^0 \\ \mathbf{f}_n{}^s \\ \mathbf{f}_n{}^c \end{Bmatrix}
= \begin{Bmatrix} \mathbf{0} \\ \mathbf{f}_{exc}{}^s \\ \mathbf{f}_{exc}{}^c \end{Bmatrix}
\tag{3.5}
$$

In this study, only first harmonics are considered. Bias term are not and higher harmonics are neglected. Therefore, Equation (3.5) reduced to

$$
\begin{bmatrix} -\omega^2\mathbf{M}+\mathbf{K} & -\mathbf{H}+\omega\mathbf{C} \\ \mathbf{H}+\omega\mathbf{C} & -\omega^2\mathbf{M}+\mathbf{K} \end{bmatrix}
\begin{Bmatrix} \mathbf{x}^s \\ \mathbf{x}^c \end{Bmatrix}
+ \begin{Bmatrix} \mathbf{f}_n{}^s \\ \mathbf{f}_n{}^c \end{Bmatrix}
= \begin{Bmatrix} \mathbf{f}_{exc}{}^s \\ \mathbf{f}_{exc}{}^c \end{Bmatrix}
\tag{3.6}
$$

Details can be found in [32].

3.2. Newton’s Method with Arc-Length Continuation Method

In order to solve nonlinear algebraic Equation (3.5), a residual vector is defined as follow

$$
\mathbf{r}\left(\mathbf{X},\omega\right) = \begin{bmatrix} -\omega^2\mathbf{M}+\mathbf{K} & -\mathbf{H}+\omega\mathbf{C} \\ \mathbf{H}+\omega\mathbf{C} & -\omega^2\mathbf{M}+\mathbf{K} \end{bmatrix}\mathbf{x} + \mathbf{f}_n - \mathbf{f}_{exc} = 0
\tag{3.7}
$$

Due to the presence of the nonlinearity, a turning point may have appeared. In order to overcome this situation, the new continuation parameter is defined. The arc-length parameter is the radius of an n-dimensional sphere, which is centered at the previous solution points (Figure 3.1). The new solution points are searched on the surface of the sphere. The equation for n-dimensional sphere with radius s and located at the previous solution point is

$$\{\mathbf{q}_k - \mathbf{q}_{k-1}\}^T \{\mathbf{q}_k - \mathbf{q}_{k-1}\} = s^2 \tag{3.8}$$

where s is the arch length parameter, k-1 is the previous solution points and k is the current solution points. With the addition of this new equation, the new vector of unknown becomes as follows

$$\mathbf{q} = \begin{Bmatrix} \mathbf{x} \\ \omega \end{Bmatrix} \tag{3.9}$$

New equation is obtained

$$h(\mathbf{x},\omega) = \{\mathbf{q}_k - \mathbf{q}_{k-1}\}^T \{\mathbf{q}_k - \mathbf{q}_{k-1}\} - s^2 = 0 \tag{3.10}$$

A single step of Newton's Methods becomes

$$\mathbf{q}_k^{\ i+1} = \mathbf{q}_k^{\ i} - \begin{bmatrix} \dfrac{\partial \mathbf{r}}{\partial \mathbf{x}} & \dfrac{\partial \mathbf{r}}{\partial \omega} \\ \dfrac{\partial h}{\partial \mathbf{x}} & \dfrac{\partial h}{\partial \omega} \end{bmatrix}_{\mathbf{x}_i \& \omega_i} \begin{Bmatrix} \mathbf{r}(\mathbf{x}_i, \omega_i) \\ h(\mathbf{x}_i, \omega_i) \end{Bmatrix} \tag{3.11}$$

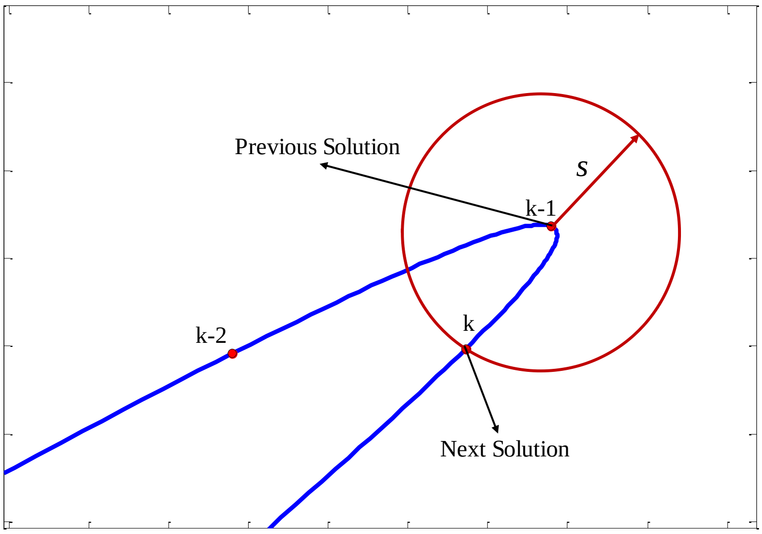

Figure 3.1. Arc-Length Continuation Method

Details can be found in [33].

3.3. Hill's Method

Arc-Length continuation algorithm provides the solution points on a solution branch. It does not give information about the stability of the solution points. Due to the presence of the nonlinearity, the stability problem may have occurred. Stability analysis in the frequency domain can be performed with a Hill's Method. Stability analysis is carried out by investigating the effect of a perturbation around a periodic solution. Perturbation is described as

$$\boldsymbol{\sigma}(t) = e^{\lambda t}\mathbf{z}(t) \tag{3.12}$$

Where $e^{\lambda t}$ is decay term, and $\mathbf{z}(t)$ is periodic term i.e:

$$\mathbf{z}(t) = \sum_{p=-N}^{N} \mathbf{z}_p e^{ip\omega t} \tag{3.13}$$

New solution is written

$$\mathbf{x}(t) = \tilde{\mathbf{x}}(t) + \boldsymbol{\sigma}(t) \tag{3.14}$$

Where $\tilde{\mathbf{x}}(t)$ known solution. Substitute Equation (3.14) to Equation (3.2)

$$\mathbf{M}\ddot{\tilde{\mathbf{x}}}(t) + \left(\mathbf{C} + \frac{\mathbf{H}}{\omega}\right)\dot{\tilde{\mathbf{x}}}(t) + \mathbf{K}\tilde{\mathbf{x}} + \boldsymbol{\psi}e^{\lambda t} + \mathbf{f}_{non}\left(\mathbf{x}(t)\right) - \mathbf{f}_{exc}(t) = 0 \tag{3.15}$$

Where

$$\boldsymbol{\psi} = \mathbf{M}\ddot{\mathbf{z}}(t) + \left(2\mathbf{M}\lambda^2 + \mathbf{C} + \frac{\mathbf{H}}{\omega}\right)\dot{\mathbf{z}}(t) + \left(\mathbf{K} + \lambda^2\left(\mathbf{M} + \mathbf{C} + \frac{\mathbf{H}}{\omega}\right)\right)\mathbf{z}(t) \tag{3.16}$$

Fourier representations of the solution terms is substituted into the Equation (3.15). Notice that, only first harmonics are considered in this study. Thus, Fourier representation of solution is:

$$\begin{aligned}\tilde{\mathbf{x}}(t) &= \tilde{\mathbf{x}}^s \sin(\omega t) + \tilde{\mathbf{x}}^c \cos(\omega t)\\ \boldsymbol{\sigma}(t) &= \left(\mathbf{z}^s \sin(\omega t) + \mathbf{z}^c \cos(\omega t)\right) e^{\lambda t}\end{aligned} \tag{3.17}$$

Substitute Equation (3.17) into Equation (3.15), we obtain

$$\boldsymbol{\Delta}_1 \tilde{\mathbf{x}} + \left(\lambda^2 \boldsymbol{\Delta}_2 + \lambda \boldsymbol{\Delta}_3 + \boldsymbol{\Delta}_1\right) \mathbf{z} e^{\lambda t} + \mathbf{f}_n\left(\tilde{\mathbf{x}} + \mathbf{z} e^{\lambda t}\right) - \mathbf{f}_{exc} = \mathbf{0} \tag{3.18}$$

Where

$$\boldsymbol{\Delta}_1 = \begin{bmatrix} -\mathbf{M}\omega^2 & -\omega\mathbf{C} - \mathbf{H} \\ \omega\mathbf{C} + \mathbf{H} & -\mathbf{M}\omega^2 \end{bmatrix} \quad , \quad \boldsymbol{\Delta}_2 = \begin{bmatrix} \mathbf{M} & \mathbf{I} \\ \mathbf{I} & \mathbf{M} \end{bmatrix} \quad , \quad \boldsymbol{\Delta}_3 = \begin{bmatrix} \mathbf{C} + \dfrac{\mathbf{H}}{\omega} & 2\omega\mathbf{M} \\ \mathbf{M} & \mathbf{C} + \dfrac{\mathbf{H}}{\omega} \end{bmatrix} \tag{3.19}$$

Nonlinear term in Equation (3.15) can be written around known solution point $\tilde{\mathbf{x}}(t)$ by Taylor series of expansion.

$$\mathbf{f}_n(\mathbf{x}) = \mathbf{f}_n(\tilde{\mathbf{x}}) + \left.\frac{\partial \mathbf{f}_n}{\partial \mathbf{x}}\right|_{\mathbf{x}=\tilde{\mathbf{x}}} \mathbf{z} e^{\lambda t} \tag{3.20}$$

Substitute Equation (3.20) into Equation (3.18),

$$\boldsymbol{\Delta}_1 \tilde{\mathbf{x}} + \mathbf{f}_n(\tilde{\mathbf{x}}) - \mathbf{f}_{exc} + \left(\boldsymbol{\Delta}_2 \lambda^2 + \boldsymbol{\Delta}_3 \lambda + \boldsymbol{\Delta}_1 + \left.\frac{\partial \mathbf{f}_n}{\partial \mathbf{x}}\right|_{\mathbf{x}=\tilde{\mathbf{x}}}\right) \mathbf{z} e^{\lambda t} = 0 \tag{3.21}$$

Notice that $\boldsymbol{\Delta}_1 \tilde{\mathbf{x}} + \mathbf{f}_n(\tilde{\mathbf{x}}) - \mathbf{f}_{exc}$ is zero by the definition in Equation (3.21). In addition, Jacobian matrix is defined

$$\mathbf{J} = \frac{\partial \mathbf{r}}{\partial \mathbf{x}} = \boldsymbol{\Delta}_1 + \frac{\partial \mathbf{f}_n}{\partial \mathbf{x}} \tag{3.22}$$

Quadratic eigenvalue problem is obtained by substituting Equation (3.22) into Equation (3.32), which is

$$\mathbf{\Delta}_2\lambda^2 + \mathbf{\Delta}_3\lambda + \mathbf{J} = \mathbf{0} \tag{3.23}$$

Equation (3.23) can be rewritten in state space form. Linear eigenvalue problem is obtained.

$$\mathbf{\Delta}_2\ddot{\mathbf{v}} + \mathbf{\Delta}_3\dot{\mathbf{v}} + \mathbf{J}\mathbf{v} = \mathbf{0} \tag{3.24}$$

Where $\boldsymbol{\tau} = \begin{Bmatrix} \boldsymbol{\tau}_1 \\ \boldsymbol{\tau}_2 \end{Bmatrix} = \begin{Bmatrix} \dot{\mathbf{v}} \\ \mathbf{v} \end{Bmatrix}$, and $\mathbf{v} = e^{\lambda}$ which is defined as

$$\begin{aligned} \mathbf{\Delta}_2 \frac{\partial \boldsymbol{\tau}_1}{\partial t} &= -\mathbf{\Delta}_1\boldsymbol{\tau}_1 - \mathbf{J}\boldsymbol{\tau}_2 \\ \frac{\partial \boldsymbol{\tau}_2}{\partial t} &= \boldsymbol{\tau}_1 \end{aligned} \tag{3.25}$$

Equation (3.24) can be rewritten as

$$\begin{bmatrix} \mathbf{\Delta}_2 & \mathbf{0} \\ \mathbf{0} & \mathbf{I} \end{bmatrix} \dot{\boldsymbol{\tau}} + \begin{bmatrix} \mathbf{\Delta}_3 & \mathbf{J} \\ -\mathbf{I} & \mathbf{0} \end{bmatrix} \boldsymbol{\tau} = \mathbf{0} \tag{3.26}$$

This will give 4N eigenvalues for single harmonic solution. Only 2N eigenvalues are valid solutions. Others have physically no meaning. For stability analysis, eigenvalues with the smallest imaginary part in modulus are considered. For the solution points where eigenvalues are greater than zero, it is unstable [34]. Details related to method can be found in [35].

As an example, two DOF system with cubic stiffness is investigated. Stability behavior is well known in the literature. Solid linear denotes stable solution, dotted lines denotes for unstable solution in Figure 3.2.

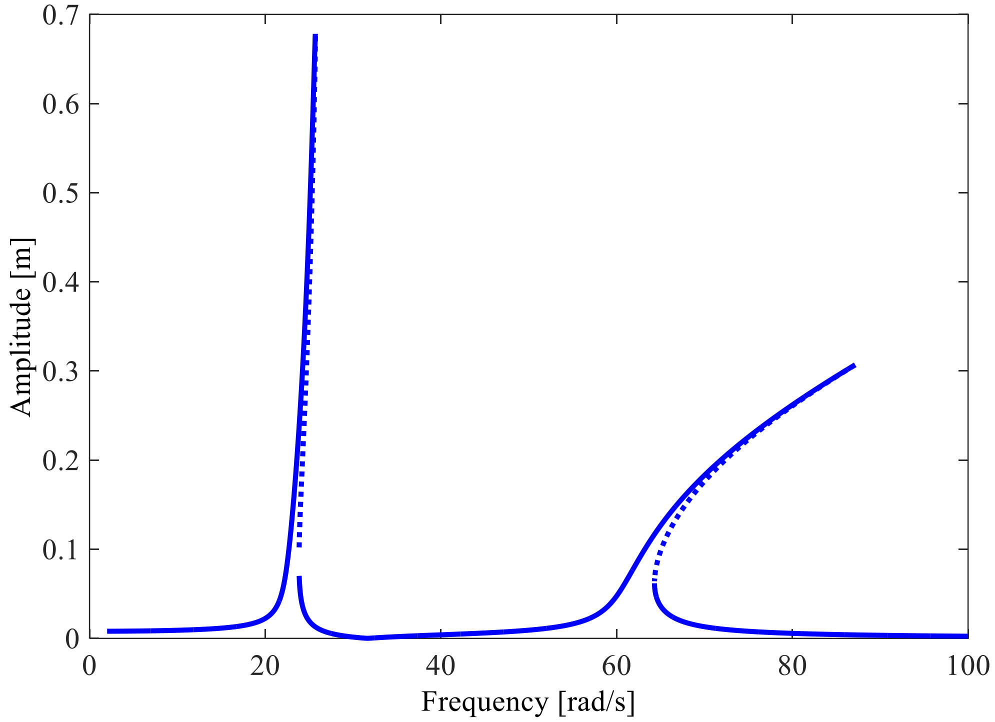

Figure 3.2. Stability of the Solution

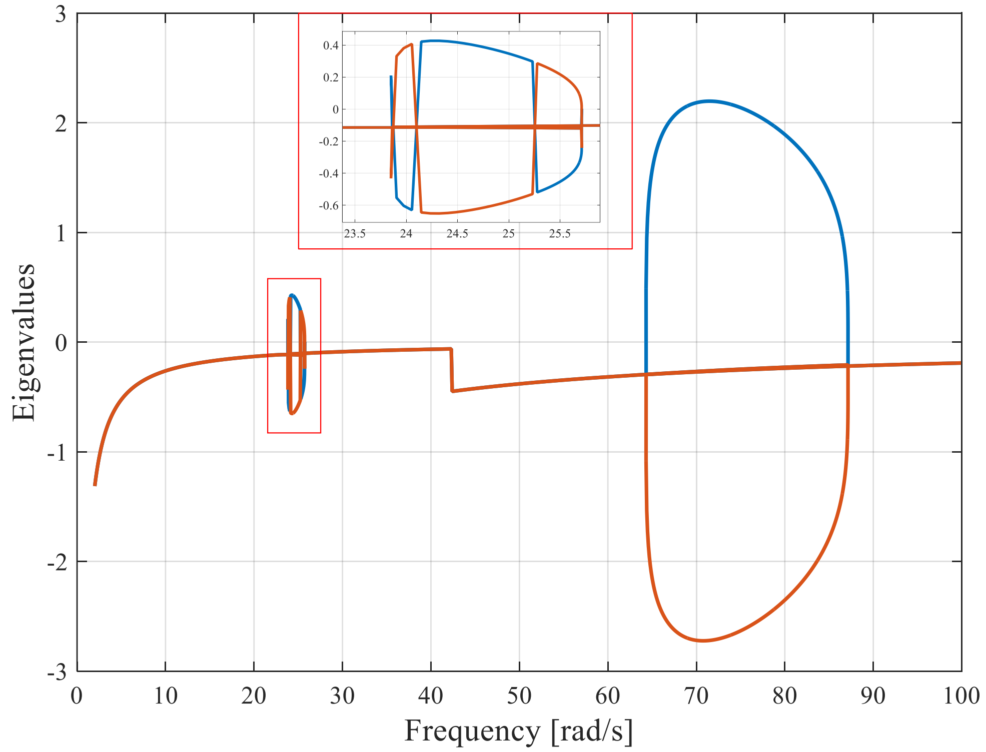

Figure 3.3. Real Part of Eigenvalues for Frequency Response

3.4. Assumed Modes Method

Exact solution of many continuous systems is sometimes difficult. In such cases, approximate analytical methods are useful. For must system, only the first few natural frequencies and natural mode have importance for the dynamic response. Contribution of the higher modes are negligible.

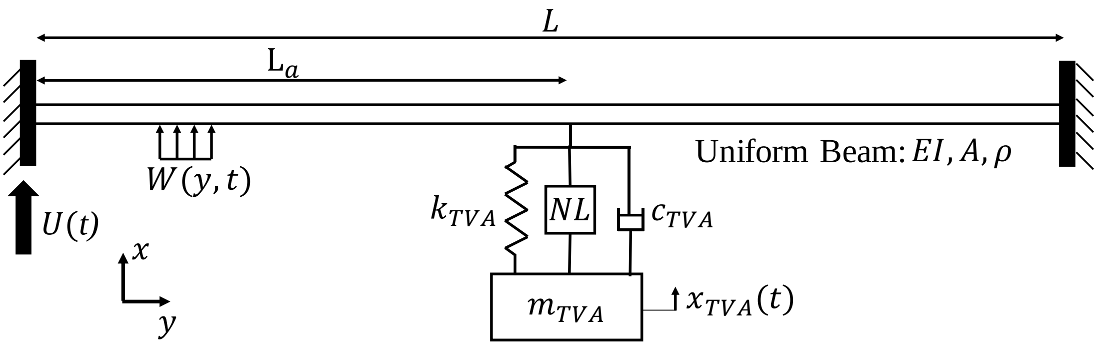

Figure 3.4 Linear Euler-Bernoulli Beam with Nonlinear TVA

Displacement of the beam (Fig. 3.3) is assumed as

$$w(y,t) = \sum_{i=1}^{n} \phi_i(y) x_i(t) \tag{3.27}$$

Where, $\phi_i(y)$ is the known trial functions that satisfy boundary conditions and, $x_i(t)$ is the unknown function of time. The beam is subjected to base excitation, $U(t)$. There is a concentrated mass connected to beam with elastic and nonlinear element, which is TVA. Beam with uniform cross-section is used. EI is the modulus of rigidity, A is cross-section of the beam and ρ the density of the beam. NL is the nonlinear element between TVA and beam. k_{TVA} and c_{TVA} the spring and damping coefficients respectively.

Energy equations of the beam is

$$
\begin{aligned}
V &= \frac{1}{2} EI \int_0^L \left(\frac{\partial^2 w(y,t)}{\partial y^2} \right)^2 dy + \frac{1}{2} k_{TVA} \left(x_{rel}(t) \right)^2 + \int F_{NL} \left(x_{rel}(t) \right) \\
T &= \frac{1}{2} EI \int_0^L \left(\frac{\partial w(y,t)}{\partial t} + U(t) \right)^2 dy + \frac{1}{2} m_{TVA} \left(\frac{\partial x_{TVA}}{\partial t} \right)^2 \\
D &= \frac{1}{2} c_{TVA} \left(\frac{\partial x_{rel}}{\partial t} \right)^2
\end{aligned}
\tag{3.28}
$$

Where $x_{rel}(t) = U(t) + w(L_a, t) - x_{TVA}(t)$ i.e. relative displacement between TVA and point of the beam where TVA is connected. Nonlinear forces are added to the potential energy equation.

In addition, inherent damping of the beam is considered. Rayleigh damping [1] is used to obtained inherent damping matrix of the beam. Mass and stiffness matrix of the beam without TVA is obtained ($\mathbf{M}_{Beam}$ & $\mathbf{K}_{Beam}$). Natural frequencies of the beam are obtained. Damping ratios are settled for selected natural frequencies. Rayleigh coefficients are obtained for those frequencies. The formula for Rayleigh coefficients are:

$$
\begin{Bmatrix} \alpha \\ \beta \end{Bmatrix} = \frac{2\omega_i \omega_j}{\omega_j^{\ 2} - \omega_i^{\ 2}} \begin{bmatrix} \omega_j & -\omega_i \\ \dfrac{1}{\omega_j} & \dfrac{1}{\omega_i} \end{bmatrix} \begin{Bmatrix} \xi_i \\ \xi_j \end{Bmatrix} \tag{3.29}
$$

For this study, only first five mode taken into consideration. Displacement vector becomes

$$
\mathbf{x} = \begin{Bmatrix} x_1 & x_2 & x_3 & x_4 & x_5 & x_{TVA} \end{Bmatrix}^T \tag{3.30}
$$

Mode shapes of the linear Euler Bernoulli Beam is used for trial functions. To obtain equation of motion of the system, Lagrange equation is used.

$$\frac{\partial}{\partial t}\left(\frac{\partial T}{\partial \dot{x}_i}\right)-\frac{\partial T}{\partial x_i}+\frac{\partial V}{\partial x_i}+\frac{\partial D}{\partial \dot{x}_i} \tag{3.31}$$

System matrix are obtained by substituting Equation (3.28) into Equation (3.31)

System matrixes are

$$\mathbf{M}=\begin{bmatrix} m_{11} & m_{12} & m_{13} & m_{14} & m_{15} & 0 \\ m_{12} & m_{22} & m_{23} & m_{24} & m_{25} & 0 \\ m_{13} & m_{23} & m_{33} & m_{34} & m_{35} & 0 \\ m_{14} & m_{24} & m_{34} & m_{44} & m_{45} & 0 \\ m_{15} & m_{25} & m_{35} & m_{45} & m_{55} & 0 \\ 0 & 0 & 0 & 0 & 0 & m_{TVA} \end{bmatrix} \tag{3.32}$$

Where

$$m_{ij}=\rho A\int_0^L \phi_i(y)\phi_j(y)\,dy \tag{3.33}$$

$$\mathbf{K}=\begin{bmatrix} k_{11} & k_{12} & k_{13} & k_{14} & k_{15} & k_{66} \\ k_{12} & k_{22} & k_{23} & k_{24} & k_{25} & k_{26} \\ k_{13} & k_{23} & k_{33} & k_{34} & k_{35} & k_{36} \\ k_{14} & k_{24} & k_{34} & k_{44} & k_{45} & k_{46} \\ k_{15} & k_{25} & k_{35} & k_{45} & k_{55} & k_{56} \\ k_{16} & k_{26} & k_{36} & k_{46} & k_{56} & k_{TVA} \end{bmatrix} \tag{3.34}$$

Where

$$\begin{aligned} k_{ij} &= EI\int_0^L \frac{\partial^2\phi_i(y)}{\partial y^2}\frac{\partial^2\phi_j(y)}{\partial y^2}dy+k_{TVA}\phi_j(L_a)\phi_j(L_a) \quad &&\text{if} \quad i\,\&\,j<6 \\ k_{i6} &= -k_{TVA}\phi_i(L_a) &&\text{if} \quad i\le 6 \end{aligned} \tag{3.35}$$

$$\mathbf{C}=\begin{bmatrix} c_{11} & c_{12} & c_{13} & c_{14} & c_{15} & c_{66} \\ c_{12} & c_{22} & c_{23} & c_{24} & c_{25} & c_{26} \\ c_{13} & c_{23} & c_{33} & c_{34} & c_{35} & c_{36} \\ c_{14} & c_{24} & c_{34} & c_{44} & c_{45} & c_{46} \\ c_{15} & c_{25} & c_{35} & c_{45} & c_{55} & c_{56} \\ c_{16} & c_{26} & c_{36} & c_{46} & c_{56} & c_{TVA} \end{bmatrix}+\alpha\begin{bmatrix} \mathbf{M}_{Beam} & \mathbf{0} \\ \mathbf{0} & \mathbf{0} \end{bmatrix}+\beta\begin{bmatrix} \mathbf{K}_{Beam} & \mathbf{0} \\ \mathbf{0} & \mathbf{0} \end{bmatrix} \tag{3.36}$$

Where

$$\begin{aligned} c_{ij} &= c_{TVA}\phi_i\left(L_a\right)\phi_j\left(L_a\right) \quad \text{if} \quad i\,\&\,j<6 \\ c_{i6} &= c_{TVA}\phi_i\left(L_a\right) \qquad\qquad \text{if} \quad i\le 6 \end{aligned} \tag{3.37}$$

Due to orthogonality relation, i.e.

$$\begin{aligned} &\int_0^L \phi_i\left(y\right)\phi_j\left(y\right)dy=0 \quad \text{if} \quad i\neq j \\ &\int_0^L \phi_i\left(y\right)\phi_j\left(y\right)dy\neq 0 \quad \text{if} \quad i=j \end{aligned} \tag{3.38}$$

Equation (3.38) are used to reduce system matrixes. Equation (3.32) and Equation (3.33) are reduced to

$$\mathbf{M}=\operatorname{diag}\left(\left\{m_1 \quad m_2 \quad m_3 \quad m_4 \quad m_5 \quad m_{TVA}\right\}\right) \tag{3.39}$$

Where

$$m_i=\rho A\int_0^L \phi_i^2 dy=0 \quad \text{if} \quad i<6 \tag{3.40}$$

Similarly, Equation (3.35) reduced to

$$
\begin{aligned}
k_{ij} &= \int_0^L \left(\frac{\partial^2 \phi_i(y)}{\partial y^2} \right) dy + k_{TVA}\phi_i^2(L_a) \quad \text{if} \quad i = j \quad \& \quad i < 6 \\
k_{ij} &= k_{TVA}\phi_i(L_a)\phi_j(L_a) \quad \text{if} \quad i \neq j \quad \& \quad i, j < 6 \\
k_{ij} &= -k_{TVA}\phi_i(L_a) \quad \text{if} \quad j = 6 \quad \& \quad i < 6
\end{aligned}
\tag{3.41}
$$

Equation (3.37) is reduced to

$$
\begin{aligned}
c_{ij} &= c_{TVA}\phi_i^2(L_a) \quad \text{if} \quad i = j \quad \& \quad i < 6 \\
c_{ij} &= c_{TVA}\phi_i(L_a)\phi_j(L_a) \quad \text{if} \quad i \neq j \quad \& \quad i, j < 6 \\
c_{ij} &= -c_{TVA}\phi_i(L_a) \quad \text{if} \quad j = 6 \quad \& \quad i < 6
\end{aligned}
\tag{3.42}
$$

Similarly, input vectors are obtained. Component comes from kinetic energy equation is

$$
\mathbf{f}^M = \left\{ f_1^M \quad f_2^M \quad f_3^M \quad f_4^M \quad f_5^M \quad 0 \right\}^T \tag{3.43}
$$

Where

$$
f_i^M = \rho A \int_0^L \phi_i(y)\, dy \quad \text{if} \quad i < 6 \tag{3.44}
$$

Component comes from energy loss equations is

$$
\mathbf{f}^C = \left\{ f_1^C \quad f_2^C \quad f_3^C \quad f_4^C \quad f_5^C \quad -c_{TVA} \right\}^T \tag{3.45}
$$

Where

$$
f_i^C = c_{TVA}\phi_i(L_a) \quad \text{if} \quad i < 6 \tag{3.46}
$$

Component comes from potential energy equations is

$$\mathbf{f}^K = \left\{ f_1^K \quad f_2^K \quad f_3^K \quad f_4^K \quad f_5^K \quad -k_{TVA} \right\}^T \tag{3.47}$$

Where

$$f_i^K = k_{TVA}\phi_i\left(L_a\right) \quad \text{if} \quad i < 6 \tag{3.48}$$

Nonlinear part is obtained

$$\mathbf{f}_{non}\left(\mathbf{x}(t), u(t)\right) = F_{NL}\left(\mathbf{x}_{rel}(t)\right)\begin{Bmatrix} \phi_1\left(L_a\right) \\ \phi_2\left(L_a\right) \\ \phi_3\left(L_a\right) \\ \phi_4\left(L_a\right) \\ \phi_5\left(L_a\right) \\ -1 \end{Bmatrix} \tag{3.49}$$

Equation of motion is obtained by combining Equation (3.32), (3.34), (3.36), (3.43), (3,45), (3,47) and (3,49).

$$\mathbf{M}\ddot{\mathbf{x}}(t) + \mathbf{C}\dot{\mathbf{x}}(t) + \mathbf{K}\mathbf{x}(t) + \mathbf{f}_{non}\left(\mathbf{x}_{rel}(t)\right) = \mathbf{f}_{exc}(t) \tag{3.50}$$

Where

$$\mathbf{f}_{exc}(t) = \mathbf{f}^M\ddot{U}(t) + \mathbf{f}^C\dot{U}(t) + \mathbf{f}^K U(t) \tag{3.51}$$

Linear results is compared with FEM Software, ANSYS. Plane stress (2D) elements are used. Parameters are

$$\begin{array}{llll} L = 0.250\,m & L_a = 0.125\,m & \rho = 7850\,kg/m^3 & A = 10^{-4}\,m^2 \\ EI = 41.67\,Nm^2 & k_{TVA} = 10^5\,N/m & m_{TVA} = 0.05\,kg & \end{array}$$

Fixed-Fixed boundary conditions are applied. Trial function is

$$\phi_i(y) = \cos\left(\beta_i y\right) - \cosh\left(\beta_i y\right) - Q_i\left(\sin\left(\beta_i y\right) - \sinh\left(\beta_i y\right)\right) \tag{3.52}$$

Where

$$Q_i = \frac{\cos(\beta_i L) - \cosh(\beta_i L)}{\sin(\beta_i L) - \sinh(\beta_i L)} \tag{3.53}$$

Notice that, each mode has different β_i value. β_i can be found

$$\cos(\beta_i L)\cosh(\beta_i L) - 1 = 0 \tag{3.54}$$

Equation (3.54) is nonlinear algebraic equation. β_i values can be obtained numerically. For initial value, $\beta_i L = (2i+1)\pi/2$ can be used. Accurate values for β_i are obtained by using Newton method. These values are substituted into Equation (3.45). Resulting mode shapes are substituted into Equation (3.44).

Modal analysis is performed and natural frequency results are compared.

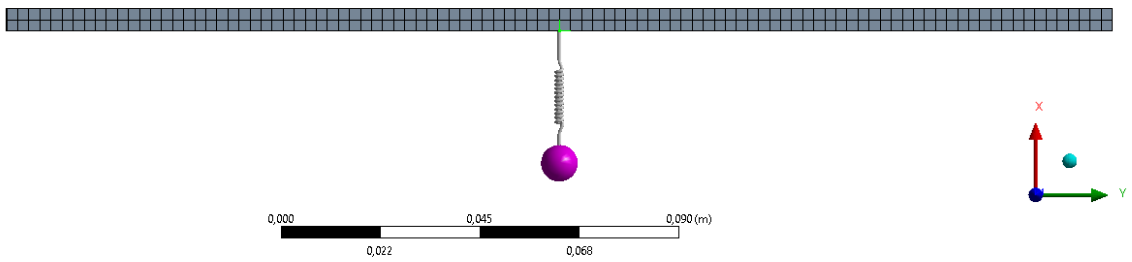

Figure 3.5 FEM Model

Table 3.1. Natural Frequency Comparison

	Analytical	**ANSYS**	**Error (%)**
1^{st} Mode	201.1 Hz	201.2 Hz	0.07
2^{nd} Mode	463.2 Hz	463.3 Hz	0.01
3^{rd} Mode	1144.2 Hz	1136.2 Hz	0.70
4^{th} Mode	2248.8 Hz	2235.1 Hz	0.61
5^{th} Mode	3707.9 Hz	3630.0 Hz	2.10
6^{Th} Mode	5547.7 Hz	5436.4 Hz	2.01

7^{th} Mode	-	7296.8 Hz	-

Details related to assumed mode method can be found in [35].

CHAPTER 4

MATHEMATICAL MODELLING

4.1. Discrete System

In this chapter, discrete linear system TVA utilized with linear and nonlinear elements is investigated. First, system with one TVA will be studied. The effects the change of the TVA parameters will be observed. After having a general idea about the effect of the linear and nonlinear elements, and then it is extended for double TVA

4.1.1. Single TVA

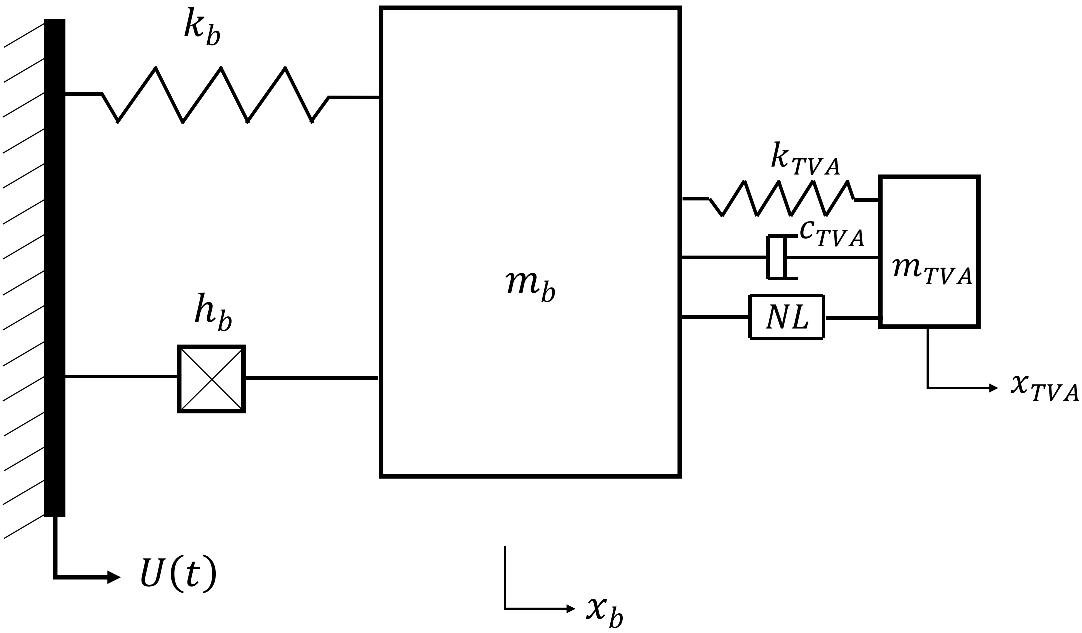

Figure 4.1. Linear SDOF System with TVAs

TVAs equipped with linear and nonlinear elements is as shown in**Error! Reference source not found.** Figure 4.1. Where m_b is the mass of the main system. m_{TVA} is the mass of the TVA, k_b and k_{TVA} are linear springs h_b is structural damping elements,

c_{TVA} is viscous damping elements. NL is the nonlinear element. As a result, two DOF system is obtained. Several nonlinear elements will be investigated separately, and their combination. In addition to nonlinear elements, linear TVAs are also investigated for reference value.

Equation of motion of the general system is

$$\begin{aligned} &m_b \ddot{x}_b + \frac{h}{\omega}\dot{x}_b + k_b x_b + c_{TVA}\dot{x}_{rel} + k_{TVA}x_{rel} + f_{non}\left(x_{rel}\right) = \frac{h}{\omega}\dot{U} + k_b U \\ &m_{TVA}\ddot{x}_{TVA} - c_{TVA}\dot{x}_{rel} - k_{TVA}x_{rel} - f_{non}\left(x_{rel}\right) = 0 \end{aligned} \tag{4.1}$$

Where $x_{rel} = x_b - x_{TVA}$ Also mass of the TVA is selected as ten percent of the main mass, i.e $m_{TVA} = m_b/10$ Loss factor for the main system is taken as one percent.

Linear and nonlinear elements will be studied in individual chapters.

4.1.1.1. Linear System

In linear system, nonlinear elements are vanished. All free parameters are viscous damping and the linear spring of the TVA. For better understanding, Equation (4.1) is nondimensionalized.

$$\begin{aligned} &\ddot{x}_b + \omega_b{}^2\left(1+i\gamma\right)x_b + 2\in\xi\omega_{TVA}\dot{x}_{rel} + \in\omega^2{}_{TVA}x_{rel} = f_{exc} \\ &\ddot{x}_{TVA} - 2\xi\omega_{TVA}\dot{x}_{rel} - \omega^2{}_{TVA}x_{rel} = 0 \end{aligned} \tag{4.2}$$

Where

$$\begin{aligned} &\in = \frac{m_{TVA}}{m_b} = 0.1 \qquad \gamma = 0.01 \qquad \omega_b{}^2 = \frac{k_b}{m_b} \\ &\omega_{TVA}{}^2 = \frac{k_{TVA}}{m_{TVA}} \qquad \xi = \frac{c_{TVA}}{2\sqrt{m_{TVA}k_{TVA}}} \qquad f_{exc} = U\left(1+i\gamma\right)\omega_b{}^2 \end{aligned} \tag{4.3}$$

Mass ratio, loss factor and excitation is specified. Only free parameters is natural frequency and the damping ratio of the TVA.

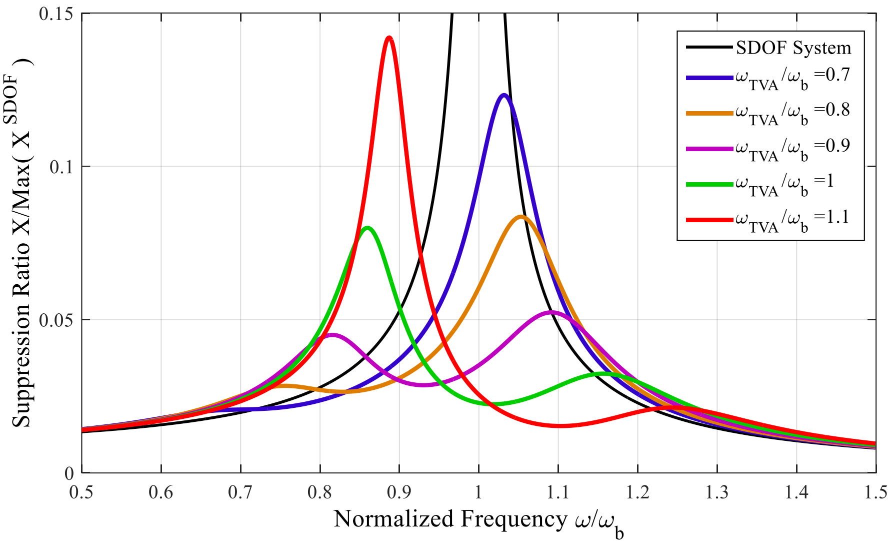

Figure 4.2. The Effect of TVA's Natural Frequency

Damping Ratio, $\xi = 0.11$

As it is seen from Figure 4.2, optimum natural frequency ratio is around 0.9. This values will be used later in optimization.

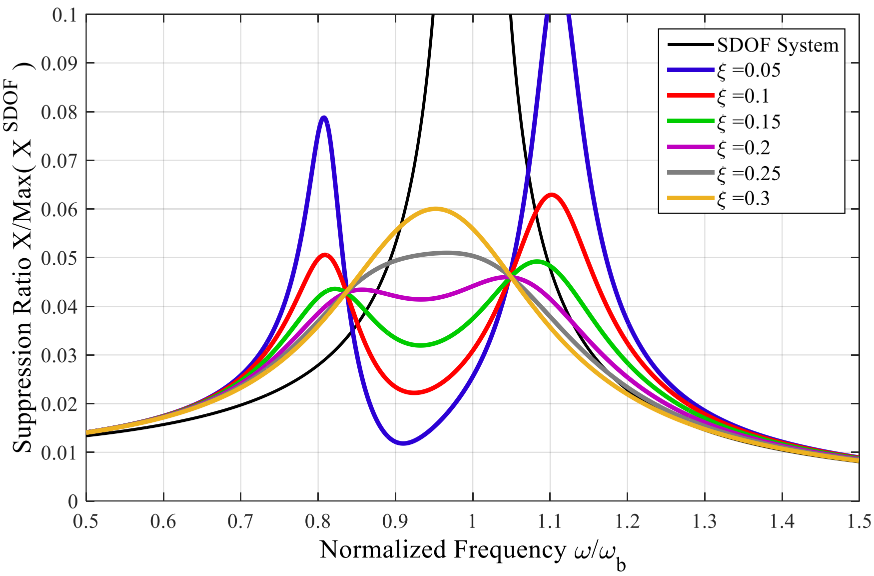

Figure 4.3. Effect of TVA's Damping Ratio

The ratio of the natural frequencies, $\omega_{TVA}/\omega_b = 0.9$

Optimum damping ratio is around 0.2. This value will be used in optimization later.

For low damping values, response at the previous resonance is low but two new resonance points are introduced nearby. For high damping values, system behaves like SDOF system.

Also, notice that, there is no *invariant point* in Figure 4.3 because the main system contains damping.

4.1.1.2. System with Cubic Damping

Cubic damping is a nonlinear force, which is proportional to third power of the relative velocity. To understand effect of the cubic damping, linear damping is vanished from Equation (4.1). Nonlinear Force is expressed as

$$f_{NL}\left(x_{rel}\right) = c_c \left(\frac{\partial x_{rel}}{\partial t}\right)^3 \tag{4.4}$$

Graphical demonstration is given in *Figure 4.4*

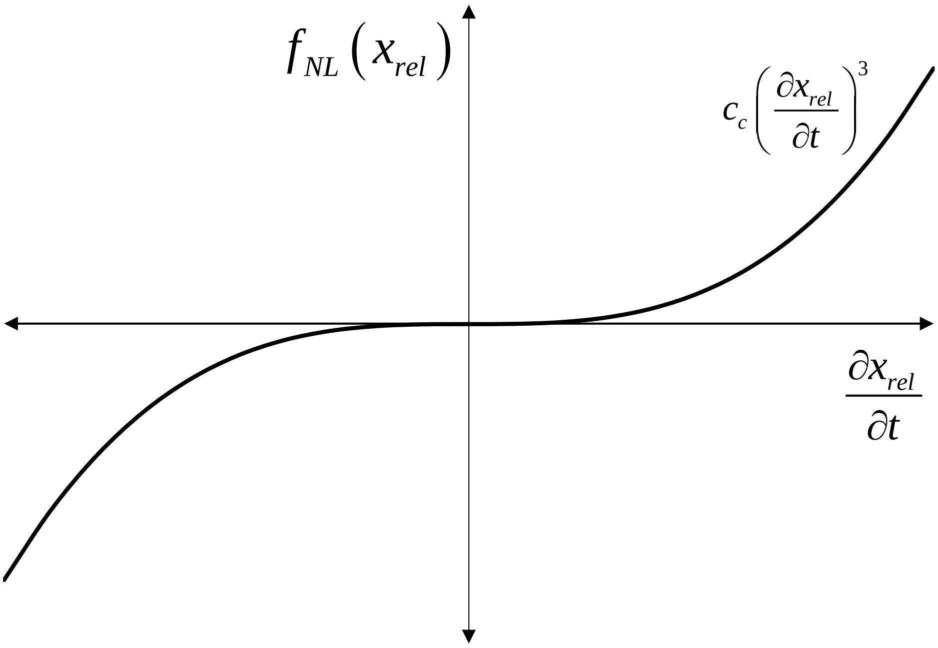

Figure 4.4 Graphical Demonstration of Cubic Damping

Equation (4.1) is rearraged to obtain generic form

$$\begin{aligned}&\ddot{x}_b + \omega_b^{\ 2}\left(1+i\gamma\right)x_b + \in \xi_c \dot{x}_{rel}^3 + \in \omega^2{}_{TVA} x_{rel} = f_{exc}\\&\ddot{x}_{TVA} - \xi_c \dot{x}_{rel}^3 - \omega^2{}_{TVA} x_{rel} = 0\end{aligned} \tag{4.5}$$

Nondimensional parameters are same as Equation (4.3), except nonlinear loss factor,

$$\xi_c = \frac{c_c}{m_{TVA}}$$

Since the equation of motion is nonlinear, it depends on input value. Input value is specified.

$$U\left(t\right) = 0.01\sin\left(\omega t\right) \tag{4.6}$$

Relative displacement for single harmonic, from Equation (3.1)

$$\frac{\partial x_{rel}\left(\theta\right)}{\partial t} = \omega x_{rel}{}^{s}\cos\left(\theta\right) - \omega x_{rel}{}^{c}\sin\left(\theta\right) \tag{4.7}$$

Equation (4.3) and Equation (4.7) are substituted into Equation (3.4). Nonlinear force coefficients for single harmonic is obtained.

$$\begin{aligned}f_n^{\ s} &= -\frac{4}{3}\xi_c \omega^3 x_{rel}{}^{c}\left(\left(x_{rel}{}^{s}\right)^2 + \left(x_{rel}{}^{c}\right)^2\right)\\f_n^{\ c} &= \frac{4}{3}\xi_c \omega^3 x_{rel}{}^{s}\left(\left(x_{rel}{}^{s}\right)^2 + \left(x_{rel}{}^{c}\right)^2\right)\end{aligned} \tag{4.8}$$

Equation (4.5) is substituted into Equation (3.6) $\mathbf{f}_n$ becomes

$$\mathbf{f}_n = \left\{\in f_n^{\ s} \quad -f_n^{\ s} \quad \in f_n^{\ c} \quad -f_n^{\ c}\right\}^T \tag{4.9}$$

Equation (4.5), (4.6), (4.7) and (4.9) are substituted into Equation (3.6). Nonlinear algebraic equation sets are obtained.

$$\begin{bmatrix} -\omega^2\mathbf{I}+\mathbf{\Omega}_b{}^2 & -\gamma\hat{\mathbf{H}} \\ \gamma\hat{\mathbf{H}} & -\omega^2\mathbf{I}+\mathbf{\Omega}_b{}^2 \end{bmatrix}\begin{Bmatrix} \mathbf{x}^s \\ \mathbf{x}^c \end{Bmatrix}+\mathbf{f}_n=0.01\begin{Bmatrix} \omega^2{}_b \\ 0 \\ \gamma\omega^2{}_b \\ 0 \end{Bmatrix} \tag{4.10}$$

Where

$$\mathbf{\Omega}_b{}^2=\begin{bmatrix} \omega_b{}^2+\in\omega_{TVA}{}^2 & -\in\omega_{TVA}{}^2 \\ -\omega_{TVA}{}^2 & \omega_{TVA}{}^2 \end{bmatrix} \quad , \quad \hat{\mathbf{H}}=\begin{bmatrix} \gamma\omega_b{}^2 & 0 \\ 0 & 0 \end{bmatrix} \tag{4.11}$$

Ratio of natural frequency would be similar with Figure 4.2 Effect of the change of the nonlinear loss factor is given in Figure 4.5.

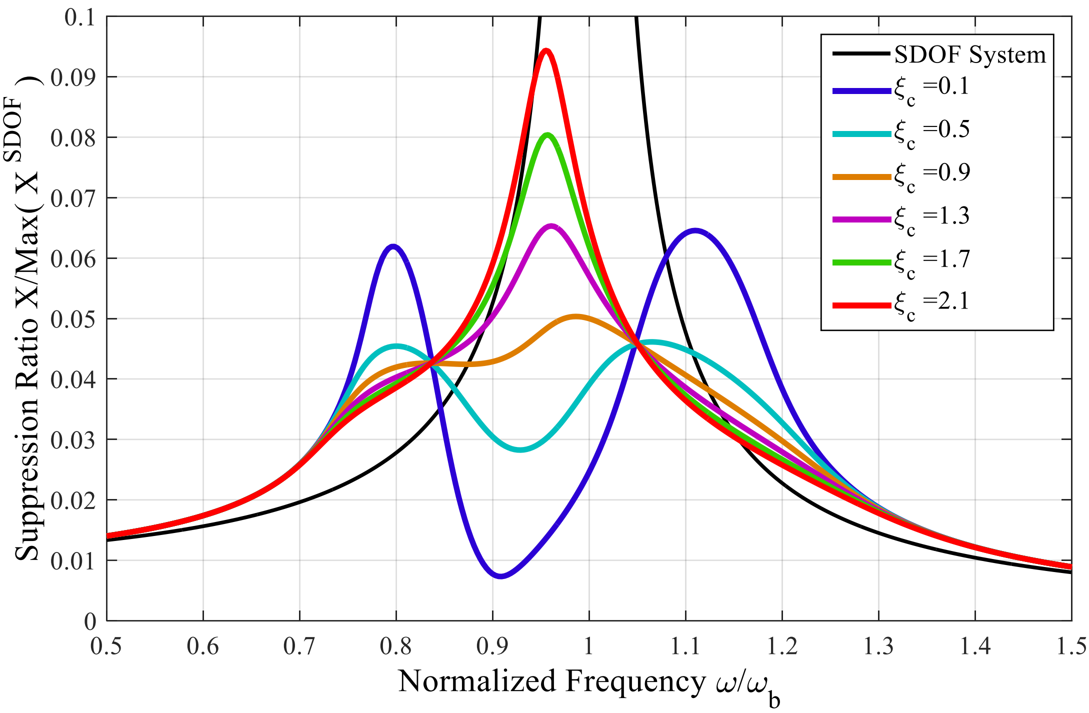

Figure 4.5. Effect of the Change of Nonlinear Damping Ratio

The ratio of the natural frequencies, $\omega_{TVA}/\omega_b=0.9$

As it is seen from the Figure 4.5, optimum value for nonlinear damping ratio is between 0.5 and 0.9. This information later will be used in optimization.

For low nonlinear damping value, system behavior is similar to classic TVA i.e. response at previous resonance is quite low, but two new resonance introduced nearby. For high nonlinear damping values, the system starts to behave like SDOF system. Behavior of a TVA with nonlinear damping seems similar to a TVA with linear damping. Except, it is more sensitive in higher amplitudes. There are sharp changes in frequency response.

4.1.1.3. System with Cubic Stiffness

Cubic stiffness is a nonlinear force, which is proportional to third power of the relative displacement. It can be hardening or softening type. In this study, hardening type will be explored. For a better understanding of the effect of the cubic stiffness, linear stiffness vanishes from Equation (4.1).

$$f_N\left(x_{rel}\right) = k_c {x_{rel}}^3 \tag{4.12}$$

Graphical demonstration is given in Figure 4.6

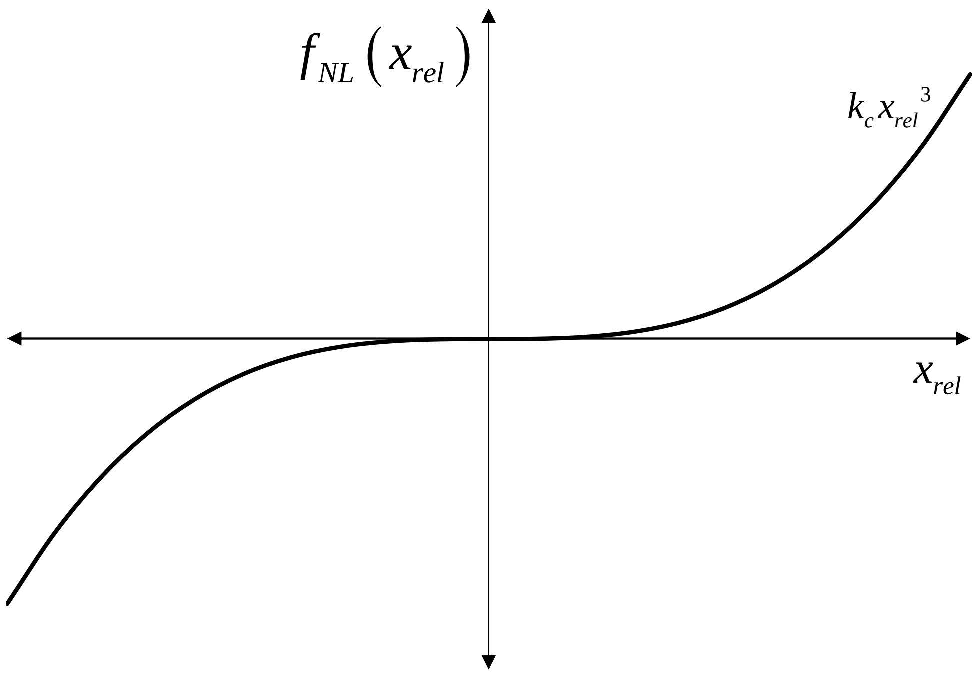

Figure 4.6. Graphical Demonstration of Cubic Stiffness

Equation (4.1) is nondimensionalized. .Notice that, it is nonlinear equation, therefore, it is input depended. Similar to cubic damping case, input value in Equation (4.6) is used.

$$\begin{aligned} &\ddot{x}_b + \omega_n{}^2 (1 + i\gamma) x_b + 2 \in \xi \omega_n \dot{x}_{rel} + \in \kappa_c x_{rel}{}^3 = f_{exc} \\ &\ddot{x}_{TVA} - 2\xi\omega_n \dot{x}_{rel} - \kappa_c x_{rel}{}^3 = 0 \end{aligned} \tag{4.13}$$

Where

$$\begin{aligned} &\in = \frac{m_{TVA}}{m_b} \quad , \quad \gamma = 0.01 \quad , \quad \omega_b{}^2 = \frac{k_b}{m_b} \\ &\xi = \frac{c_{TVA}}{2m_{TVA}\omega_b} \quad , \quad \kappa_c = \frac{k_c}{m_{TVA}} \quad , \quad f_{exc} = 0.01(1 + i\gamma)\omega_n{}^2 \end{aligned} \tag{4.14}$$

Free parameters of TVA are damping ratio and the cubic spring parameter.

Relative displacement for single harmonic is

$$x_{rel}(\theta) = x_{rel}{}^s \sin(\theta) + x_{rel}{}^c \cos(\theta) \tag{4.15}$$

Similarly nonlinear force coefficients are obtained by substituting Equation (4.12) and Equation (4.15) into Equation (3.4)

$$\begin{aligned} f_n{}^s &= \frac{4}{3}\kappa_c x_{rel}{}^s \left(\left(x_{rel}{}^s \right)^2 + \left(x_{rel}{}^c \right)^2 \right) \\ f_n{}^c &= \frac{4}{3}\kappa_c x_{rel}{}^c \left(\left(x_{rel}{}^s \right)^2 + \left(x_{rel}{}^c \right)^2 \right) \end{aligned} \tag{4.16}$$

Nonlinear force vector is constructed by using Equation (4.16)

$$\mathbf{f}_n = \left\{ \in f_n{}^s \quad -f_n{}^s \quad \in f_n{}^c \quad -f_n{}^c \right\}^T \tag{4.17}$$

Equation (4.9) rearranged by using Equation (4.16). As a result, nonlinear algebraic equation is obtained by substituting Equations (4.6), (4.13), (4.15) and (4.17) into Equation (3.6).

$$\begin{bmatrix} -\omega^2\mathbf{I}+\mathbf{\Omega}_b{}^2 & -\gamma\hat{\mathbf{H}}-\omega\hat{\mathbf{C}} \\ \gamma\hat{\mathbf{H}}+\omega\hat{\mathbf{C}} & -\omega^2\mathbf{I}+\mathbf{\Omega}_b{}^2 \end{bmatrix}\begin{Bmatrix} \mathbf{X}^s \\ \mathbf{X}^c \end{Bmatrix}+\mathbf{f}_n=0.01\begin{Bmatrix} \omega^2{}_b \\ 0 \\ \gamma\omega^2{}_b \\ 0 \end{Bmatrix} \tag{4.18}$$

Where

$$\mathbf{\Omega}_b{}^2=\begin{bmatrix} \omega_b{}^2 & 0 \\ 0 & 0 \end{bmatrix} \quad , \quad \hat{\mathbf{H}}=\begin{bmatrix} \gamma\omega_b{}^2 & 0 \\ 0 & 0 \end{bmatrix} \quad , \quad \hat{\mathbf{C}}=\begin{bmatrix} 2\in\xi\omega_b & -2\in\xi\omega_b \\ -2\xi\omega_b & 2\xi\omega_b \end{bmatrix} \tag{4.19}$$

Since there is no linear stiffness element between masses, TVA does not have a natural frequency. For same reason, definition of damping ratio in Equation (4.3) and Equation (4.14) are different. Effects of the change of the cubic stiffness related parameter and damping ratio are demonstrated in Figure 4.7 and Figure 4.8.

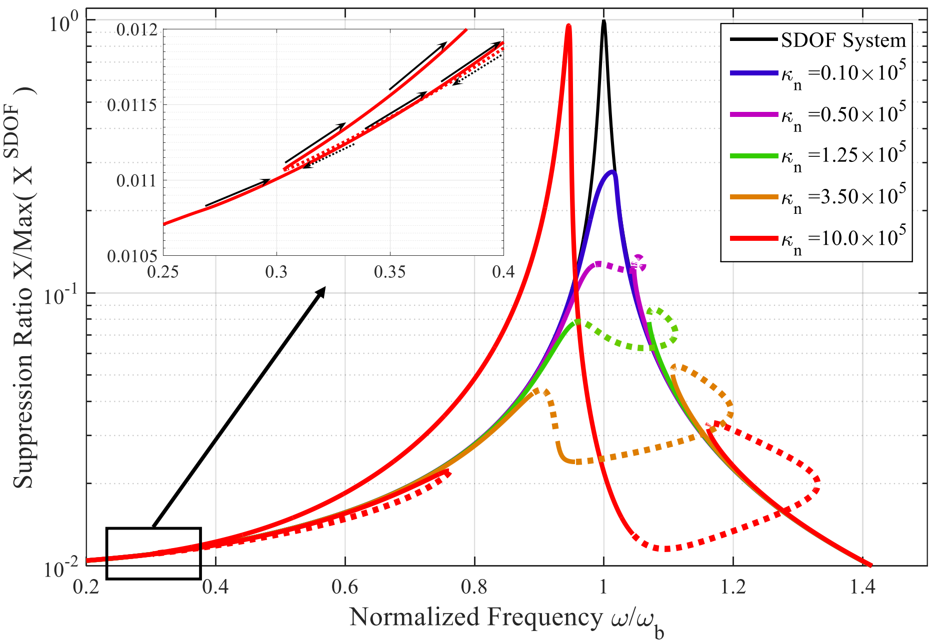

Figure 4.7 The Effect of the Change of the Cubic Stiffness Parameter

Damping ratio is $\xi=0.09$ Dotted lines indicate unstable solution points.

When cubic stiffness value is low, suppression ratio is also low. The reason is, at low amplitudes, nonlinear spring behaves like soft spring. As the stiffness parameters increase, amplitude decrease up to certain value. After certain threshold value, jump phenomena is observed. After that point, increase in cubic stiffness parameter does not affect the maximum amplitude, but the characteristic of the FRF changes.

In addition, there is no stable solution in certain frequency range for some cubic stiffness values. Response for those regions are not harmonic, it is chaotic or quasi-periodic [29]. This phenomenon will be investigated in later in this study.

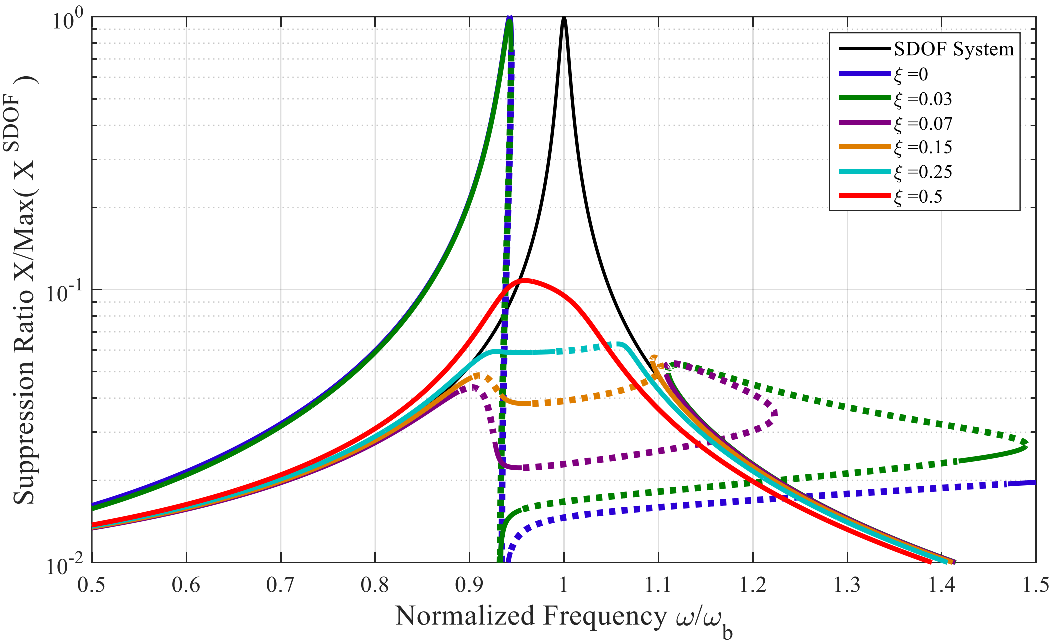

Figure 4.8 The Effect of the Change of the Damping Ratio

Cubic Stiffness is $\kappa_c = 3.50 \times 10^5$. Dotted lines indicate unstable solution points.

From Figure 4.8, at low damping values, jump is observed. After certain damping value, jump is disappeared. As damping gets higher and higher, amplitudes are increased, system starts to behave like SDOF system. Also, unstable region is affected by damping value. At low damping values, wide frequency region is unstable. As damping increase, the unstable region gets narrower. After certain damping value, unstable region is not observed.

Also, notice that, damping values are lower than the Linear System when considering preferable solutions.

4.1.1.4. Dry Friction Damping

Friction force is defined as the resistance of the motion when one body is tangentially in contact with another body [37]. Macro-slip friction model is used in this study due to its mathematical simplicity. Details of the model used in this study is given in the papers [38], [39]. Macro-slip friction model is shown in Figure 4.8. Hysteresis curve for single harmonic motion is shown in the Figure 4.9.

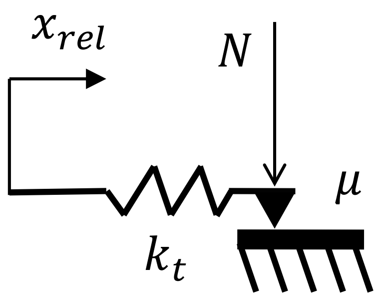

Figure 4.9. Macro-slip Friction Model

Where k_t is contact stiffness, N is the normal load acting upon the contact surface,μ is the friction coefficient, and x_{rel} is the relative displacement between terminals.

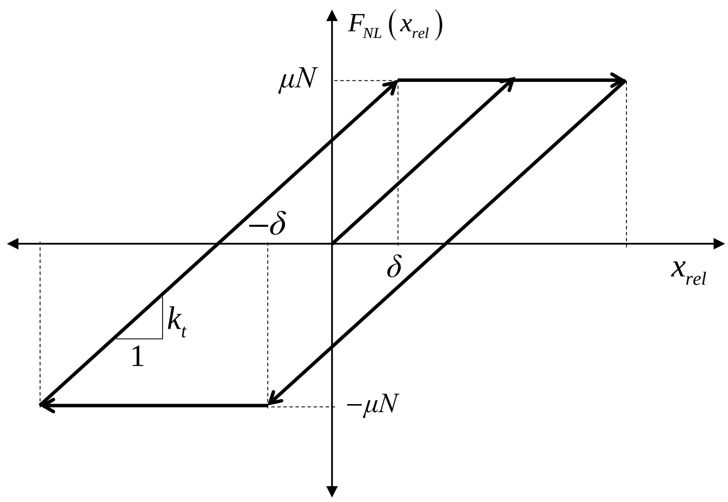

Figure 4.10. Hysteresis Curve for Single Harmonic Motion

When the force on the nonlinear element is less than slip force, μN it stick and acts like stiffness element. When the force on the nonlinear elements reaches to slip force, μN, it starts to slip until relative velocity becomes zero (i.e $\dot{x}_{rel} = 0$). The point, where the slip starts, is breaking point, δ.

Nonlinear force can be expressed as follows

if $\delta < x_{\max}$

$$f_{NL}(\theta) = \begin{cases} -\mu N + k_t\left(x_{rel}(\theta) + \delta\right) & \text{if} \quad \psi_1 < \theta < \psi_2 \\ -\mu N & \text{if} \quad \psi_2 < \theta < \psi_1 + \pi \\ \mu N - k_t\left(x_{rel}(\theta) + \delta\right) & \text{if} \quad \psi_1 + \pi < \theta < \psi_2 + \pi \\ \mu N & \text{if} \quad \psi_2 + \pi < \theta < \psi_1 + 2\pi \end{cases} \tag{4.20}$$

if $\delta > x_{\max}$

$$f_{NL}(\theta) = k_t x_{rel}(\theta)$$

Where

$$x_{\max} = \sqrt{\left(x_{rel}{}^{s}\right)^2 + \left(x_{rel}{}^{c}\right)^2} \quad , \quad \delta = \frac{2\mu N - k_t x_{\max}}{k_t}$$
$$\psi_1 = \tan^{-1}\left(\frac{x_{rel}{}^{s}}{x_{rel}{}^{c}}\right) \quad , \quad \psi_2 = \cos^{-1}\left(\frac{\delta}{x_{\max}}\right) + \psi_1 \tag{4.21}$$

$x_{rel}(\theta)$, $x_{rel}{}^{s}$ and $x_{rel}{}^{c}$ are introduced in Equation (4.15).

Friction will act as damper element. Therefore, to see the effect of the dry friction better, linear damping elements are vanished. Equation (4.1) is nondimensionalized. Input value in Equation (4.6) is used.

$$\begin{aligned} &\ddot{x}_b + \omega_b{}^2(1 + i\gamma)x_b + \in \omega_{TVA}{}^2 x_{rel} + \in \hat{f}_{NL}(x_{rel}) = f_{exc} \\ &x_{TVA} - \omega_{TVA}{}^2 x_{rel} - \hat{f}_{NL}(x_{rel}) = 0 \end{aligned} \tag{4.22}$$

Where

$$\in = \frac{m_{TVA}}{m_b} \quad , \quad \gamma = 0.01 \quad , \quad \omega_b{}^2 = \frac{k_b}{m_b}$$
$$\omega_{TVA}{}^2 = \frac{k_{TVA}}{m_{TVA}} \quad , \quad \hat{f}_{NL} = \frac{f_{NL}}{m_{TVA}} \quad , \quad \hat{f} = 0.01(1+i\gamma)\,\omega_n{}^2 \tag{4.23}$$

In addition, parameters of the friction force $F_N\left(x_{rel}\right)$ are nondimensionalized

$$\omega_t{}^2 = \frac{k_t}{m_{TVA}} \quad , \quad \xi_{\mu N} = \frac{\mu N}{m_{TVA}} \tag{4.24}$$

Similarly, nonlinear force coefficients are obtained by substituting Equation (4.15), Equation (4.20) and Equation (4.14) into Equation (3.4)

$$f_N{}^s = \frac{1}{\pi}\left(2\omega_t{}^2 x_{\max}\left(\cos\left(\psi_2\right) - \cos\left(\psi_1\right) - 4\xi_{\mu N}\cos\left(\psi_2\right)\right)\right) + \omega_t{}^2 x_{rel}{}^s\Gamma_1 + \omega_t{}^2 x_{rel}{}^c\Gamma_2$$
$$f_N{}^c = \frac{1}{\pi}\left(2\omega_t{}^2 x_{\max}\left(\sin\left(\psi_1\right) - \sin\left(\psi_2\right) + 4\xi_{\mu N}\sin\left(\psi_2\right)\right)\right) + \omega_t{}^2 x_{rel}{}^s\Gamma_2 + \omega_t{}^2 x_{rel}{}^c\Gamma_3 \tag{4.25}$$

Where

$$\Gamma_1 = \frac{1}{2\pi}\left(2\psi_2 - 2\psi_1 + \sin\left(2\psi_1\right) - \sin\left(2\psi_2\right)\right)$$
$$\Gamma_2 = \frac{1}{2\pi}\left(\cos\left(2\psi_1\right) - \cos\left(2\psi_2\right)\right) \tag{4.26}$$
$$\Gamma_3 = \frac{1}{2\pi}\left(2\psi_2 - 2\psi_1 - \sin\left(2\psi_1\right) + \sin\left(2\psi_2\right)\right)$$

Nonlinear force vector is constructed by using Equation (4.25)

$$\mathbf{f}_n = \left(\in f_n{}^s \quad -f_n{}^s \quad \in f_n{}^c \quad -f_n{}^c\right)^T \tag{4.27}$$

Equation (4.9) rearranged by using Equation (4.22). As a result, nonlinear algebraic equation is obtained by substituting Equations (4.6), (4.15) and (4.27) into Equation (3.6).

$$\begin{bmatrix} -\omega^2\mathbf{I}+\mathbf{\Omega}_n{}^2 & -\gamma\hat{\mathbf{H}} \\ \gamma\hat{\mathbf{H}} & -\omega^2\mathbf{I}+\mathbf{\Omega}_n{}^2 \end{bmatrix} \begin{Bmatrix} \mathbf{x}^s \\ \mathbf{x}^c \end{Bmatrix} + \mathbf{f}_n = 0.01 \begin{Bmatrix} \omega^2{}_b \\ 0 \\ \gamma\omega^2{}_b \\ 0 \end{Bmatrix} \tag{4.28}$$

Where

$$\mathbf{\Omega}_b{}^2 = \begin{bmatrix} \omega_b{}^2 + \in \omega_{TVA}{}^2 & -\in \omega_{TVA}{}^2 \\ -\omega_{TVA}{}^2 & \omega_{TVA}{}^2 \end{bmatrix} \quad , \quad \hat{\mathbf{H}} = \begin{bmatrix} \gamma\omega_b{}^2 & 0 \\ 0 & 0 \end{bmatrix} \tag{4.29}$$

There are three free parameters. These are the linear spring between TVA and the main system, contact stiffness and slip force. Natural frequency ratios would be similar with *Figure 4.1* therefore, effect of the change of the natural frequency ratio is not plotted.

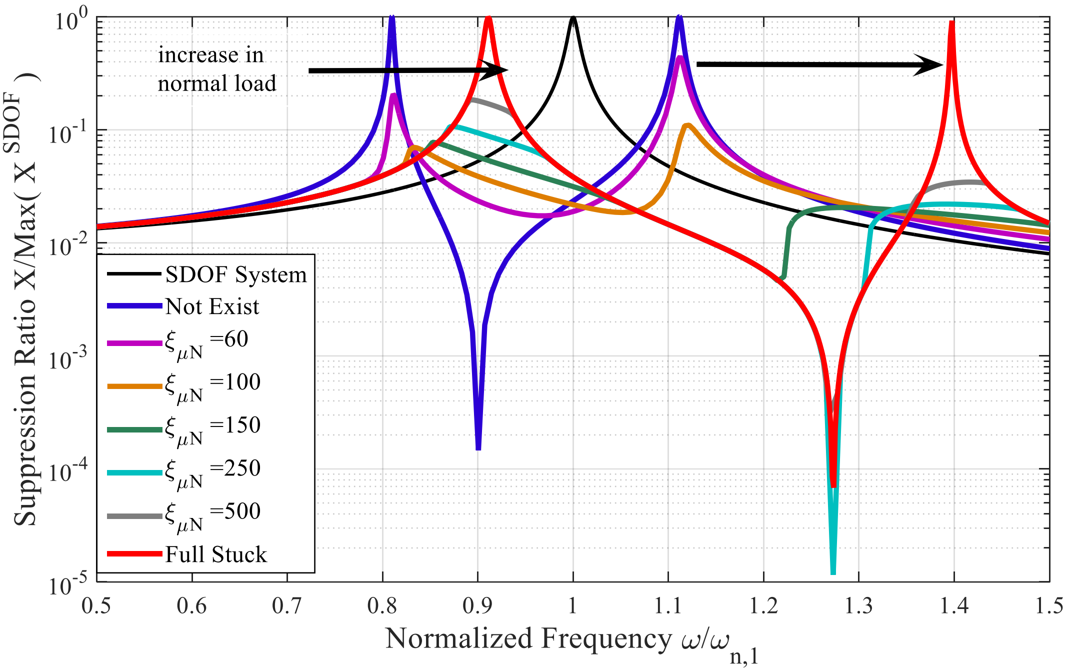

Figure 4.11. Effect of the Change of the Normal Load Parameter

$$\omega_{TVA} = \omega_{TVA} = 0.9\omega_b$$

From the Figure 4.11, it is seen that, low slip load cannot suppress the amplitude levels effectively. Adequate suppression level is observed for friction values around

$\xi_{\mu N} \cong 150-250$ For higher friction values, it starts to stick and acts like just stiffness element. These values will be used in optimization later.

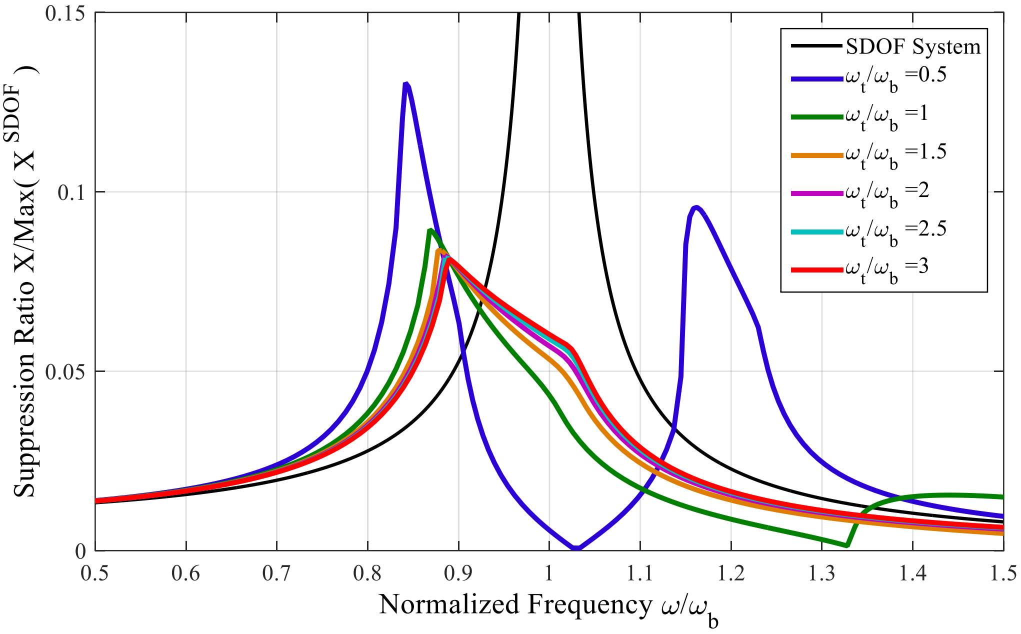

Figure 4.12 Effect of the Change of the Contact Stiffness

$\omega_{TVA} = 0.9\omega_b$ and $\xi_{\mu N} = 200$

From Figure 4.12, for low contact stiffness value, suppression level is also quite low, because relative displacement cannot exceed breaking point, δ nonlinear elements behaves like a linear soft spring. As the contact stiffness value increases, relative displacement more easily reach the breaking point, and nonlinear elements start to slip and exert friction force on the system. In addition, second natural frequency shifts to right with lower amplitude value in higher contact stiffness value. After certain value, contact stiffness does not have significant importance on the suppression level.

4.1.1.5. Cubic Stiffness and Dry Friction Damping

Combination of nonlinear elements may have also distinct behavior. Viscous elements are removed from Equation (4.9) and friction force is added in Equation (4.20). Same nondimensionalization procedure is applied.

$$
\begin{aligned}
&\ddot{x}_b + \omega_b \left(1 + i\gamma\right) x_b + \in \hat{F}_{NL}\left(x_{rel}\right) + \in \kappa_c x_{rel}{}^3 = f_{exc} \\
&\ddot{x}_{TVA} - \hat{F}_{NL}\left(x_{rel}\right) - \kappa_c x_{rel}{}^3 = 0
\end{aligned} \tag{4.30}
$$

There are three free parameter, which are normal load, contact stiffness and cubic stiffness.

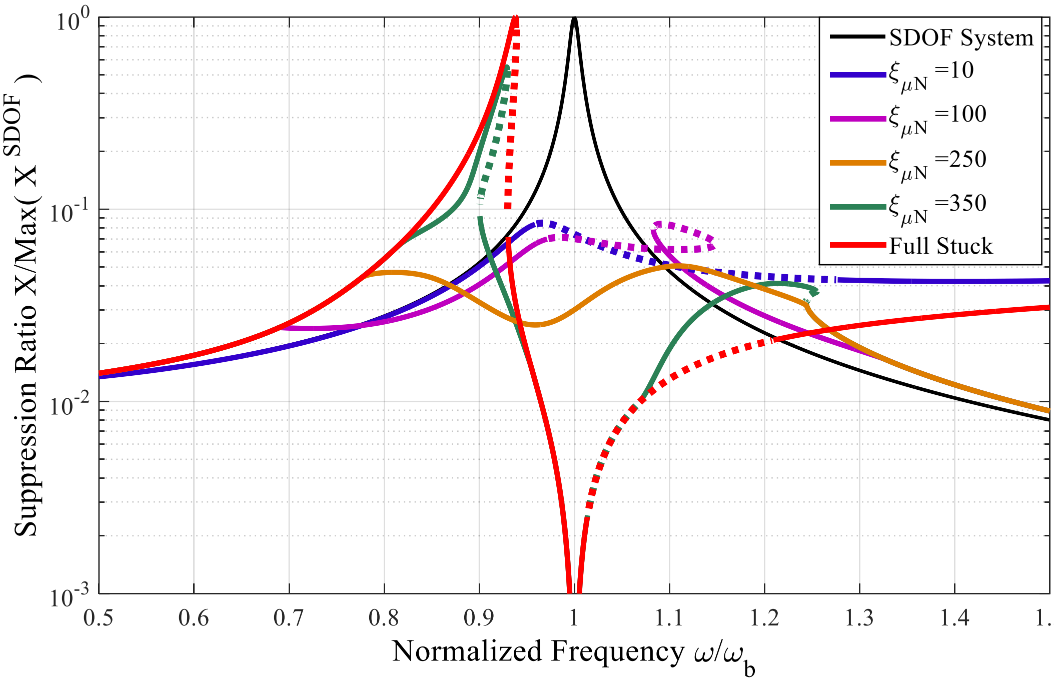

Figure 4.13. The Effect of the Change of the Normal Load

$\kappa_c = 10^5$ and $\omega_t = 0.9\omega_b$. Dotted lines indicate unstable solution points.

When the slip force is zero, since no other damping element attached on the system, peculiar behavior observed in frequency response. As normal load increased, better suppression performance is observed.

Notice that, there was a frequency interval with no stable solution in cubic stiffness case. In this case, however, there is no frequency region with unstable region is observed.

Further increase in slip force decreases suppression levels. It starts to stick and acts like stiffness element. When full stuck is occurred, the system behaves like TVA with cubic and linear stiffness with no damping.

These values will be used in optimization later.

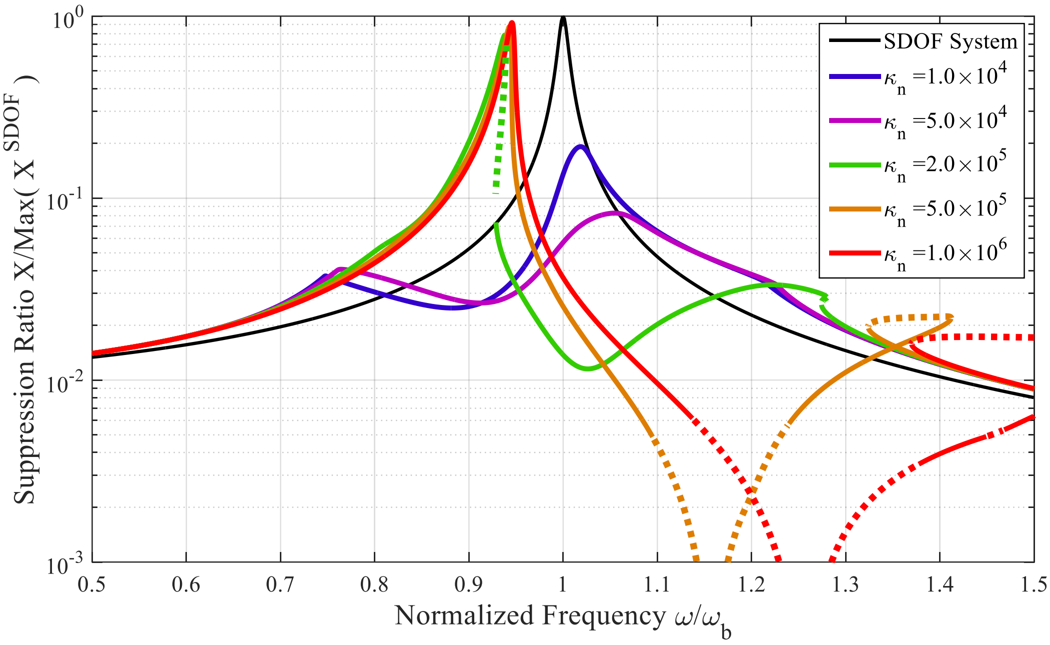

Figure 4.14. The Effect of the Change of the Cubic Stiffness Parameter.

$\xi_{\mu N} = 250$ and $\omega_t = 0.9\omega_n$ Dotted lines indicate unstable solution points.

For low cubic stiffness values, suppression level is low. Since dry friction damper element contains stiffness element, certain level of suppression is observed. As the cubic stiffness increased, adequate suppression is observed.

Further increase in cubic stiffness value badly affect the suppression level. After certain level, maximum amplitude value does not change, however topology of the frequency response is changing. Unlike Figure 4.6 changes in FRF by changing cubic stiffness parameter is smoother.

Frequency interval with no stable solution is observed high cubic stiffness parameters. That region is not observed for moderate level cubic stiffness parameters. Therefore, stability behavior makes it more useful when comparing TVA with cubic stiffness and viscous damping.

These values later used in optimization.

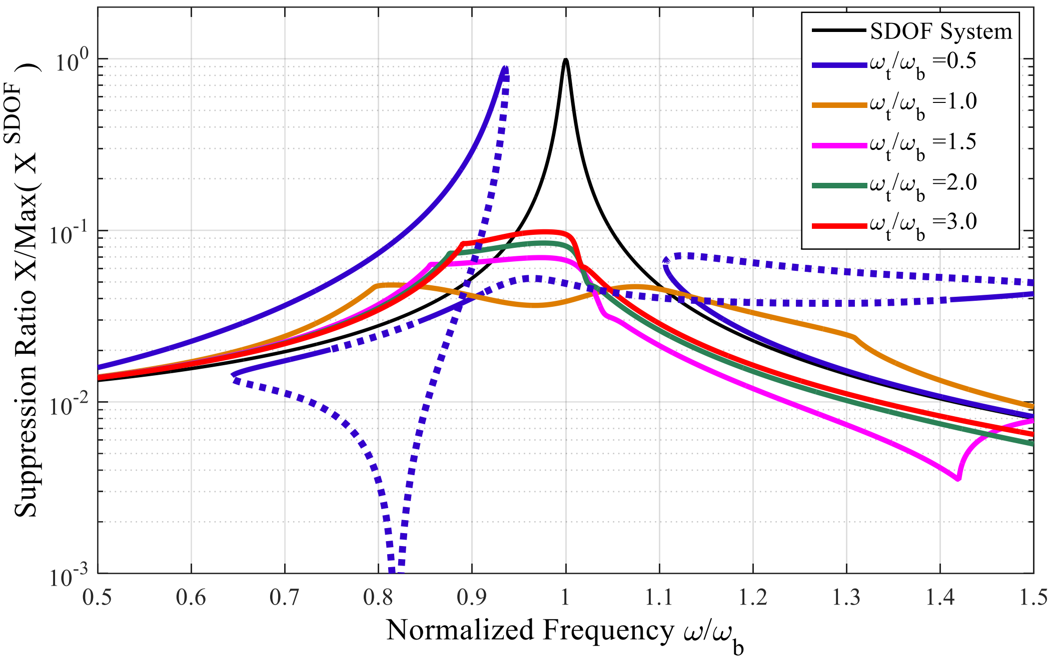

Figure 4.15. The Effect of the Change of the Contact Stiffness Parameter

$\kappa_c = 10^5$ and $\xi_{\mu N} = 250$ Dotted lines indicate unstable solution points.

For low contact stiffness value, the effect of the friction damper is low because relative displacement is not big enough to exceed braking point. Thus friction damping is act likes soft spring. As contact stiffness value goes higher, adequate suppression level is observed. Further increase in contact stiffness value, reduces suppression level also shifts second natural frequency to right.

Moreover, for contact stiffness values, unstable solution is observed.

4.1.1.6. Cubic Stiffness and Cubic Damping

Combination of nonlinear elements may have also distinct behavior. Viscous elements are removed from Equation (4.9) and cubic damping in Equation (4.4) is added. After non-dimensional procedure is applied.

$$\begin{aligned}&\ddot{x}_b+\omega_b{}^2(1+i\gamma)x_b+\in\xi_c\dot{x}_{rel}{}^3+\in\kappa_c x_{rel}{}^3=f_{exc}\\&\ddot{x}_{TVA}-\xi_c\dot{x}_{rel}{}^3-\kappa_c x_{rel}{}^3=0\end{aligned}\tag{4.31}$$

There are two free parameter, which are cubic stiffness and cubic damping.

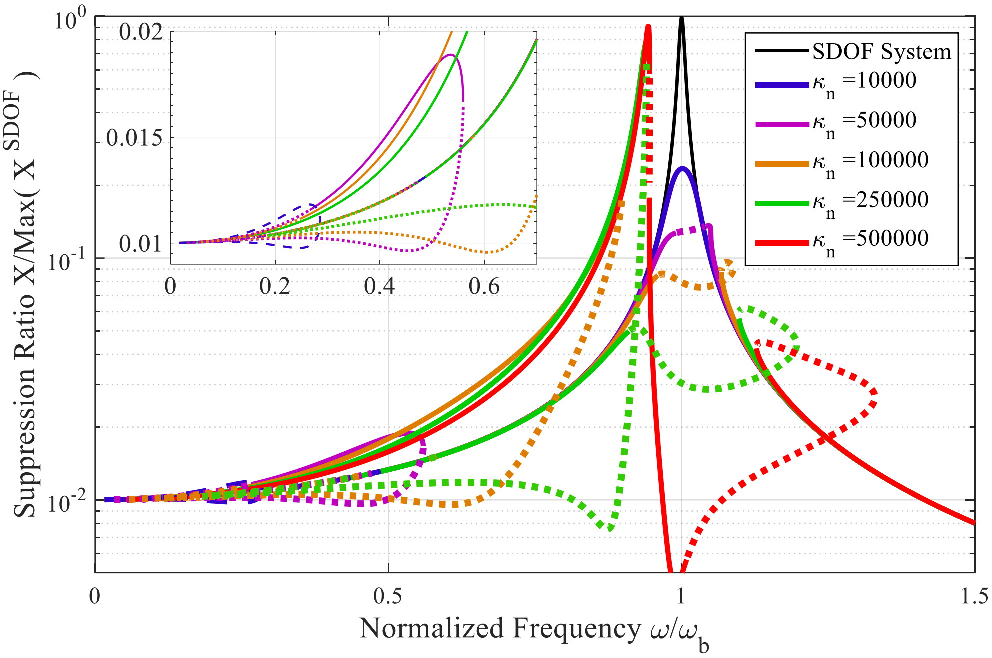

Figure 4.16. The Effect of the Change of the Cubic Stiffness Parameter

$\xi_c = 0.09$ Solid lines indicates stable solution points; dotted lines indicate unstable solution points.

Behaviour of the TVA with cubic stiffness and cubic damping is similar with TVA with cubic stiffness and linear damping. For small cubic stiffness values, suppression level is low. The suppression level gets better with increase in cubic stiffness until it reach a threshold value. Jump phenomena is observed. After that point, maximum value does not change. Increase in cubic stiffness changes the topology of the frequency response curve.

Stability behavior is similar to TVA with cubic stiffness with viscous damper. There is a frequency internal with no stable solution. This region is located around previous resonance point.

This values will be used in optimization later.

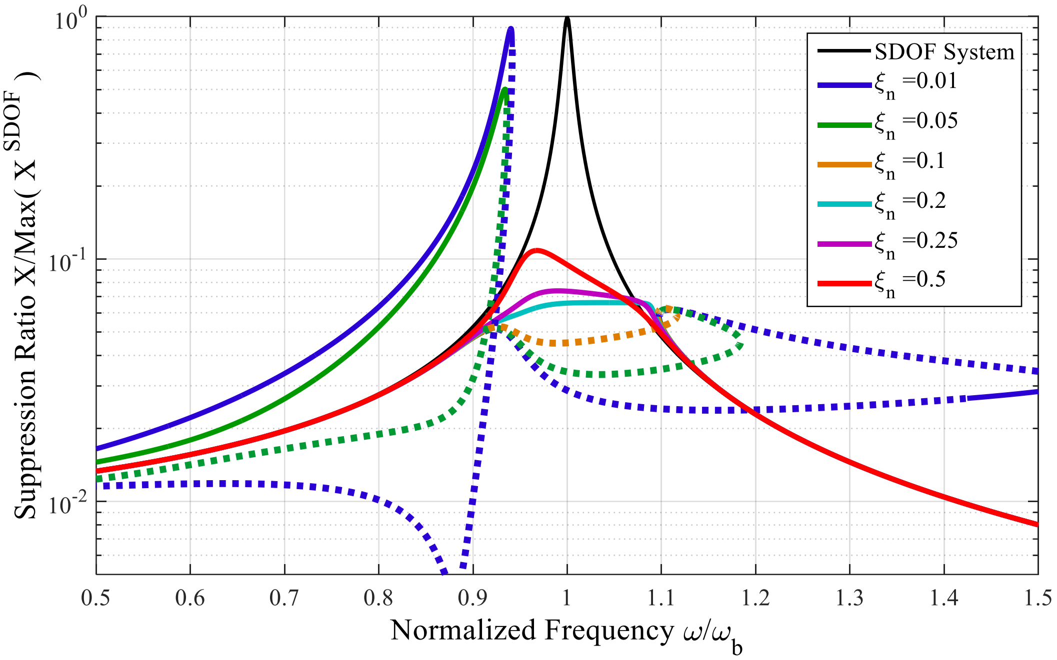

Figure 4.17 The Effect of the Change of the Cubic Damping Parameter

$\kappa_c = 2.5\times10^5$ Dotted lines indicate unstable solution points.

The effect of the change of the cubic damping parameter is similar to change in viscous damping. Increase in cubic damping value cancels out the jump. Further increase in cubic damping parameter increases amplitude levels.

For low cubic damping values, there is a frequency interval with no stable solution. This interval vanishes by increasing cubic damping values.

Notice that, unlike Figure 4.8, increase in cubic damping does not suddenly increases the maximum value. However, unstable frequency interval vanished. This values and this information might be used later in optimization.

4.1.2. Double TVA

By the use of multiple TMDs and nonlinear elements, it is aimed to suppress the vibrations of the structures in a broader frequency range.

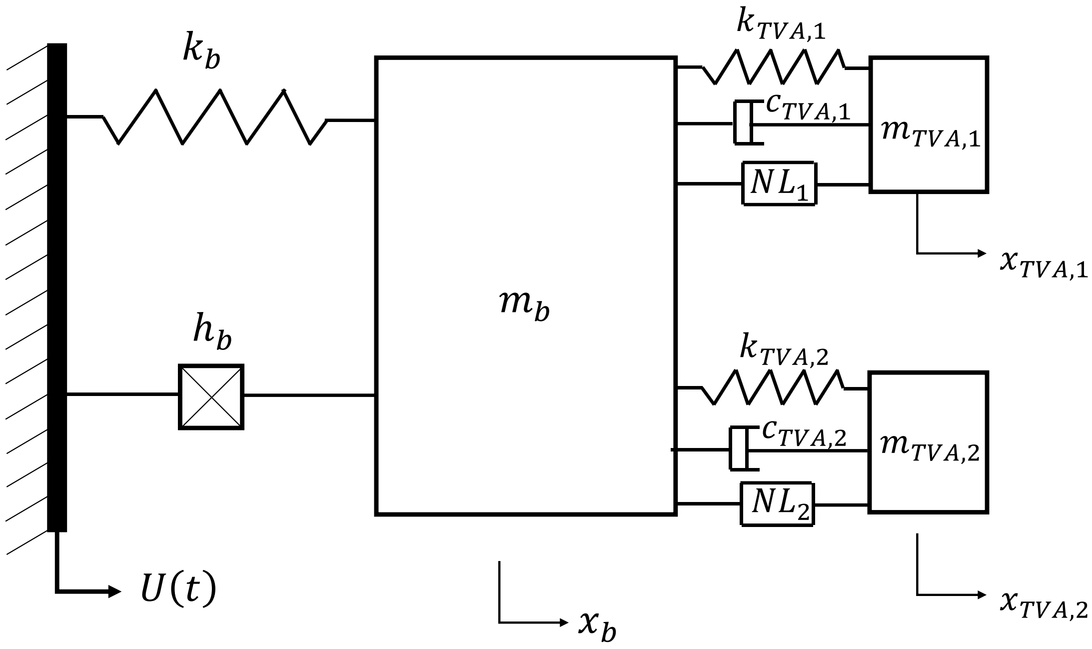

Figure 4.18. SDOF Systems with Two TMDs Utilizing Dry Friction Dampers

Single DOF linear system equipped with two nonlinear TVAs is shown in Chapter 5.1.1. Where m_b is the mass of the main system. $m_{TVA,j}$ are the masses of the TVSs. k_b and $k_{TVA,j}$ are linear springs h_b is structural damping elements. $c_{TVA,j}$ are viscous dampers. NL_j are nonlinear elements.

Equation of motion of the general system is

$$\begin{aligned}
&m_b\ddot{x}_b + h_b/\omega\,\dot{x}_b + k_b x_b + \sum_{j=1}^{2}\left(c_{TVA,j}\dot{x}_{rel,j} + k_{TVA,j}x_{rel,j} + f_{NL,j}\left(x_{rel,j}\right)\right) = f_{exc}\\
&m_{TVA,1}\ddot{x}_{TVA,1} - c_{TVA,1}\dot{x}_{rel,1} - k_{TVA,1}x_{rel,1} - f_{NL,1}\left(x_{rel,1}\right) = 0\\
&m_{TVA,2}\ddot{x}_{TVA,2} - c_{TVA,2}\dot{x}_{rel,2} - k_{TVA,2}x_{rel,2} - f_{NL,2}\left(x_{rel,2}\right) = 0
\end{aligned} \tag{4.32}$$

Where $x_{rel,j} = x_b - x_{TVA,j}$ .total mass of the TVA is selected as ten percent of the main mass, i.e $m_{TVA,j} = m_b/20$ Loss factor for the main system is taken as one percent and $f_{exc} = h_b/\omega\dot{U} + k_b U$

Nonlinear force vector would be

$$\mathbf{f}_{non} = \begin{Bmatrix} f_{NL,1} + f_{NL,2} \\ f_{NL,1} \\ f_{NL,2} \end{Bmatrix} \tag{4.33}$$

Linear and nonlinear elements will not be studied individually in this chapter.

4.2. Continuous System

Response of a linear Euler-Bernoulli beam with TVA with equipped with linear and nonlinear elements is investigated. Equation (3.50) is used. Topology is similar with ones, shown in previous chapter.

Equation (3.50) is further extended for multi TVAs for first and second mode cancelation is considered

CHAPTER 5

RESULTS

TVAs parameters are optimized by genetic algorithm (GA) of MATLAB. Optimum values are used as an initial guess in gradient based optimization, fminunc of MATLAB.

Different cost functions are considered. The first is the maximum response value because the aim of the vibration suppression is to minimize maximum value. The second cost function is the area of the response above unity. It is shown in Figure 5.1. When the system contains a lot of DOF or subjected to random excitation, considering only the resonance point might not give desired suppression characteristic. [40].

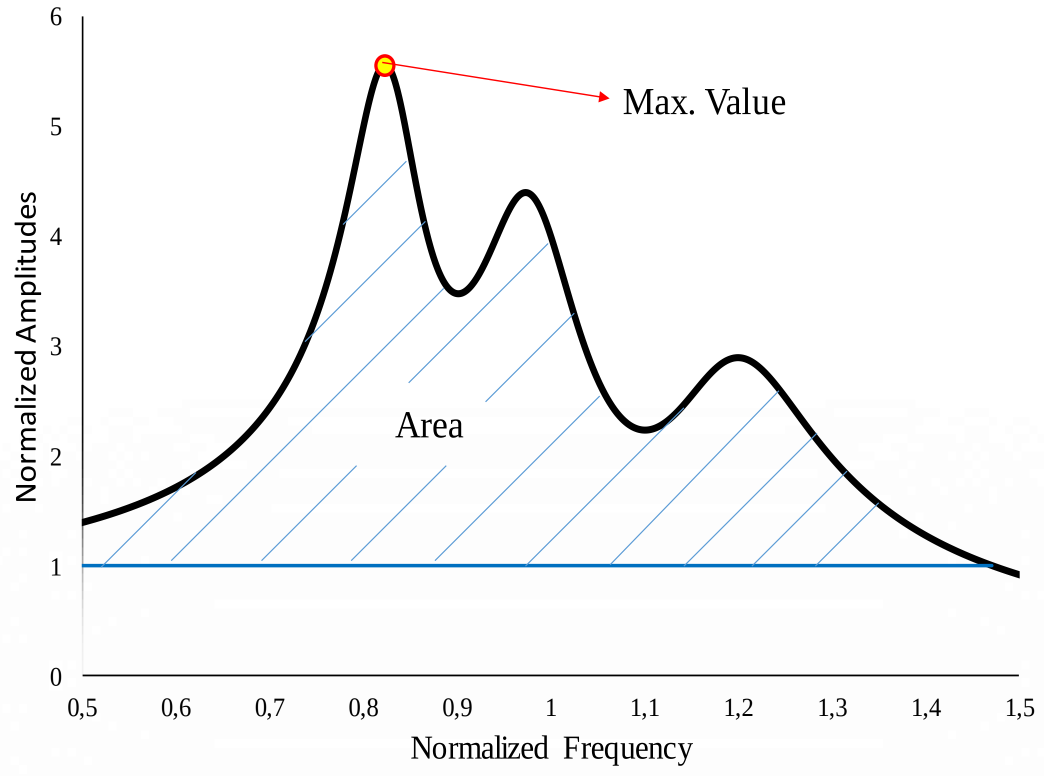

Figure 5.1. Definition of Cost Functions

Also combination of normalized maximum values and normalized areas are used. The results are compared in Figure 5.2 and Figure 5.3. In Figure 5.2, single TVA is optimized, in Figure 5.3, two TVAs are optimized.

The maximum value is used because one of the aim in the vibration suppression is essentially to reduce maximum vibration amplitude.

The system is excited by unity base excitation. Every value above unity is amplification. It is also desired to minimize all those amplified values. Therefore, the area above unity is defined.

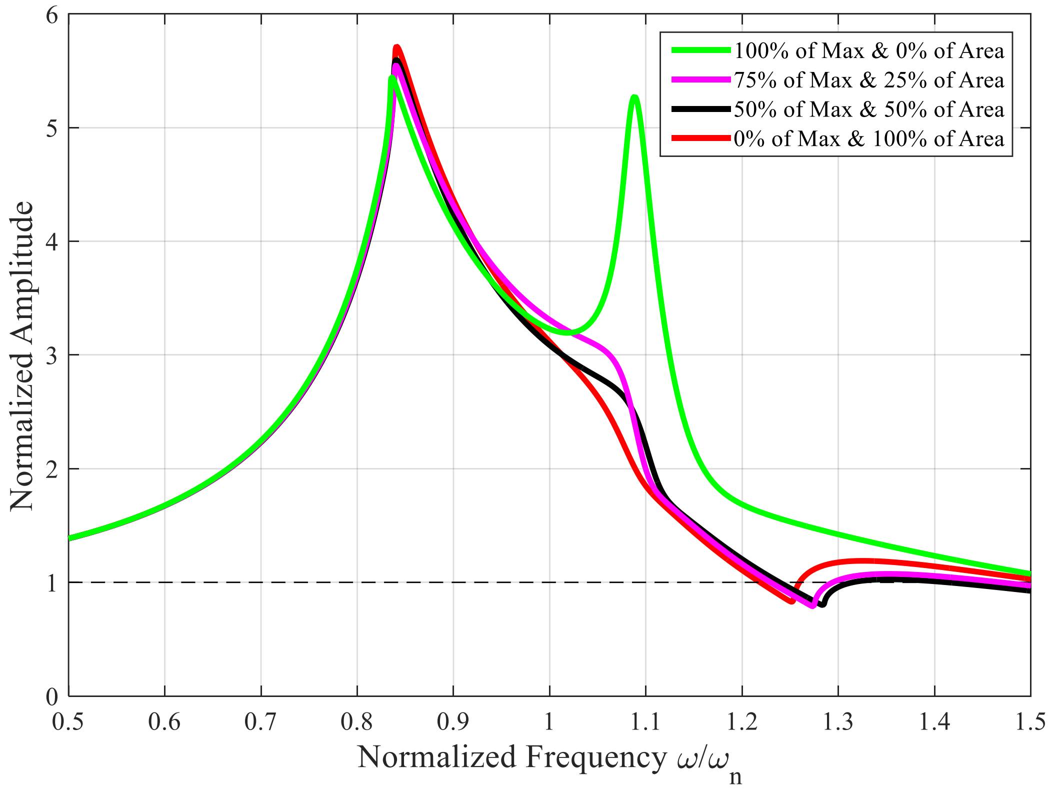

Figure 5.2 Comparison of Cost Functions in single TVA Optimization

Normalized response of the system with single TVA is shown in Figure 5.2. When the weight of the integral of the displacement amplitude is zero, i.e 100% Max, second resonance peak occurs. This is due to the fact that only the maximum displacement amplitude is used as the cost function and hence, optimization resulted in two peaks with equal amplitudes. When the weight of the maximum displacement of the main system is zero, i.e 100% Area, amplitude of the resonance peak is larger. This is due to the fact that the area under the frequency response function is minimized without considering the amplitudes of the resonance peaks.

The differences in maximum values are mathematical. It is seen that 100 % of maximum is not preferable. However, for other cost functions, the difference is not clear. Therefore, cost function are compared in multi TVA optimization.

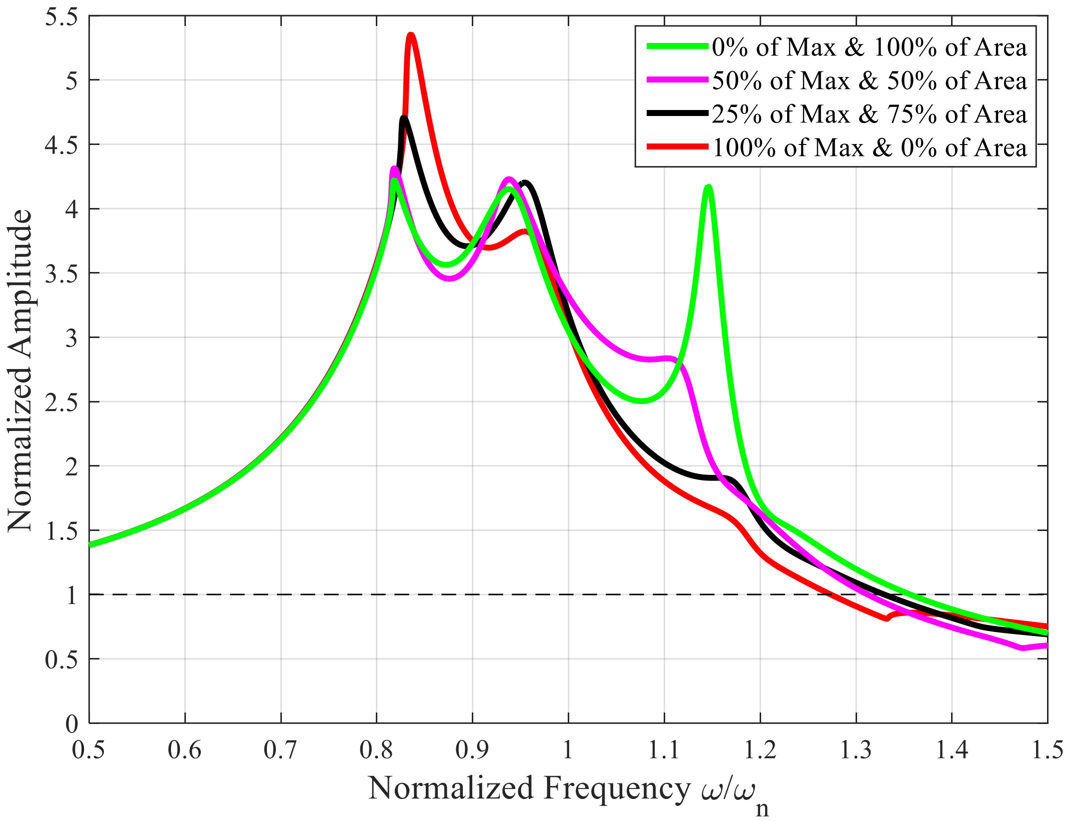

Figure 5.3 Comparison of Cost Functions in two TVAs Optimization

When the weight of the integral of the displacement amplitude is zero, i.e 100% Max, This is due to the fact that only the maximum displacement amplitude is used as the cost function and hence, optimization resulted in three peaks with equal amplitudes. When the weight of the maximum displacement of the main system is zero, i.e 100% Area, amplitude of the first resonance peak is larger. This is due to the fact that the area under the frequency response function is minimized without considering the amplitudes of the resonance peaks.

Combinations of normalized area and normalized amplitude are also considered. Notice that, between 100% of Max & 0% of Area and 50% of Max & 50% of Area, the differences are mathematical. Amplitude level in 25% of Max, slightly higher than the 50 % of Max.

When considering the general physical behavior, combination of area and maximum value is more effective. It is selected as ultimate cost function in further analysis.

5.1. Discrete System

Parameters of the system under investigation are $m_b = 1kg$, $k_b = 3948\, N/m$, $h_b = 39.5\, N/m$ and $U = 0.01\, m$. Mass of TVA is ten percent of the total mass. Remaining parameters are optimized.

5.1.1. Single TVA

Mass of the TVA is taken as $m_{TVA} = 0.1 m_b$

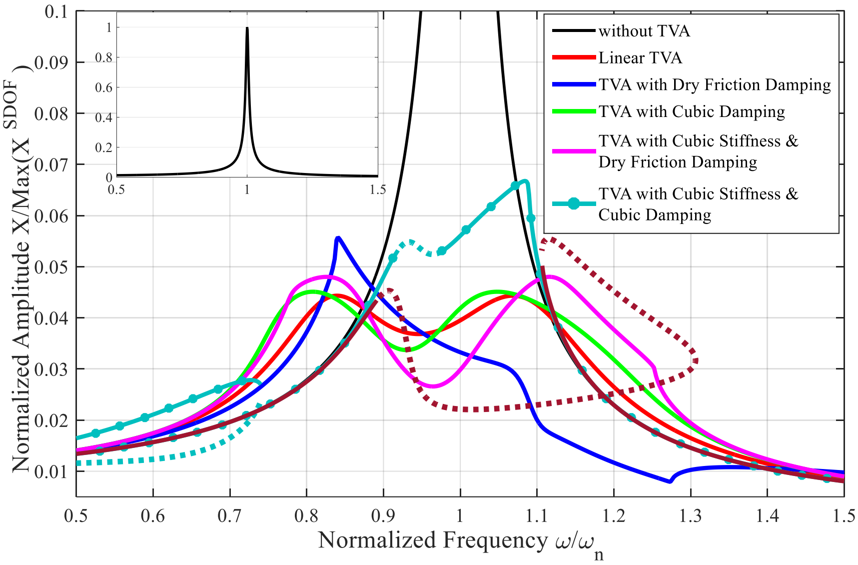

Figure 5.4 Comparison of single TVA Configurations.

Dotted lines denote unstable solutions. Solid lines denote stable solutions.

Linear TVA has good suppression behavior. It suppress more than 95% of vibration amplitude. When comparing the system without TVA, It has a higher vibration amplitude between normalized frequencies of 0.5 to 0.85. It has very effective suppression around resonance of the main.

TVA equipped with friction damper has also effective. It has higher vibration amplitude than linear TVA between normalized frequencies of 0.8 to 0.95. After that frequency, it has more effective suppression performance.

TVA with cubic stiffness and viscous damping i.e. Nonlinear Energy Sink (NES) has lower amplitude except between normalized frequency of 1.1 to 1.35. However, there is a frequency interval with no stable solution. It indicates that, at those frequencies, there are different solution point, which will be investigated later.

TVA with cubic damping quite similar to linear TVA. The difference is mathematical.

TVA with cubic stiffness and dry friction damper has similar behavior with linear TVA. Its performance slightly worse. Notice that, there is no frequency interval with unstable solutions. Adding friction damper solves the stability problem in cubic stiffness.

TVA with cubic stiffness and cubic damper has the worst suppression performance when comparing the others. It has a frequency interval with no stable solution; also, it has a dual solution before the normalized frequency of 0.75.

The other cost function parameter is the area which defined in Figure 5.1.

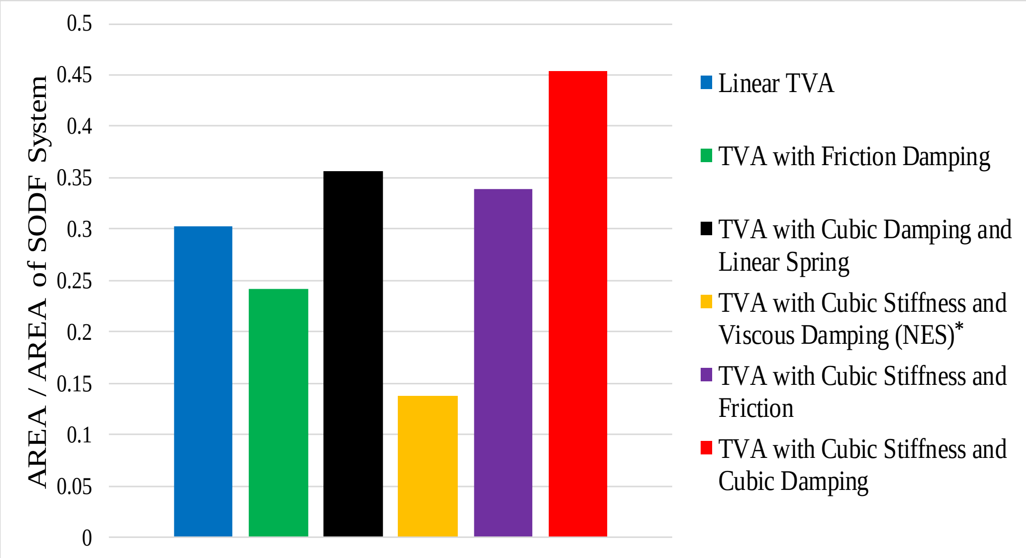

Figure 5.5 Comparison of single TVA Configurations in Terms of Defined Area

*Area of NES is calculated with including unstable frequency region

All parameters are given in Table 5.1. Parameters of Single TVA Configurations

Table 5.1. *Parameters of Single TVA Configurations*

Configuration	**Parameters**
Linear TVA	$k_{TVA} = 316.\,N/m \quad c_{TVA} = 2.0\,Ns/m$
TVA with Dry Friction Damping	$k_{TVA} = 270\,N/m \quad k_t = 598.5\,N/m$ $\mu N = 12.95\,N$
TVA with Cubic Stiffness and Viscous Damping (NES)	$k_c = 3.2\times10^4\,N/m^3 \quad c_{TVA} = 0.6\,Ns/m$
TVA with Cubic Damping	$k_{TVA} = 322.8\,N/m \quad c_c = 0.061\,Ns^3/m^3$
TVA with Cubic Stiffness and Friction Damping	$k_c = 1.13\times10^4\,N/m^3 \quad \mu N = 24\,N$ $k_t = 324.4$
TVA with Cubic Stiffness and Cubic Damping	$k_c = 2.36\times10^4\,N/m^3 \quad c_c = 0.045\,Ns^3/m^3$

Notice that, for linear TVA $\omega_{TVA} = 57.1\ rad/s$, $\omega_{TVA}/\omega_b = 0.91$ and $\xi = 0.18$

5.1.2. Multi TVAs

Dual TVAs are also considered.

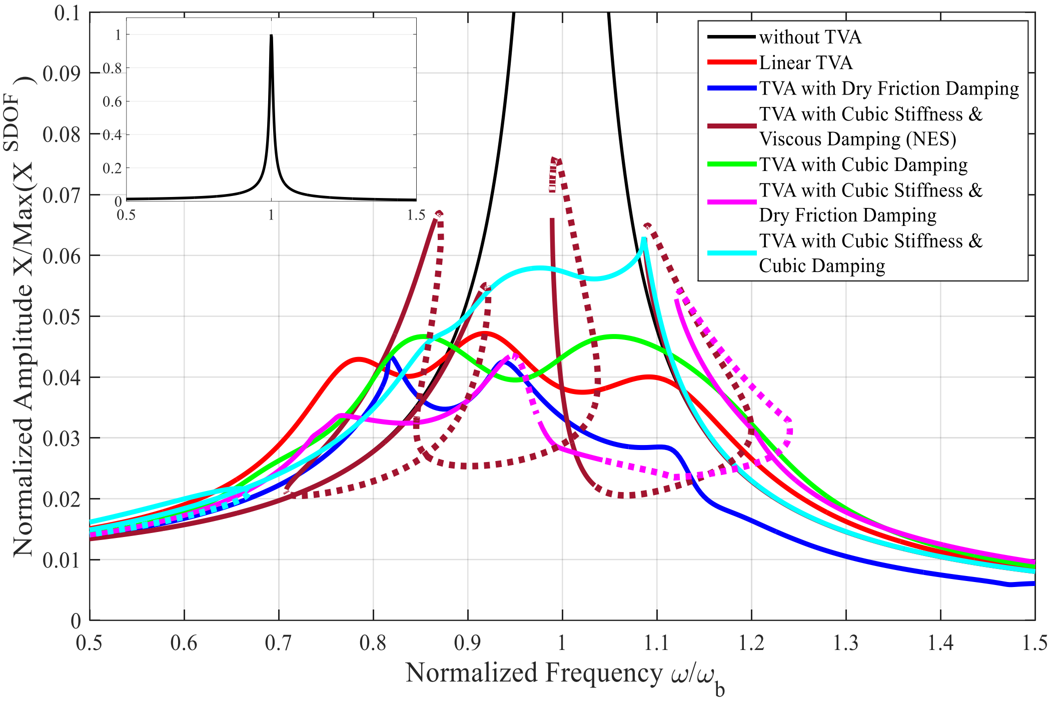

Figure 5.6 Comparison of multi TVAs Configurations.

Dotted lines denote unstable solutions. Solid lines denote stable solutions.

Linear multi TVA configuration has similar suppression ratio when comparing to linear single TVA configuration. Therefore, for linear system, usage of multiple TVA is not advantageous.

Configuration of multi TVAs equipped with dry friction damper is advantageous when comparing to single TVA with dry friction damper. It has also slightly better suppression regime than linear configuration. Multiple TVAs with dry friction dampers are more advantageous than single TVA configuration.

Configuration of multi TVAs with cubic stiffness and viscous damping has more complex behavior than single. It has four peaks and frequency intervals with no stable solutions.

Configuration of multi TVA with cubic damping is similar with linear multi TVA configuration but it is slightly worse. In addition, adding another TVA with cubic damper does not improve suppression level.

Configuration of multi TVAs with cubic stiffness and dry friction is worse than single TVA configuration. It has a higher amplitude between normalized frequency of 1.15 to 1.25. It has also frequency intervals with no stable solution.

Configuration of multi TVAs with cubic stiffness and cubic damper has the worst suppression performance when comparing the others.

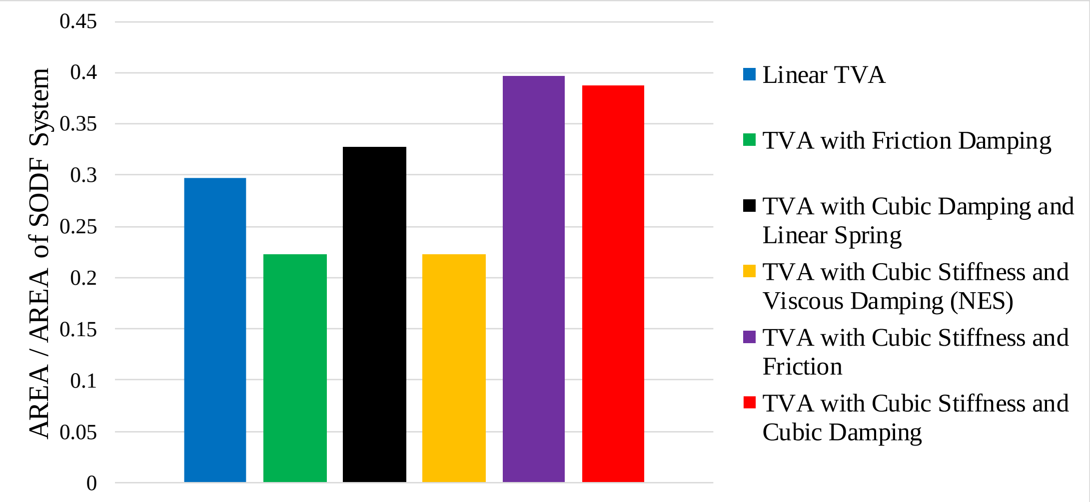

Figure 5.7 Comparison of multi TVAs Configurations. Dashed lines denote unstable solutions. Solid lines denote stable solutions.

From Figure 5.7, it is seen that, adding another cubic stiffness to the system does not improve suppression behavior.

Table 5.2. *Parameters of Multi TVA Configurations*

Configuration	**Parameters**
Linear TVAs	$k_{TVA,1} = 193.7\, N/m \quad c_{TVA,1} = 0.87\, Ns/m$ $k_{TVA,2} = 140.7\, N/m \quad c_{TVA,2} = 0.74\, Ns/m$

TVAs with Dry Friction Damping	$k_{TVA,1} = 183.8\,N/m$ $k_{TVA,2} = 138.9\,N/m$ $k_{t,1} = 430.4\,N/m$ $k_{TVA,2} = 558.6\,N/m$ $\mu N_1 = 5.6\,N$ $\mu N_2 = 4.2\,N$
TVAs with Cubic Stiffness and Viscous Damping (NES)	$k_{c,1} = 11487.3\ N/m^3$ $c_{TVA,1} = 0.42\,Ns/m$ $k_{c,2} = 6718.1\ N/m^3$ $c_{TVA,2} = 0.20\,Ns/m$
TVAs with Cubic Damping	$k_{TVA,1} = 178.2\,N/m$ $c_{c,1} = 0.015\,Ns^3/m^3$ $k_{TVA,2} = 121.0\,N/m$ $c_{c,2} = 0.058\,Ns^3/m^3$
TVAs with Cubic Stiffness and Friction Damping	$k_{c,1} = 2920.0\,N/m^3$ $k_{c,2} = 11802.1\,N/m^3$ $k_{t,1} = 154.9\,N/m$ $k_{TVA,2} = 259.8\,N/m$ $\mu N_1 = 11.21\,N$ $\mu N_2 = 5.03\,N$
TVAs with Cubic Stiffness and Cubic Damping	$k_{c,1} = 14990.8\ N/m^3$ $c_{c,1} = 0.051\,Ns^3/m^3$ $k_{c,2} = 12626.3\ N/m^3$ $c_{c,2} = 0.020\,Ns^3/m^3$

Notice that, for linear system, $\omega_{TVA,1} = 62.6\ rad/s$, $\omega_{TVA,2} = 56.0\ rad/s$, $\omega_{TVA,1}/\omega_b = 0.99$, $\omega_{TVA,2}/\omega_b = 0.84$, $\xi_1 = 0.14$ and $\xi_2 = 0.13$

To sum up, multiple TVAs is not effective except ones with dry friction dampers. Adding TVA with cubic stiffness increases the complexity of the system and does not improve the suppression level.

5.1.3. Comparison and Further Comments

Best configurations are single linear TVA, single TVA with NES and configuration of multi TVAs with dry friction damping.

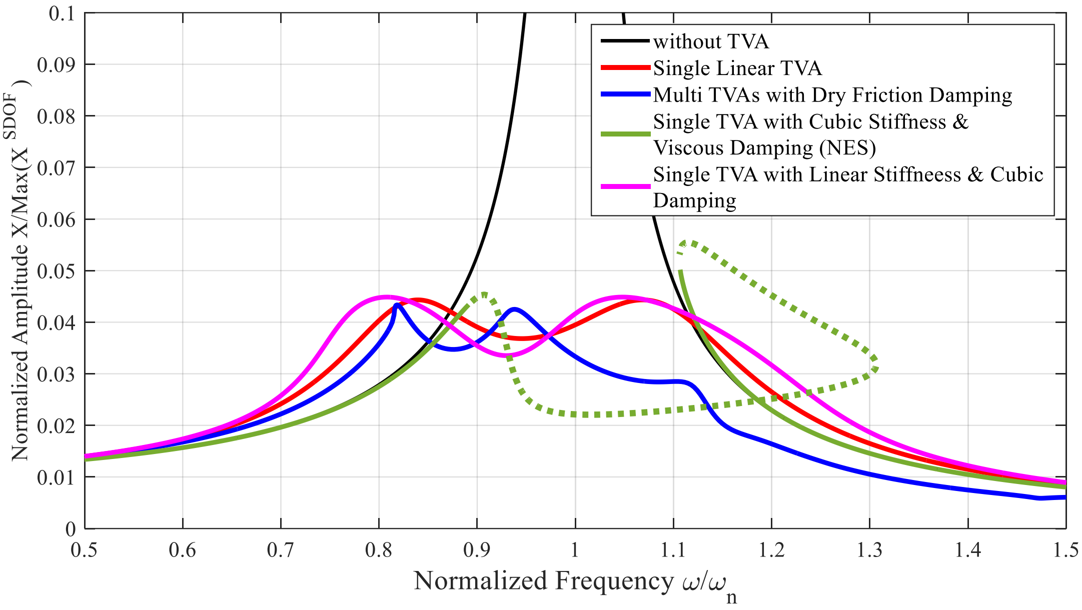

Figure 5.8. Best Configurations. Dashed lines denote unstable solutions. Solid lines denote stable solutions.

Configuration of multi TVAs with dry friction damping is slightly better when comparing with single linear TVA. It has lower amplitude except between normalized frequency of 0.9 to 0.95.

NES seems effective. However, due to stability behavior, further investigation is required.

Time domain solution is performed at certain frequencies. ODE45 of MATLAB is used to solve nonlinear differential equation in time domain. All initial values are take as zero and solution is performed for 100 seconds. Last one seconds are investigated. Maximum and minimum values are taken. $\left(x_{\max} - x_{\min}\right)/2$ is displayed. In addition, time history is investigated and periodicity is checked. This process is applied at specified frequencies.

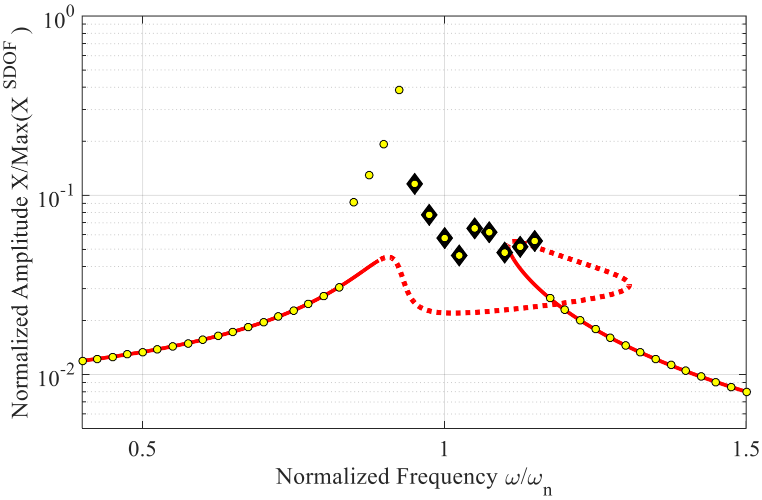

Figure 5.9. Comparison of Time Domain Solution and Frequency Domain Solution. Solid lines denote stable solutions. Dashed Lines denotes unstable solution.

From Figure 5.9, it is seen that, there is another solution after normalized frequency of 0.8. There is a bifurcation at some frequency. Solution points with no periodic solution is marked with black diamonds. These points will be investigated later.

The points obtained by time domain solution is used as an initial guess to follow other solution paths.

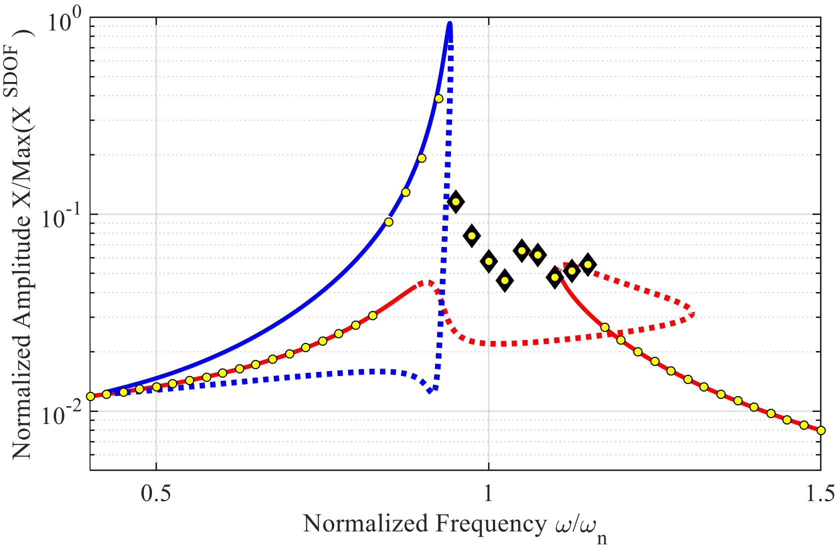

Figure 5.10 Comparison of Time Domain Solution and Extended Frequency Domain Solution. Solid lines denote stable solutions. Dashed Lines denotes unstable solution.

There is a bifurcation before normalized frequency of 0.42. These points can be seen more clearly in Figure 5.12, i.e. response of the TVA.

Figure 5.8 is updated as

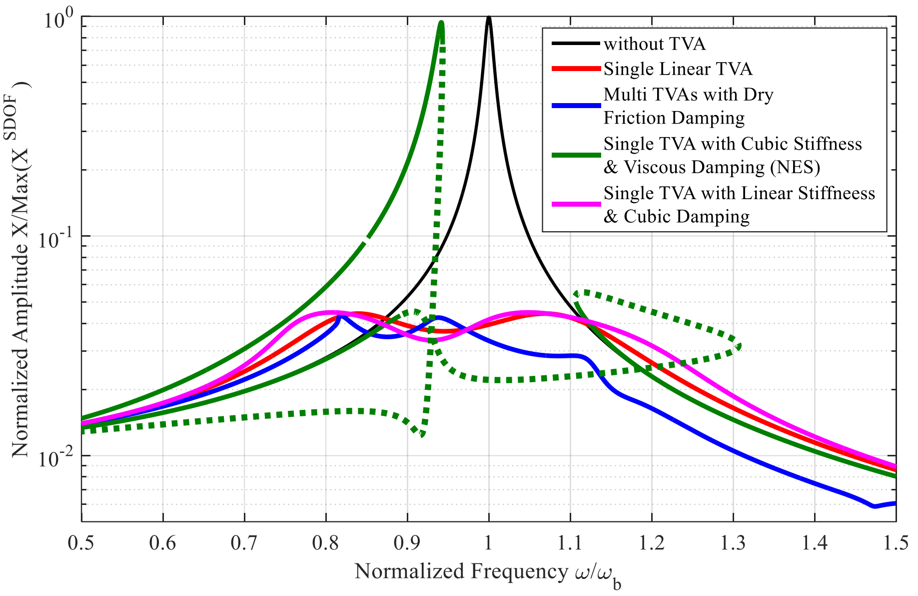

Figure 5.11. Best Configurations Updated.

Dotted lines denote unstable solutions. Solid lines denote stable solutions.

In addition, the solution point around resonance does not converge to another solution curve. There are no harmonic solution at those frequencies. Vibration at those frequencies might be chaotic. There are several ways to identify chaotic vibration. [41]

- **Sensitive to initial condition (Butterfly Effect):** Different initial values results different steady state solution.
- **Frequency Spectrum:** Broadband frequency excitation is observed.
- **Phase Plane:** If the response is periodic, phase plane orbits traced out a closed curve.

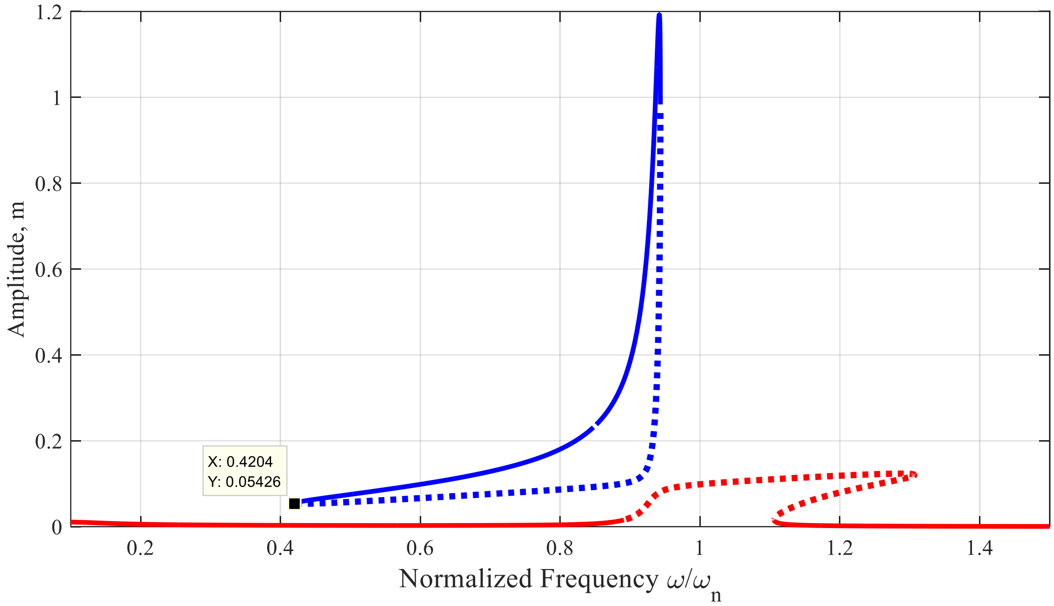

Figure 5.12 Response of the TVA. Solid lines denote stable solutions.

Dotted lines denote unstable solutions. Solid lines denote stable solutions.

Time response is obtained at normalized frequency 1, i.e. 10 Hz for 100 s for different initial conditions. Last second is presented in Figure 5.13

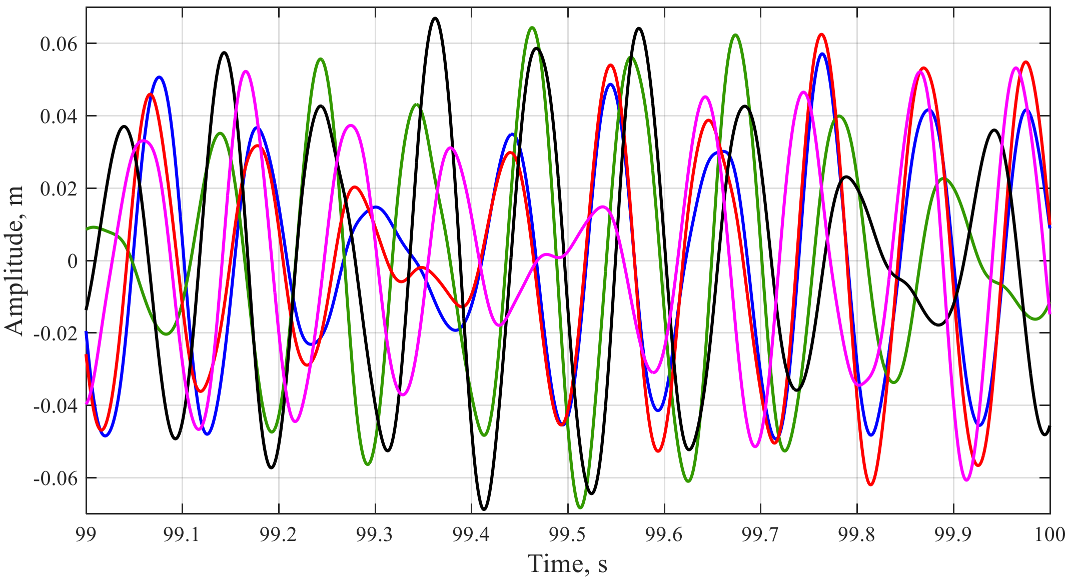

Figure 5.13: Time History with Different Initial Guesses

Change in initial guess, changes the steady state solution as it is seen in Figure 5.13.

At same frequency, i.e. 10 Hz, frequency spectrum is obtained by using FFT of MATLAB.

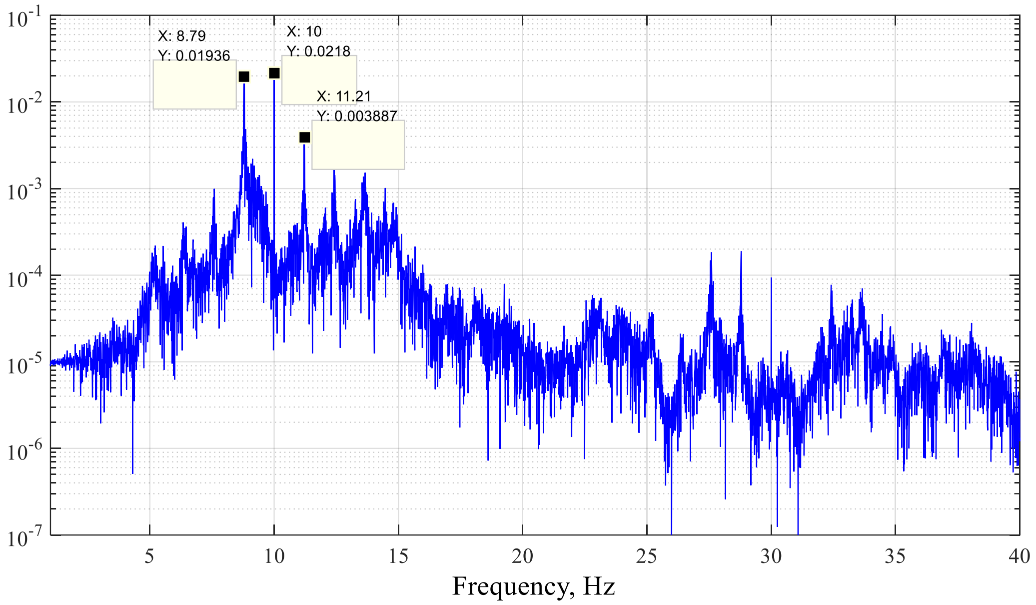

Figure 5.14: Single Sided Amplitude Spectrum of $x_b(t)$ when excitation frequency is 10 Hz

The excitation frequency is 10 Hz. In frequency spectrum, excitation frequency and its higher harmonics are expected (See Figure 5.15). However, broadband frequency excitation is observed. The values are higher around excitation frequency.

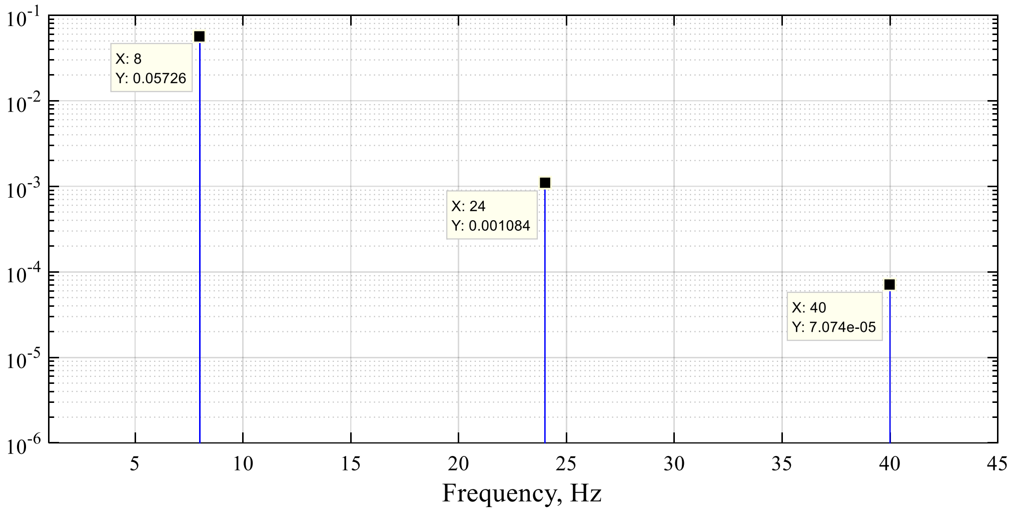

Figure 5.15: Single Sided Amplitude Spectrum of $x_b(t)$ when excitation frequency is 8 Hz

Finally, phase plan is obtained.

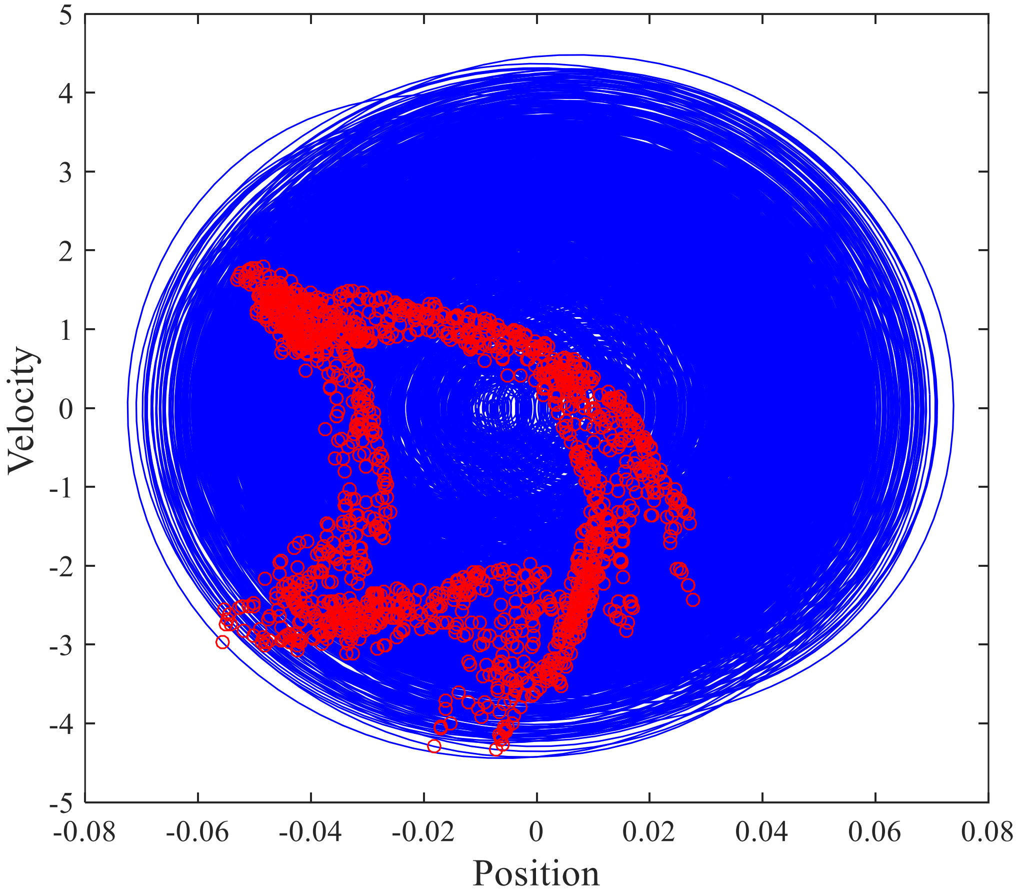

Figure 5.16: Phase Plane of $x_b(t)$ when excitation frequency is 10 Hz

Trajectory does not follow a closed loop. The solution at that frequency is chaotic. Normally trajectory follows a closed loop, like in Figure 5.17.

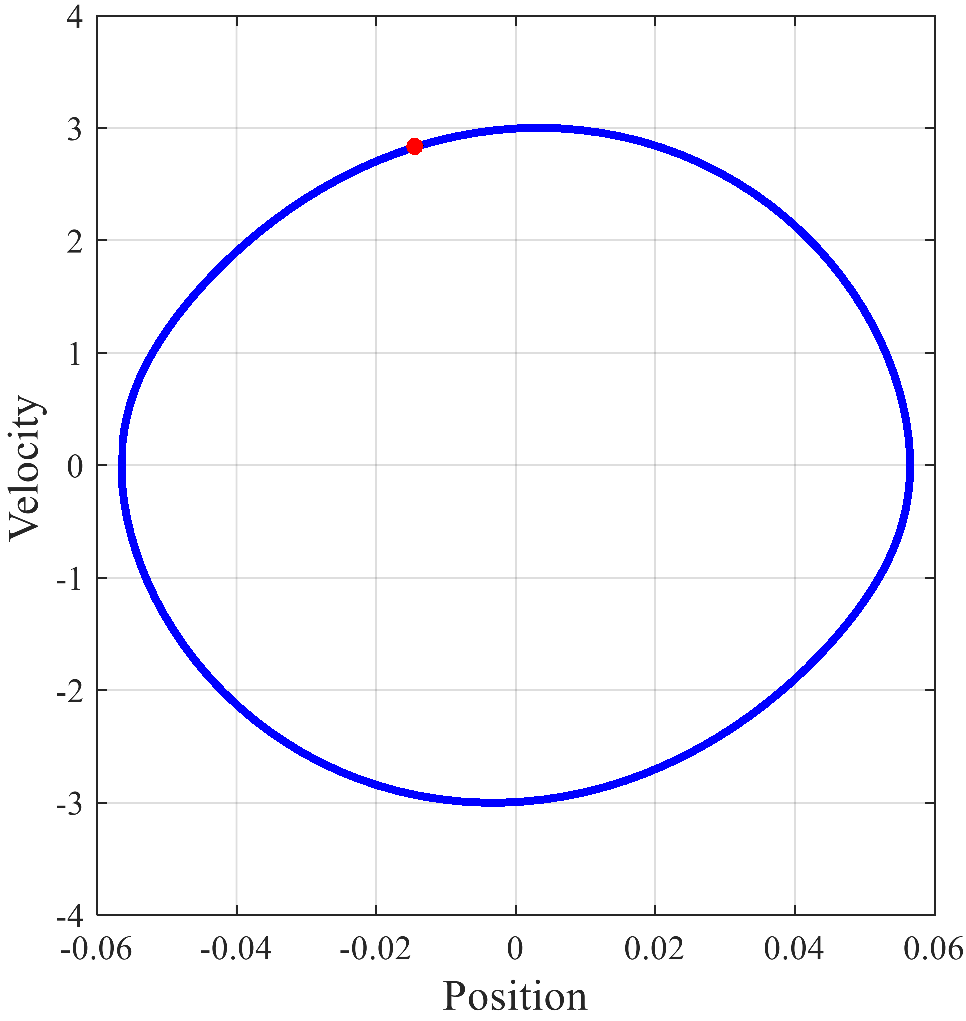

Figure 5.17: Phase Plane of $x_b(t)$ when excitation frequency is 8 Hz

In conclusion, NES is not effective in vibration suppression under harmonic excitation due to stability problem. Some studies in literature [30] claim that NES is more effective than linear TVA under harmonic excitation. However, this study claims opposite.

Notice that damping values in the linear system is quite higher when comparing to NES. For same damping value, the suppression performance of the NES might be better [42]. However, in this study, best parameter is selected. Such comparisons and analogies are not considered.

5.1.4. Effects of Mistuning

TVAs are generally effective when the all values are optimum. However, if values diverges from optimum value, suppression of TVA is worsened. In this chapter, effects of mistuning will be investigated.

Mistuning can be observed in both primary system and TVA. In primary system, natural frequency might be differed from the design value. In TVA, elastic element and dissipative element might be different from optimum value. Finally, input value can be differed.

Parameters are changed from 80 % to 120 %. Normalized maximum values are presented.

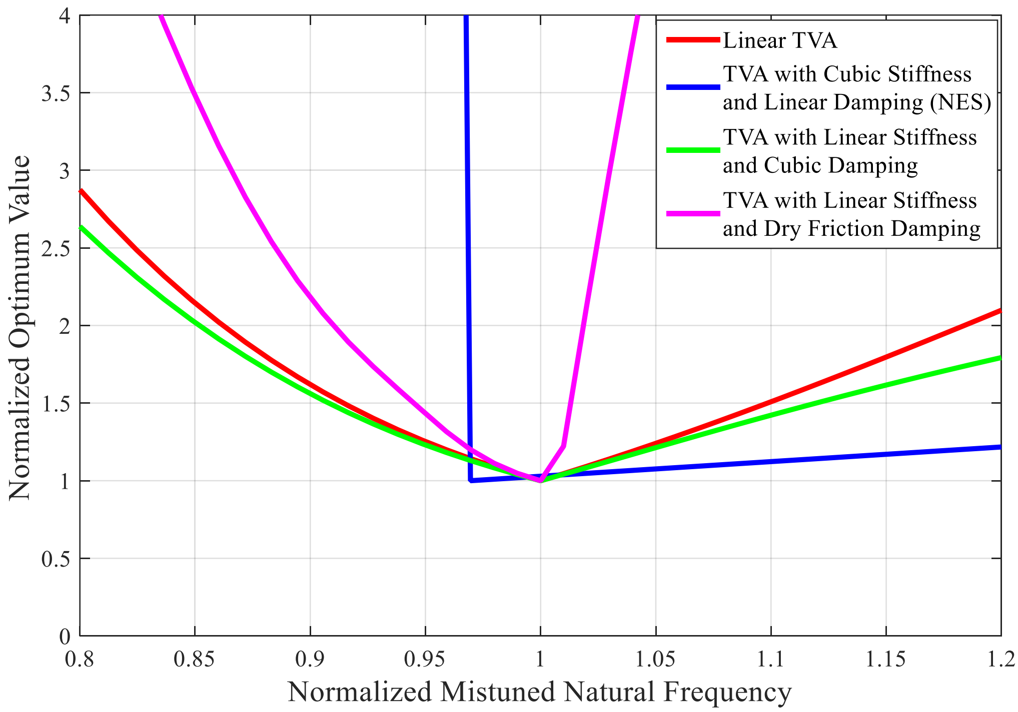

Figure 5.18: Effect of the Mistuning of the Natural Frequency of the Primary System

In Figure 5.18, natural frequency of the primary system is reduced and increased 20%. TVAs optimized for design value is used. It is seen that TVA with cubic damping have similar performance when comparing to linear TVA when system is detuned. TVA with dry friction damper is more sensitive to change in natural frequency. Amplitude of the system increase more drastically with increasing natural frequency. If friction is considered as equivalent viscous damping, it is inversely proportional with frequency [43]. Thus, performance of TVA with friction damping is worse when the system frequency is increased. NES is the most sensitive TVA configuration. After certain parameter exceed, it jumps.

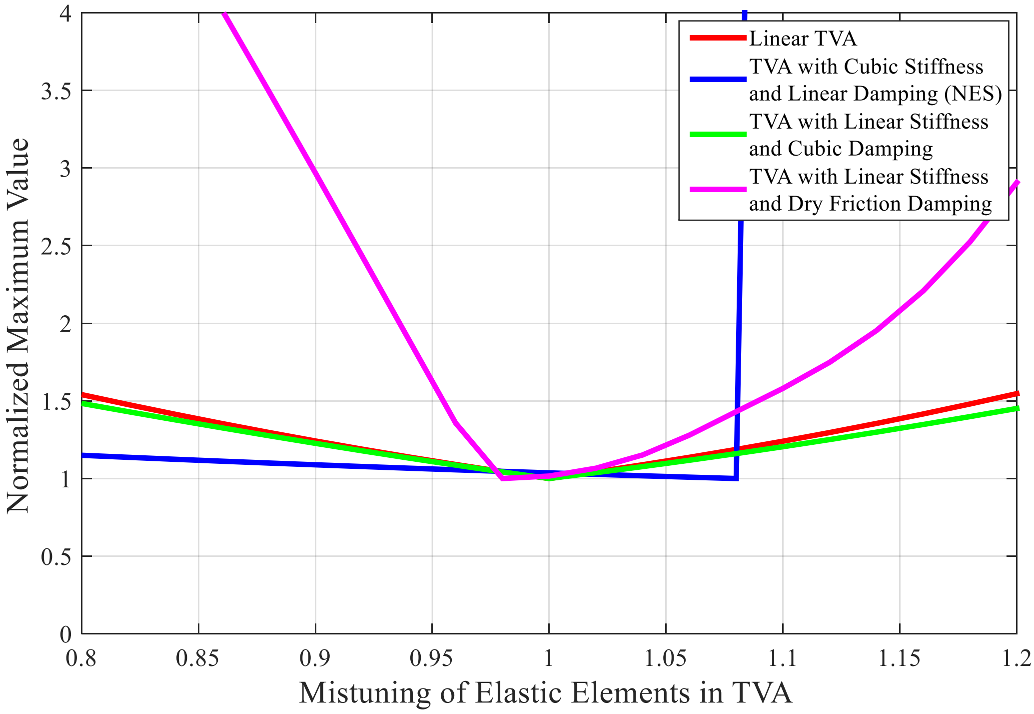

Figure 5.19: Effect of the Mistuning of the Elastic Elements in TVA

In Figure 5.19, elastic member in TVA is changed. In NES, elastic member is cubic stiffness. In all other configuration, it is linear stiffness. The configuration is similar with Figure 5.18. Behavior of the TVA with cubic damping is similar with linear one. TVA with dry friction damper is more sensitive to parameter change. The reason is similar with previous case. .NES is the most sensitive configuration.

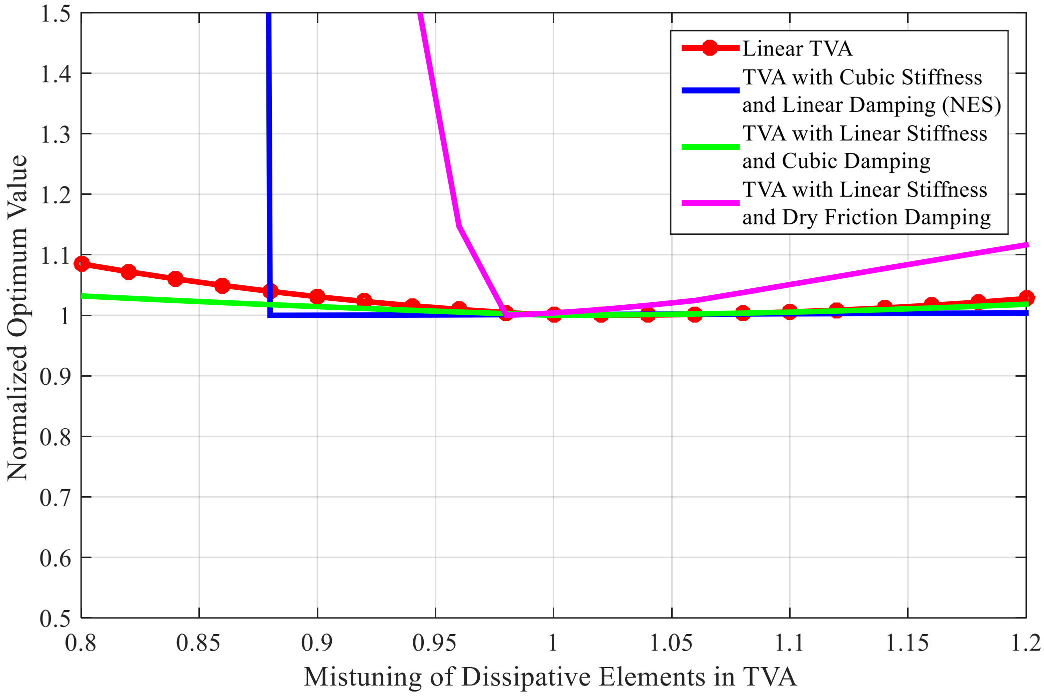

Figure 5.20: Effect of the Mistuning of the Dissipative Elements in TVA

In Figure 5.20, dissipative elements in TVA are changed. In linear TVA and NES, dissipative element is linear damping. In TVA with cubic damping, dissipative element is cubic damping and in TVA with dry friction damping, dissipative element is dry friction. Linear TVA and TVA with cubic damping have similar behavior. TVA with dry friction damping is more sensitive in lower values.

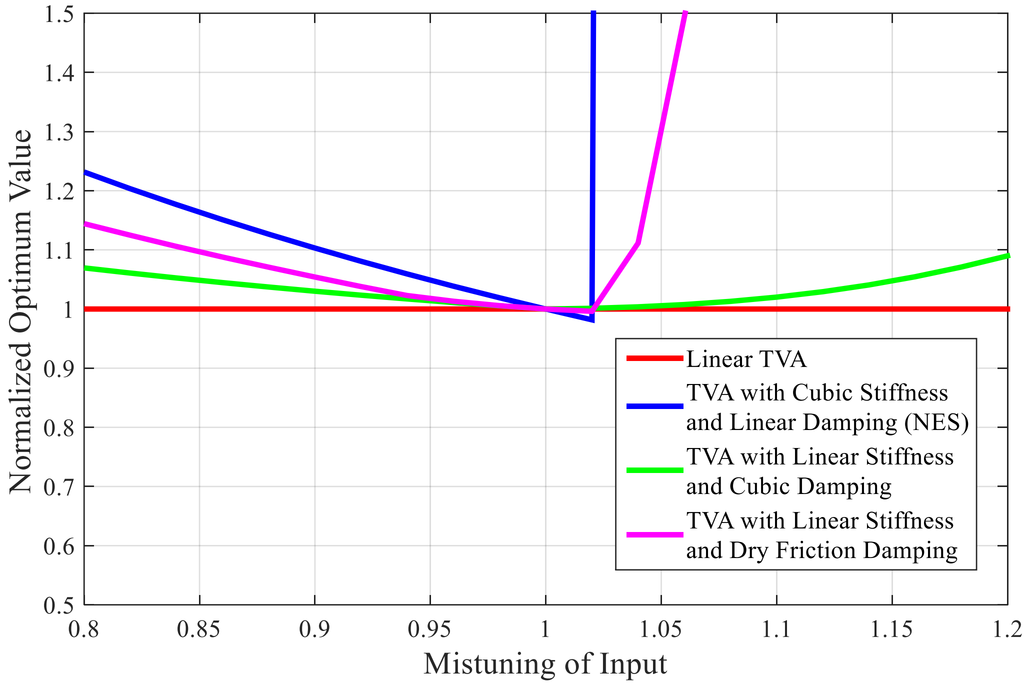

Figure 5.21: Effect of the Mistuning of the Input

In Figure 5.21, input value is changed. Performance of linear TVA does not change because the system is linear. TVA with dry friction damper is similar to TVA with cubic damping when the input is lower than design value. When input is higher, performance of TVA with dry friction damper is worse. NES sensitive to parameter change, it jumps.

5.2. Continuous System

To obtain more realistic and accurate results, TVA configurations with continuous system is studied. In this chapter linear Euler-Bernoulli beam under harmonic excitation. Both ends are fixed supported. Solution for other boundary condition is given in the appendix.

Parameters of the system is $L = 1m$, $EI = 9\,Nm^2$, $A = 60\,mm^2$, $\rho = 7850\ kg/m^3$ and $u = 1\ mm$.

Inherit damping of the beam is calculated by using Equation (3.29). Base excitation cannot excite second mode. Therefore, first and second mode is considered.

$$\boldsymbol{\omega}_b = \sqrt{eig\left(\mathbf{K}_{Beam}, \mathbf{M}_{Beam}\right)} = \begin{Bmatrix} 97.80 \\ 269.5 \\ 528.5 \\ 873.6 \\ 1306 \end{Bmatrix} rad/s \tag{5.1}$$

Damping ratio is taken as one percent for both mode.

$$\xi_1 = \xi_3 = 0.01 \tag{5.2}$$

$$\alpha = 0.01 \frac{2\omega_1 \omega_3}{\omega_1 + \omega_3} = 1.65 \tag{5.3}$$

$$\beta = 0.01 \frac{2}{\omega_1 + \omega_3} = 3.19 \times 10^{-5} \tag{5.4}$$

Inherit damping of the beam is constructed as

$$\mathbf{C}_{Beam} = \alpha \mathbf{M}_{Beam} + \beta \mathbf{K}_{Beam} \tag{5.5}$$

Base excitation cannot excite second mode. Therefore, first and the third mode cancelation is considered. Ineffective TVA configurations are excluded. Single and multi linear TVA configurations, single and multi TVA with dry friction configurations are studied. In addition, NES are also studied.

Location for TVA is selected for maximum suppression.

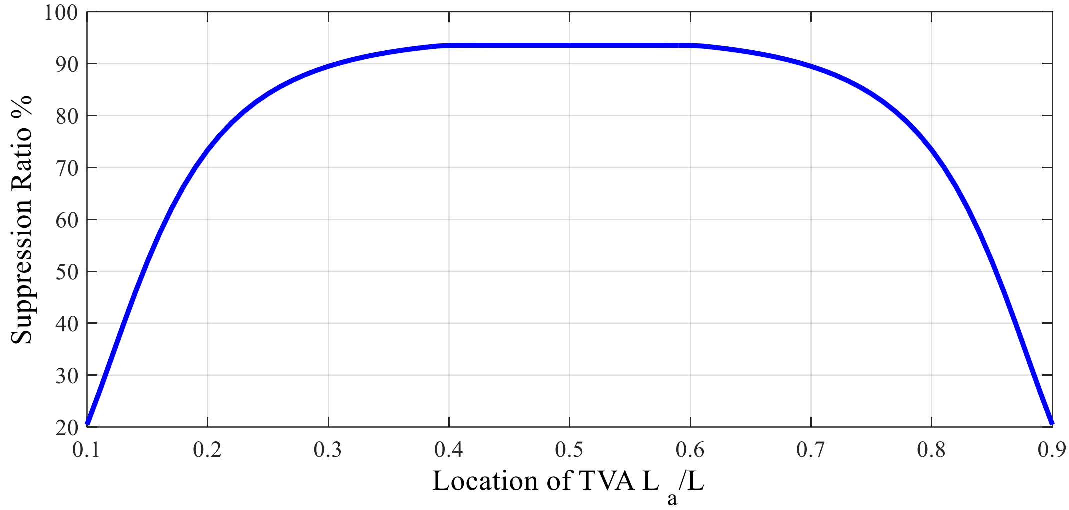

Figure 5.22 Effect of the Location of the TVA on Suppression Ratio

From Fig. 5.18, it is seen that, optimum location is $L_a = 0.5L$

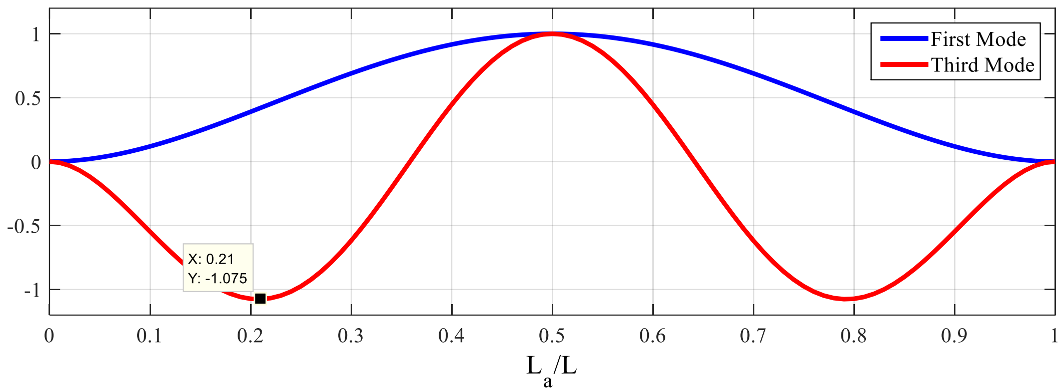

Figure 5.23 Effect of the Location of the TVA on Suppression Ratio

To cancel out third mode, TVA can also locate $L/2$ However, for optimization, other locations, which has a peak, are also checked. These locations are 0.21L, and 0.79L. Single the beam is symmetric and TVA is located at the middle, only one of the is considered. Response of these two are same.

5.2.1. First Mode Cancelation

Total mass of the TVAs are ten percent of the main system, i.e. $m_{TVA} = 0.1\rho AL$. For double TVAs, masses are equal to each other.

Selected TVA configurations are optimized:

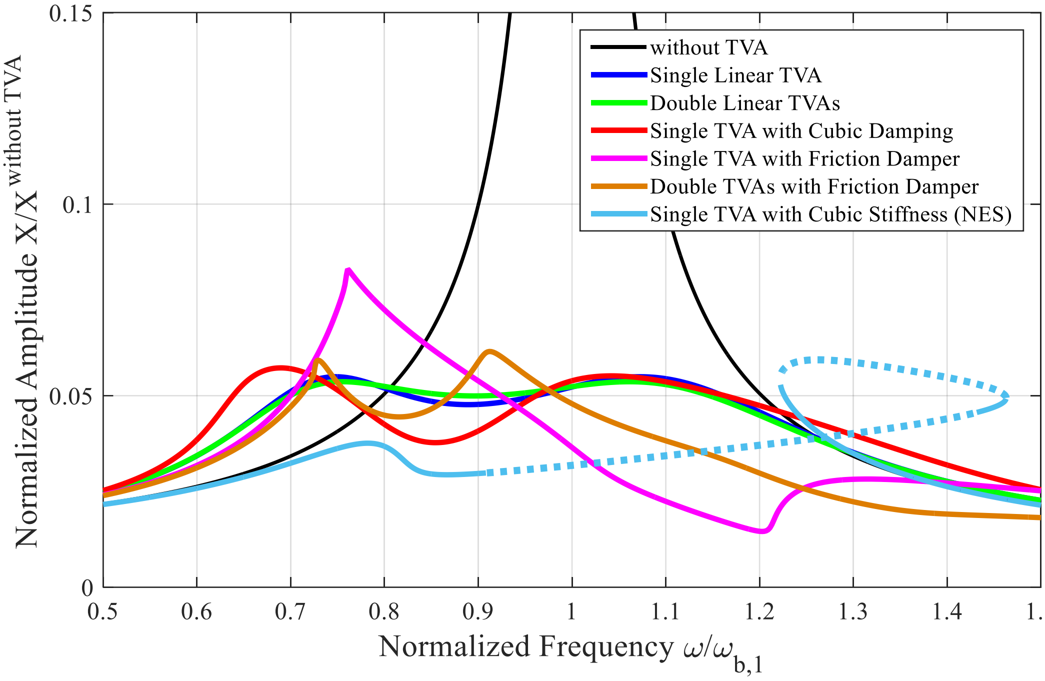

Figure 5.24 TVA Configurations to Cancel Out First Mode

Single TVA with friction damper has higher amplitude than linear response between normalized frequencies 0.7 to 0.95. After that value, it has better suppression regime.

Configuration of double TVAs with friction dampers has higher amplitude between normalized frequencies 0.8 to 0.95. For other frequency region, it has slightly better suppression regime.

Single TVA with cubic damping, single linear TVA and multi linear TVA have similar suppression behavior.

NES seems effective; however, it is ineffective due to its stability behavior. It is studied in previous chapter in detail.

Parameters are given in Table 5.3.

Table 5.3. *Parameters of TVA Configuration to Cancel Out First Mode*

Configuration	Parameters
Single Linear TVA	$k_{TVA} = 300.8\ N/m \quad c_{TVA} = 2.08\, Ns/m$
Double Linear TVAs	$k_{TVA,1} = 177.9\, N/m \quad c_{TVA,1} = 1.18\, Ns/m$ $k_{TVA,2} = 131.4\, N/m \quad c_{TVA,1} = 0.88\, Ns/m$
Single TVA with Dry Friction Damping	$k_{TVA} = 156.7\, N/m \quad \mu N = 1.45\, N$ $k_t = 700.0\, N/m$
Double TVAs with Dry Friction Damping	$k_{TVA,1} = 129.8\, N/m \quad k_{TVA,2} = 189.4\, N/m$ $\mu N_1 = 0.34\, N \quad \mu N_2 = 0.62\, N$ $k_{t,1} = 599.9\, N/m \quad k_{t,2} = 995.5\, N/m$
TVA with Cubic Stiffness and Viscous Damping (NES)	$k_c = 93.2\times10^5\ N/m^3 \quad c_{TVA} = 0.68\, Ns/m$
TVAs with Cubic Damping	$k_{TVA} = 297.2\, N/m \quad c_c = 8.19\, Ns^3/m^3$

5.2.2. First and Third Modes Cancelation

Base excitation cannot excite second mode of the fixed -fixed beam. The next mode, which can be excited by base excitation, is the third mode.

By designing TVAs for the first mode, response of the third mode can be also reduced, because, overall damping of the system is increased.

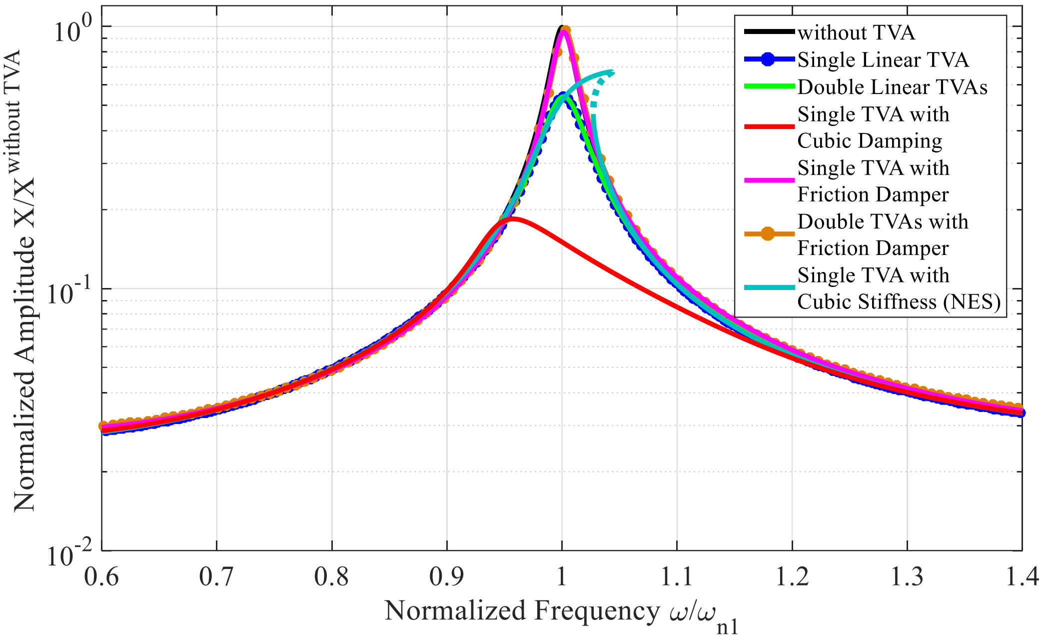

Figure 5.25 Effect of Previous TVA Configurations at Third Mode.

In previous chapter, TVA configurations are optimized to cancel out first mode. Their effect on third mode is given in Fig. 5.18. It is seen that, configurations of TVA with friction dampers do not contribute suppression. The reason is friction is not effective in higher frequencies. Consider friction damper as an equivalent viscous damper. The damping coefficient is proportional to $1/\omega$ [43]. Therefore, it is lower in high frequencies.

Linear TVA configurations have a contribution because overall damping of the system is increased. Similar suppression behavior is observed in NES. They act as low spring with high damping.

Best suppression is observed in cubic damping. Because overall damping of the system is increased and damping force is proportional to third power of the velocity. Therefore, it is more effective when compare to others

In the next study, two TVAs with different configurations are optimized. Each of them is optimized to suppress one mode.

Total mass of the TVAs are kept same. In first optimization, mass of the first and second TVA is equal.

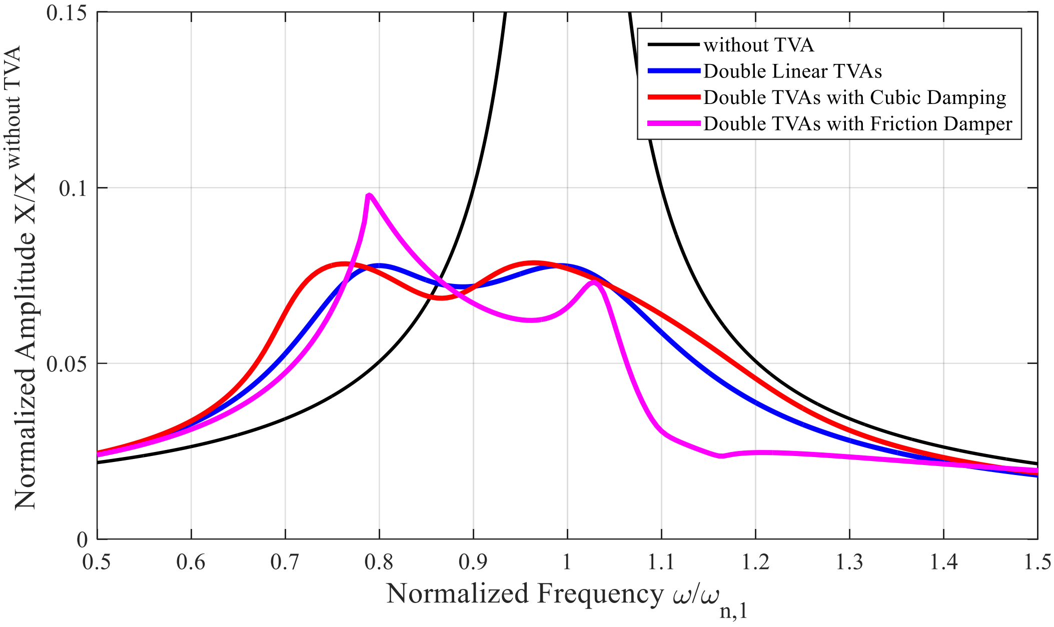

Figure 5.26 Suppression in First Mode at $L/2$

In Figure 5.26, frequency values are normalized with the first natural frequency of the beam without TVA. The amplitudes are normalized with the response of the beam at the first resonance.

TVA with friction damper has higher value than linear system between normalized frequencies 0.75 to 0.9.

Behavior of the TVA with cubic damping is similar to linear one.

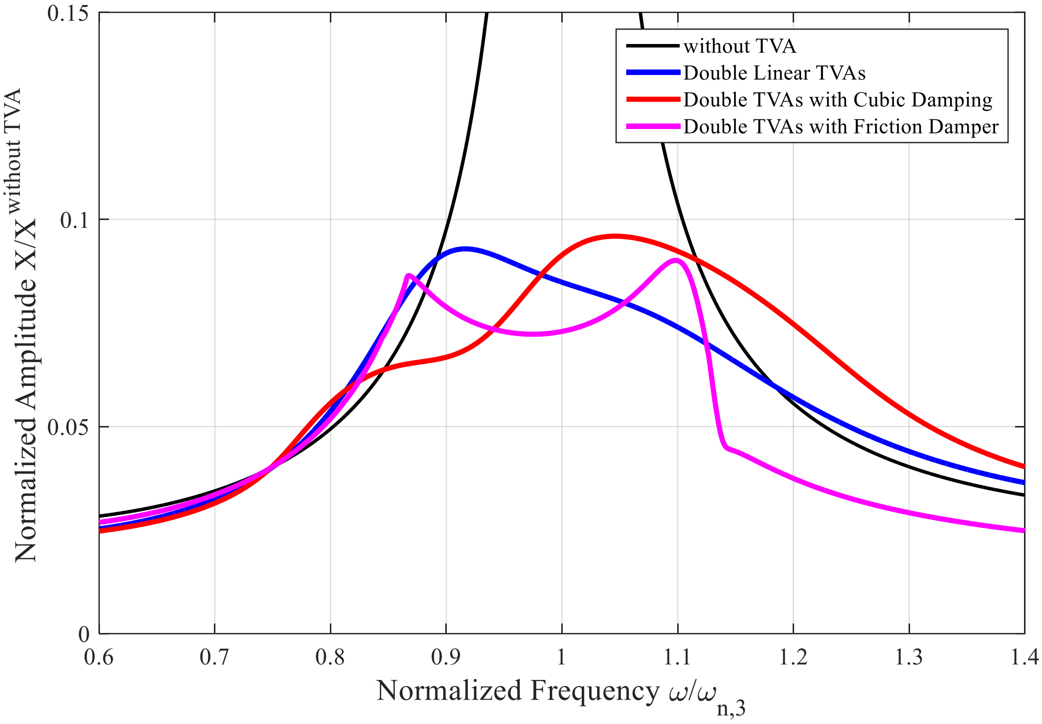

Figure 5.27 Suppression in Third Mode at $L/2$

TVA with friction damper has higher value than linear system between normalized frequencies 1.05 to 1.15. After that frequency, it is slightly lower.

Table 5.4. *Parameters of TVA Configuration to Cancel Out First Two Mode*

Configuration	**Parameters**	
TVA with Dry Friction Damper	$k_{TVA,1} = 136.0\ N/m$ $k_{t,1} = 416.0\ N/m$ $\mu N_1 = 0.75\ N$	$k_{TVA,2} = 5114.9\ N/m$ $k_{t,2} = 93926\ N/m$ $\mu N_2 = 8.56\ N$
TVA with Cubic Damping	$k_{TVA,1} = 163.7\ N/m$ $k_{TVA,2} = 4852.7\ N/m$	$c_{c,1} = 1.05\ Ns^3/m^3$ $c_{c,2} = 0.64\ Ns^3/m^3$
Linear TVA	$k_{TVA,1} = 163.4\ N/m$ $k_{TVA,2} = 5459.2\ N/m$	$c_{TVA,1} = 0.82\ Ns/m$ $c_{TVA,2} = 5.0\ Ns/m$

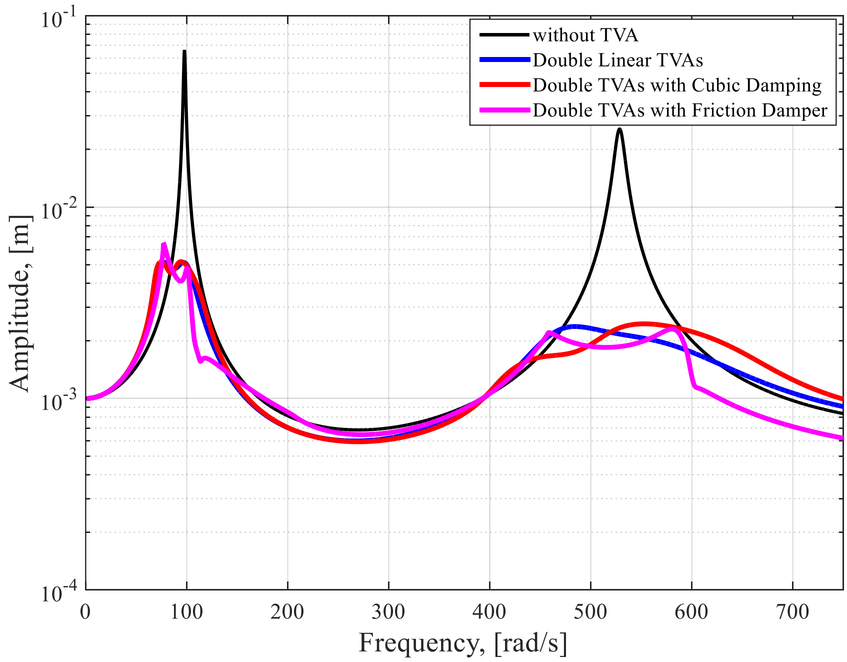

Figure 5.28 Vibration Suppression at $L/2$

Vibration suppression performance is generally better in first mode. In higher mode, amplitude level decrease due to the nature of the structure.

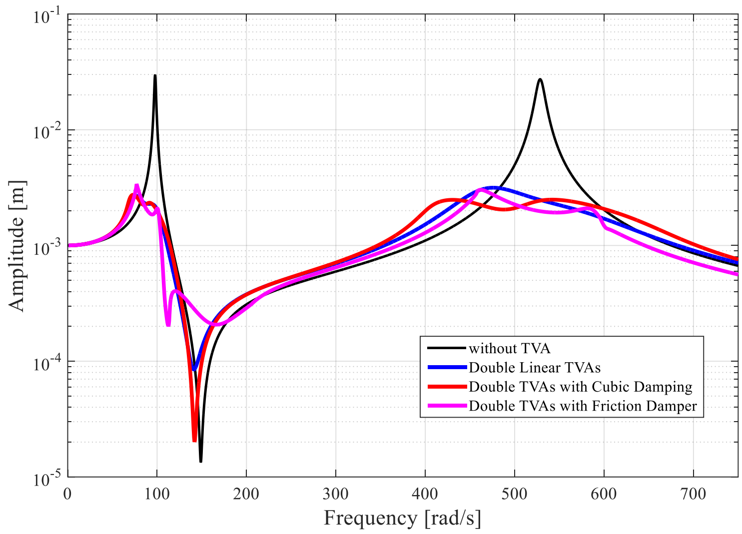

Figure 5.29 Vibration Suppression at 0.21L

CHAPTER 6

CONCLUSION AND FUTURE WORK

6.1. Conclusion

In this study, vibration reduction of structures by using Tuned Vibration Absorber is studied. Linear primary structure is considered. Both linear and nonlinear TVAs are studied.

For primary structure, discrete and continuous systems are considered. The continuous system is linear Euler Bernoulli Beam. TVA is investigated. The system is subjected to sinusoidal base excitation. Parameters of the nonlinear TVA is optimized to minimize vibration values of the primary system. Assumed modes method is used to model the Euler-Bernoulli beam. Nonlinear differential equations of motion are converted to a set of nonlinear algebraic equations by using Harmonic balance Method (HBM). The resulting set of nonlinear algebraic equations is solved by Newton's Method with Arc-Length continuation. Hill's method is used to evaluate stability of the solutions obtained. Genetic Algorithm (GA) of MATLAB is used. Results comes from genetic algorithm is used as initial guess for gradient base optimization algorithm. For gradient base optimization, fminunc of MATLAB is used.

For discrete system, SDOF lightly damped structure is considered. Linear and nonlinear TVA configurations are optimized to reduce vibration response of the primary structure. The nonlinear elements considered in this study are cubic damping, dry friction damper and cubic stiffness. TVA with cubic stiffness and viscous damping is names as NES in this study, similar with literature. Besides single TVA, use of multiple TVAs is considered. The optimum results are obtained and results are compared. NES seems very effective in terms of vibration suppression however; there are unstable regions in frequency response. Further investigation is carried out and it is found out that, there is another solution branch with higher amplitude, and a frequency region with chaotic solutions. Therefore, NES is not as effective as it seems under harmonic base excitation. The configurations are close to each other. Differences are slight.

For continuous system, lightly damped Euler Bernoulli beam is considered. First and third mode cancelation is considered. Results are presented. It is seen that, viscous and cubic damping is slightly better when first and third mode cancelation is considered.

6.1.1. Future Work

In this study, optimization is carried out for harmonic base excitation. It is not quite realistic in real case. Optimization can be extend for different type of loading such as random.

The primary systems in this study are simple system. However, in real engineering applications, primary system is more complex. Such systems are generally modelled by using Finite element methods. Coupling methods can be used to combine complex primary structure and nonlinear TVA. As a results, TVA is optimized for more realistic system.

REFERENCES

[1] Connor, J. and Laflamme, S. (2014). *Structural Motion Engineering*, doi: 10.1007/978-3-319-06281-5.

[2] Watt, P. (1883). On a Method of Reducing the Rolling of Ships at Sea. *Trans Inst Naval Archit*, 24, 165–190,

[3] Frahm, H. (1911) Device for Damping Vibrations of Bodies. US Patent No. 989958.

[4] Ordmondroyd, J. and Den Hartog, J.P. (1928). The Theory of Dynamic Vibration Absorber, *Transactions of the American Society of Mechanical Engineers*, 50, 9-22.

[5] Den Hartog, J. P. (1947). *Mechanical Vibration*, *N.Y. 3rd ed*. McGraw-Hill, New York.

[6] Bapat, V.A. and Kumaraswamy, H.V. (1979). Effect of Primary System Damping On the Optimum Design Of an Untuned Viscous Dynamic Vibration Absorber, *Journal of Sound and Vibration*, 63 (4), 469-474

[7] Ioi, T. and Ikeda, K. (1978). On the Dynamic Vibration Damped Absorber of the Vibration System, *Bulletin of JSME*, 21 (151), 64-71

[8] Randall SE, Halsted DM, III, Taylor DL. (1981) Optimum Vibration Absorbers for Linear Damped Systems. *ASME. J. Mech. Des*. 103(4):908-913.

[9] Iwanami, K. and Seto, K. (1984). An Optimum Design Method for the Dual Dynamic Damper and its Effectiveness, *Bulletin of JSME*, 27, 1965-1973.

[10] Igusa, T and Xu, K. (1994). Vibration Control Using Multiple Tuned Mass Dampers, *Journal of Sound and Vibration*, 175 (4), 491-503.

[11] Young, D. (1952). Theory of Dynamic Vibration Absorbers for Beams, *Proceedings of the First U.S. National Congress of Applied Mechanics*, 83 (12), 91-96.

[12] Neubert, V. H. (1964) Dynamic Absorbers Applied to a Bar That Has Solid Damping, *The Journal of the Acoustical Society of America*, 36 (4), 673-680.

[13] Jacquot, R. G. (1978). Optimal Dynamic Vibration Absorbers for General Beam Systems, *Journal of Sound and Vibration*, 60 (4), 535-542.

[14] Warburton, G. B. and Ayorinde, E. O. (1980). Optimum Absorber Parameters for Simple Systems, *Earthquake Engineering and Structural Dynamics,* 8 (3), 197-217.

[15] Özgüven, H. N. and Çandır, B. (1985). Suppressing the First and Second Resonances of Beams by Dynamic Vibration Absorbers, *Journal of Sound and Vibration*, 111 (3), 377-390.

[16] Esmailzadeh, E. and Jalili, N. (1998). Optimum Design of Vibration Absorbers for Structurally Damped Timoshenko Beams, *Journal of Vibration and Acoustics*, 120 (4), 833-841.

[17] Roberson, R. E. (1952). Synthesis of a Nonlinear Dynamic Vibration Absorber, *Journal of the Franklin Institute*, 254 (3), 205-220.

[18] Hunt, J. B. and Nissen, J. C. (1981). The Broadband Dynamic Vibration Absorber, *Journal of Sound and Vibration*, 83 (4), 573-578.

[19] Natsiavas, S. (1992). Steady State Oscillations and Stability of Non-Linear Dynamic Vibration Absorbers, *Journal of Vibration and Acoustics*, 156 (2), 227-245.

[20] Inaudi, J. A. and Kelly, J. M. (1995). Mass Damper Using Friction-Dissipating Devices, *Journal of Engineering Mechanics*, 121 (1), 142-149.

[21] Ricciardelli, F. and Vickery, B. J. (1999). Tuned Vibration Absorbers with Dry Friction Damping, *Earthquake Engineering and Structural Dynamics,* 28 (7), 707-723.

[22] Gewei, Z. and Basu, B. (2010). A Study on Friction-Tuned Mass Damper: Harmonic Solution and Statistical Linearization, *Journal of Vibration and Control*, 17 (5), 721-731.

[23] Carmona, J. E. C., Avila, S. M. and Doz, G. (2017). Proposal of a Tuned Mass Damper With Friction Damping to Control Excessive Floor Vibrations, *Engineering Structures*, 148, 81-100.

[24] Pisal, A. Y. (2015). Seismic Response of Multi-Story Structure with Multiple Tuned Mass Friction Dampers, *International Journal of Advanced Structural Engineering (IJASE)*, 7 (1), 81-92.

[25] Sinha, A. and Trikutam, K. T. (2018), Optimal Vibration Absorber with a Friction Damper, *Journal of Vibration and Acoustics*, 140 (2), 1-7.

[26] Gendelman, O.V., Vakakis, A.F., Manevitch, L.I. and McCloskey, R. (2001). Energy Pumping in Nonlinear Mechanical Oscillators I: Dynamics of The Underlying Hamiltonian System, *Journal of Applied Mechanics* 68 (1), 34-41.

[27] Vakakis, A.F. and Gendelman, O.V. (2001). Energy Pumping in Nonlinear Mechanical Oscillators II: Resonance Capture, *Journal of Applied Mechanics*, 68 (1), 42-48.

[28] Jiang, X., McFarland, D.M., Bergman, L.A., Vakakis, A.F. (2003). Steady State Passive Nonlinear Energy Pumping in Coupled Oscillators: Theoretical and Experimental Results. *Journal of Nonlinear Dynamics*, 33 (1), 87-102.

[29] Gendelman, O.V., Gourdon, E. and Lamarque, C.H. (2006). Quasiperiodic Energy Pumping in Coupled Oscillators Under Periodic Forcing, *Journal of Sound and Vibration*, 294 (4-5), 651-662.

[30] Parseh, M., Dardel, M. and Ghasemi, M.H. (2015). Investigating The Robustness of Nonlinear Energy Sink in Steady State Dynamics of Linear Beams with Different Boundary Conditions, *Communications in Nonlinear Science and Numerical Simulation*, 29 (1-3), 50-71.

[31] Gourc, E., Elce, L. D., Kerschen, G., Michon, G., Aridon, G. and Hot, A. (2016). Performance Comparison between a Nonlinear Energy Sink and a Linear Tuned Vibration Absorber for Broadband Control, *Nonlinear Dynamics*, 1, 83-95.

[32] Nayfeh, A. H. and Mook, D. T. (1995). *Nonlinear Oscillations*, DOI:10.1002/9783527617586

[33] Cigeroglu, E and Samandari, H. (2012). Nonlinear Free Vibration of Double Walled Carbon Nanotubes by Using Describing Function Method with Multiple Trial Functions, *Physica E,* 46, 160-173.

[34] Detroux, T., Renson, L., Masset, L., and Kerschen, G. (2015). The Harmonic Balance Method for Bifurcation Analysis of Large-Scale Nonlinear Mechanical Systems, *Computer Methods in Applied Mechanics and Engineering*, 296, 18-38.

[35] Lazarus, A, and Thomas, O. (2010). A Harmonic-Based Method for Computing the Stability of Periodic Solutions of Dynamical Systems, *Comptes Rendus Mécanique,* 338 (9), 510-517.

[36] Rao, S. S. (2006). *Vibration of Continuous Systems*, DOI:10.1002/9780470117866

[37] Bhushan B. (2013). *Principles and applications of tribology*, 2nd edn. Wiley-Interscience, Ohio

[38] Erisen, Z., E. and Cigeroglu, E. (2012). Frequency Domain Optimization of Dry Friction Dampers on Buildings under Harmonic Excitation, *Topics on the Dynamics of Civil Structures*, 1, 113-126.

[39] Cigeroglu, E. and Ozguven, H. (2006). Nonlinear Vibration Analysis of Bladed Disks with Dry Friction Dampers, *Journal of Sound and Vibration*, 295 (3-5), 1028-1043.

[40] Asami, T., Nishihara, O. and Baz, A. M. (2002). Analytical Solutions to H∞ and H2 Optimization of Dynamic Vibration Absorbers Attached to Damped Linear Systems, *Journal of Vibration and Acoustics*, 124(2), 284-295.

[41] Moon, F. C. (2004). *Chaotic Vibrations: An Introduction for Applied Scientists and Engineers*, DOI:10.1002/3527602844

[42] Vakakis, A.F., Gendelman, O.V., Bergman, L.A., McFarland, D.M., Kerschen, G., and Lee, Y.S (2009). *Nonlinear Targeted Energy Transfer in Mechanical and Structural Systems*, DOI.ORG/10.1007/978-1-4020-9130-8

[43] Sinha, A. (2010). *Vibration of Mechanical Systems,* DOI: 10.1017/CBO9780511778087

A. Beam with Simply Supported at Both End